REPORT NO.
UCB/SEMM-87/08

STRUCTURAL ENGINEERING,
MECHANICS AND MATERIALS

SOLUTION METHODS FOR DAMPED LINEAR DYNAMIC SYSTEMS

by

Harn-Ching Chen

Faculty Investigator: R. L. Taylor

NOVEMBER 1987

DEPARTMENT OF CIVIL ENGINEERING
UNIVERSITY OF CALIFORNIA AT BERKELEY
BERKELEY, CALIFORNIA

Structural Engineering, Mechanics and Materials Division

Report NO. UCB/SEMM-87/08

SOLUTION METHODS FOR

DAMPED LINEAR DYNAMIC SYSTEMS

by

Harn-Ching Chen

Department of Civil Engineering
University of California
Berkeley, California 94720

November 1987

Solution Methods for Damped Linear Dynamic Systems

Harn-ching Chen

Department of Civil Engineering

University of California, Berkeley

Abstract

This dissertation considers solution methods for damped linear structural systems which are subjected to transient loading. To accommodate a range of possible applications, the damping is assumed to be non-proportional to mass and stiffness and may also be large and/or lumped. Some important characteristic properties of the damped system are presented. The second-order equations of motion are reduced to a first-order set by doubling the size of the problem to facilitate the subsequent analysis and computation.

The Rayleigh-Ritz method is generalized for the matrix pencil associated with a damped system. A projection method is discussed as an alternative. Both provide a basis for computing partial eigensolutions of a large damped dynamic system.

The subspace iteration method is modified to extract eigensolutions of a damped dynamic system. The iteration vectors are arranged in such a way that only real arithmetic is required to describe the complex solution vectors. The algorithm is implemented to solve some typical numerical examples.

The Lanczos method also is extended to find eigensolutions of a damped dynamic system. The loss of orthogonality between Lanczos vectors is investigated and two schemes are presented to restore the required orthogonality. The algorithm presented can take full advantage of the symmetry and sparsity of the associated matrices and also involves only real arithmetic during the solution process. The algorithm is implemented and tested with the numerical examples introduced in the subspace solution.

Within the framework of mode superposition, a number of choices are discussed for finding the response of a dynamic system subjected to initial conditions and external loadings. In particular, the eigenvectors are used to transform the equations of motion into a set of uncoupled equations. A closed form solution and a numerical solution to the uncoupled equations are presented. An example is shown to illustrate the mode displacement method for the analysis of a transient dynamic problem.

Acknowledgements

I am indebted to Professor Robert L. Taylor for his support and encouragement during the course of this research. His advice and guidance are essential to this work and are also invaluable to my studies at Berkeley.

I would like to express my gratitude to Professor Beresford N. Parlett for many helpful discussions and for the computer program he provided for finding eigensolutions of an undamped system by the Lanczos method.

I would like to thank Professor Edward L. Wilson for serving on my Dissertation Committee and reading this dissertation.

The last but not the least, I would like to thank my wife Wen-ling and all my family members for their unlimited love and understanding throughout my graduate studies at Berkeley.

This research was sponsored by Lawrence Livermore National Laboratory under Contract Number UCB Eng-6619 with the University of California, Berkeley. This support and the interest of Dr. G. L. Goudreau are gratefully acknowledged.

Table of Contents

Chapter 1
Introduction

1.1 Necessity of the study

In analyzing the dynamic response of linear structures, the equation of motion of a damped system can be expressed as

$$\mathbf{M}\,\ddot{\mathbf{q}}(t) + \mathbf{C}\,\dot{\mathbf{q}}(t) + \mathbf{K}\,\mathbf{q}(t) = \mathbf{f}(t) \tag{1.1.1}$$

where **M**, **C**, **K** are the n by n mass, damping, stiffness matrices respectively and $\ddot{\mathbf{q}}(t)$, $\dot{\mathbf{q}}(t)$, $\mathbf{q}(t)$ are the n by 1 acceleration, velocity, displacement vectors respectively.

A common practice for solving this problem starts with finding the normal modes of vibration of the corresponding undamped system, that is, solving the following eigenproblem

$$\mathbf{K}\,\boldsymbol{\psi} = \omega^2\,\mathbf{M}\,\boldsymbol{\psi} \tag{1.1.2}$$

where ω and $\boldsymbol{\psi}$ are the modal frequency and shape of the corresponding undamped system. From these modal quantities, a set of uncoupled equations of motion in terms of the normal coordinates of the system can be obtained. Each of these equations corresponds to one mode of vibration and can be solved individually. The effect of damping is taken into account by adding a term which represents the suitable modal damping ratio to these uncoupled equations. The response of the system is then obtained by superposing various modal contributions. This leads to the so-called *mode superposition method*.

The solution obtained in this way is exact only when the damping matrix **C** is *proportional*; that is, **C** is of such a form that it can be diagonalized by the same transformation that uncouples the undamped systems as shown in [C1]. When **C** is not proportional, the above method is still used frequently and the solution is taken as an approximation. This approximation may be close to the exact solution when damping is very small. For large damping and/or lumped damping, this type of approximation may not be appropriate.

Although the analysis for damped systems has been in the literature (e.g., [H2]) for years, its use is still limited for the following two major reasons : (1) Inclusion of the damping matrix in the mathematical model increases the cost disproportionately in solving the resulting eigenproblem; (2) Complex quantities are required during the solution process and the physical interpretation of these complex quantities is difficult to identify. In many circumstances, the effect of damping is important and thus must be included directly in the analysis in order to obtain a reliable solution. For example, in some structure-foundation systems, the damping matrix cannot be modeled well by the proportional terms only. In the control of some flexible systems such as robot arms and space structures, damping is introduced through passive systems and actuators which may be isolated at a few locations in the form of lumped dampers. To accommodate all these possibilities, one has to include the damping matrix into the model and analyze the system as a damped one. Therefore, this work is directed to studying Eq.(1.1.1) considering a nonproportional damping matrix **C** and to developing methods for efficient analysis of such systems.

1.2 Scope of the study

The present study is focused on viscously damped nongyroscopic systems, where the associated damping matrix is symmetric. To include situations where the source of damping comes only from lumped dampers, we allow the damping matrix to be low-ranked. Therefore, the damping matrix is positive semi-definite. In the dynamic analysis of undamped structures, the inertia of the nonessential degrees of freedom are often neglected to reduce the computational effort. As a consequence of this practice, the mass matrix **M** does not have full rank and the number of finite eigenvalues of the system is reduced to the rank of **M**. Because of the presence of the damping matrix **C**, the number of finite eigenvalues of a damped system is not apparent if the rank of **M** is less than the order n of the system. For the convenience of discussion, we assume that the symmetric mass matrix is full-ranked and thus positive-definite even though the algorithm developed can still be used to solve systems where **M** is not full-ranked. The stiffness matrix is symmetric and positive definite (or positive semi-definite if there exist rigid body modes).

In Chapter 2 some basic properties of the eigensolutions of a damped dynamic system are given. Emphasis is on the difference between a damped system and the corresponding undamped system. The second-order differential equation of motion given by Eq.(1.1.1) is reduced to a first-order one by doubling the size of the problem. This is a state equation approach in the context of control theory. The eigensolutions associated with the resulting linear system, represented by the pencil (**A**, **B**), have the desirable orthogonality property, which can be used for decoupling the equation of motion.

In Chapter 3 we discuss some theoretical bases for computing a small set of eigensolutions of a large dynamic system. To take advantage of the sparsity of the associated matrices, we focus on methods in which the system matrices are used only in forming matrix-vector multiplications and divisions. In this way, the symmetry and sparsity of the associated matrices are exploited to reduce the storage space and computational effort and thus to increase the size of the problem that can be handled by the program. The stationary property of the Rayleigh quotient, which is widely used in the analysis of $\omega^2 \mathbf{M} \psi = \mathbf{K} \psi$, is generalized for an indefinite matrix pencil (**A**, **B**). The projection method, which treats the problem from a geometric point of view, is also discussed as an alternative. Both provide a theoretical basis for the partial solution of a large eigenproblem.

In Chapter 4 the subspace iteration method is extended to extract the least dominant set of eigenpairs of a damped system. The iteration vectors are arranged in such a way that only real arithmetic is employed in dealing with complex vectors. Therefore, both the storage space and computational effort are reduced substantially for the extraction of the damped modes. In spite of this, the subspace iteration method for solving the damped system is still expensive compared to its use for solving the corresponding undamped problem. This is shown by examples.

In Chapter 5 we deduce a variant of the Lanczos algorithm that can be used to find the eigensolutions of the indefinite matrix pencil $(\mathbf{A}, \mathbf{B})$. The infamous phenomenon of loss of orthogonality between Lanczos vectors is discussed and a method to restore the orthogonality or semi-orthogonality by a full re-orthogonalization or a partial re-orthogonalization scheme respectively. The matrix pencil $(\mathbf{A}, \mathbf{B})$ is projected onto the subspace spanned by the Lanczos vectors to obtain a reduced tri-diagonal system. The solutions of this reduced system are the Rayleigh-Ritz approximation to the eigensolutions of $(\mathbf{A}, \mathbf{B})$. The quality of this approximation can be measured by a residual norm, which is readily obtained from the algorithm and requires no extra computational effort. The effectiveness and efficiency of the algorithm is shown by solving some numerical examples.

In Chapter 6 the eigenvectors are used to transform the original set of equations of motion into a set of uncoupled equations. A closed form solution to the uncoupled equation and its physical interpretation are given. A numerical method for solving the so-called *discrete time system* is also derived for practical use. A numerical example is shown to illustrate the mode superposition method for the analysis of a transient problem.

Summary and suggested future research are given in Chapter 7.

Chapter 2
Some Properties of Eigensolutions

2.1 Eigensolutions

The homogeneous form of equation (1.1.1) is simply

$$\mathbf{M}\,\ddot{\mathbf{q}}(t) + \mathbf{C}\,\dot{\mathbf{q}}(t) + \mathbf{K}\,\mathbf{q}(t) = \mathbf{0} \tag{2.1.1}$$

It possesses a solution of the type

$$\mathbf{q}(t) = e^{\lambda t}\,\mathbf{w} \tag{2.1.2}$$

where λ is the eigenvalue and $\mathbf{w}$ is the eigenvector of the system which are to be determined. Substituting this solution into Eq.(2.1.1), we obtain the characteristic equation

$$(\,\lambda^2\,\mathbf{M} + \lambda\,\mathbf{C} + \mathbf{K}\,)\,\mathbf{w} = \mathbf{0} \tag{2.1.3}$$

This is a quadratic eigenproblem and is computationally more complicated than the linear eigenproblem, which arises from an undamped system. A nontrivial solution exists if, and only if, the determinant of the coefficient matrix of Eq.(2.1.3) is zero; that is,

$$\det\,(\,\lambda^2\,\mathbf{M} + \lambda\,\mathbf{C} + \mathbf{K}\,) = 0 \tag{2.1.4}$$

If $\mathbf{M}$ is nonsingular, then the left side of Eq.(2.1.4) is a real polynomial of degree $2n$ in λ and hence the equation possesses $2n$ roots, although they are not necessarily all distinct. If some of these roots are complex, they occur in conjugate pairs. Therefore, the number of real roots is even. We can arrange these roots in either real pairs or complex conjugate pairs. For a real pair of eigenvalues, the associated eigenvectors are also a real pair. For a complex conjugate pair of eigenvalues, the associated eigenvectors are also a complex conjugate pair. For the purpose of discussion, we assume that there are nc complex conjugate pairs of eigensolutions and nr

real pairs of eigensolutions. We can arrange these eigenvalues as follows

$$\alpha_1\ ,\ \bar{\alpha}_1\ ,\ .\ .\ .\ .\ ,\ \alpha_{nc}\ ,\ \bar{\alpha}_{nc}\ ,\ \beta_1\ ,\ \hat{\beta}_1\ ,\ .\ .\ .\ ,\ \beta_{nr}\ ,\ \hat{\beta}_{nr} \tag{2.1.5}$$

where

$$\alpha_j = \alpha_{Rj} + \alpha_{Ij}\ i^* \qquad \bar{\alpha}_j = \alpha_{Rj} - \alpha_{Ij}\ i^* \tag{2.1.6a}$$

and

$$\beta_j \geq \hat{\beta}_j \tag{2.1.6b}$$

The corresponding eigenvectors are

$$\phi_1\ ,\ \bar{\phi}_1\ ,\ .\ .\ .\ .\ ,\ \phi_{nc}\ ,\ \bar{\phi}_{nc}\ ,\ \psi_1\ ,\ \hat{\psi}_1\ ,\ .\ .\ .\ .\ ,\ \psi_{nr}\ ,\ \hat{\psi}_{nr} \tag{2.1.7}$$

where

$$\phi_j = \phi_{Rj} + \phi_{Ij}\ i^* \qquad \bar{\phi}_j = \phi_{Rj} - \phi_{Ij}\ i^* \tag{2.1.8}$$

Here α_{Rj}, α_{Ij}, β_j and $\hat{\beta}_j$ are real-valued scalars, ϕ_{Rj}, ϕ_{Ij}, ψ_j and $\hat{\psi}_j$ are real-valued vectors, and i^* is the imaginary unit $\sqrt{-1}$. Note that the eigenpairs mentioned above have been arranged in the following order for the convenience of subsequent discussion

$$|\alpha_1| = |\bar{\alpha}_1| < |\alpha_2| = |\bar{\alpha}_2| <\ ,\ .\ .\ .\ .\ ,< |\alpha_{nc}| = |\bar{\alpha}_{nc}| \tag{2.1.9a}$$

$$|\beta_1| < |\beta_2| <\ ,\ .\ .\ .\ ,< |\beta_{nr}| \tag{2.1.9b}$$

We can define a damped system to be *stable*, *neutrally stable* or *unstable*. If the real parts of the eigenvalues are all negative, the system is stable; if the real parts of the eigenvalues include at least one zero and the rest negative, the system is neutrally stable; and if the real parts of the eigenvalues include at least one positive, the system is unstable. Note that for real eigenvalues the real part refers to the eigenvalues themselves.

With regard to the stability of a damped system, the following theorem gives us an *a priori* condition for the system to be at least neutrally stable.

Theorem 2.1 : If **M** is positive definite, **C** and **K** are positive semi-definite, then the associated damped system is stable or neutrally stable.

proof : Let λ and **w** be an eigenpair; i.e,

$$(\lambda^2 \mathbf{M} + \lambda \mathbf{C} + \mathbf{K}) \mathbf{w} = \mathbf{0} \tag{2.1.10}$$

Premultiplying the above by $\bar{\mathbf{w}}^T$ we have

$$m\lambda^2 + c\lambda + k = 0 \tag{2.1.11}$$

where $m = \bar{\mathbf{w}}^T \mathbf{M} \mathbf{w}$, a real scalar, and c, k defined similarly. Under the prescribed conditions, we have $m > 0$ and $c, k \geq 0$.

If **w** is complex, the real part of λ is

$$Re(\lambda) = \frac{-c}{2m} \leq 0 \tag{2.1.12}$$

If **w** is real, it follows by inspection of Eq.(2.1.11) that λ must be negative. This is because the left-hand side of Eq.(2.1.11) can only vanish if $\lambda \leq 0$. If zero λ's exist then $k = 0$ for some **w**, implying that **K** is singular under the prescribed conditions; conversely, if **K** is singular then there exists at least one zero λ. □

Since the dynamic systems we consider in this study satisfy the conditions prescribed in the above theorem, all the eigenvalues we find in this study lie in the left-half of the complex plane or the imaginary axis. That is, all α_{Rj}, β_j, and $\hat{\beta}_j$ are either negative or zero.

2.2 Modal quantities

In the analysis of an undamped dynamic system, the eigenvectors, i.e., the solutions of Eq.(1.1.2), are used to decouple the equation of motion. Each of the resulting decoupled equations corresponds to a vibration mode and can be treated individually. These decoupled equations, called modal equations, can be looked upon as a set of independent single degree-of-freedom, SDOF, systems. The knowledge of a typical SDOF system can be applied directly to any of the modal equations and the behavior of the system can be easily understood by studying the set of SDOF systems. Unfortunately, the eigenvectors of a damped system, i.e., the solutions listed in Eq.(2.1.5), do not decouple the equation of motion Eq.(1.1.1) since they do not simultaneously diagonalize **M**, **C** and **K**, as will be shown later. Although the eigenvectors of a damped system do not diagonalize the associated matrices of the damped system, they are related to the modal quantities, such as modal mass, damping and stiffness. We want to show in the following how the eigenvectors of a damped system are related to the modal quantities. This relation gives insight into the behavior of the damped dynamic system. We begin by showing the characteristics of vibration contained in a typical SDOF damped system.

For a SDOF damped dynamic system, the characteristic equation can be represented by a quadratic equation as

$$m\lambda^2 + c\lambda + k = 0 \qquad (2.2.1)$$

where m, c and k is the associated (modal) mass, damping and stiffness. For this system, the critical damping is $2(km)^{\frac{1}{2}}$ and the damping ratio is

$$\xi = \frac{c}{2(km)^{\frac{1}{2}}} \qquad (2.2.2)$$

Depending on the magnitude of the damping ratio, the solution of Eq.(2.2.1) falls into one of the following three cases :

(1) Underdamped case ($0 < \xi < 1$)

We have roots twinned in complex conjugate pairs

$$\lambda = -\xi\omega \pm \tilde{\omega}\, \mathrm{i}^* \qquad (2.2.3)$$

where ω is the undamped frequency and $\tilde{\omega}$ is the damped frequency, given by

$$\omega = \left(\frac{k}{m}\right)^{\frac{1}{2}} \qquad \tilde{\omega} = \omega(1 - \xi^2)^{\frac{1}{2}} \qquad (2.2.4)$$

(2) Critically damped case ($\xi = 1$)

We have negative double roots

$$\lambda = -\omega \tag{2.2.5}$$

(3) Overdamped case ($\xi > 1$)

We have two different negative real roots

$$\lambda = -\xi\omega \pm \omega(\xi^2 - 1)^{\frac{1}{2}} \tag{2.2.6}$$

The underdamped solution of Eq.(2.2.3) corresponds to α and $\bar{\alpha}$ while the overdamped solution of Eq.(2.2.6) corresponds to β and $\hat{\beta}$ according to the notation introduced in the last section. Note that β, the *primary* root, is the one with the plus sign in Eq.(2.2.6) while $\hat{\beta}$, the *secondary* root, is the one with the minus sign in accordance with our convention. Since the critically damped case can be viewed as a special example of the overdamped case and solutions of both cases are real-valued, we combine them together and call them overdamped case in future discussions for the sake of simplicity.

For a general n DOF damped dynamic system, there are n pairs of eigensolutions as described in the last section. In these n pairs of eigensolutions, each complex conjugate pair corresponds to an underdamped mode of vibration and each real pair corresponds to an overdamped mode of vibration. For any pair of eigenvectors $(\lambda, \mathbf{w})$ and $(\tilde{\lambda}, \tilde{\mathbf{w}})$, either complex or real, we define $\tilde{\mathbf{w}}^T \mathbf{M} \mathbf{w}$, $\tilde{\mathbf{w}}^T \mathbf{C} \mathbf{w}$ and $\tilde{\mathbf{w}}^T \mathbf{K} \mathbf{w}$ as the *modal mass*, *modal damping* and *modal stiffness* of this mode since they represent the three real-valued coefficients of a quadratic equation like Eq.(2.2.1) and the solutions of the quadratic equation are the eigenvalues λ and $\tilde{\lambda}$. To justify this claim, we demonstrate in the following both the complex case and the real case.

For a complex pair of solutions represented by $(\alpha, \boldsymbol{\phi})$ and $(\bar{\alpha}, \bar{\boldsymbol{\phi}})$, we can pre-multiply their characteristic equations $\alpha^2 \mathbf{M} \boldsymbol{\phi} + \alpha \mathbf{C} \boldsymbol{\phi} + \mathbf{K} \boldsymbol{\phi} = \mathbf{0}$ and $\bar{\alpha}^2 \mathbf{M} \bar{\boldsymbol{\phi}} + \bar{\alpha} \mathbf{C} \bar{\boldsymbol{\phi}} + \mathbf{K} \bar{\boldsymbol{\phi}} = \mathbf{0}$ by $\bar{\boldsymbol{\phi}}^T$ and $\boldsymbol{\phi}^T$, respectively, to obtain

$$\alpha^2\, \bar{\phi}^T \mathbf{M}\, \phi + \alpha\, \bar{\phi}^T \mathbf{C}\, \phi + \bar{\phi}^T \mathbf{K}\, \phi = 0 \tag{2.2.7a}$$

and

$$\bar{\alpha}^2\, \phi^T \mathbf{M}\, \bar{\phi} + \bar{\alpha}\, \phi^T \mathbf{C}\, \bar{\phi} + \phi^T \mathbf{K}\, \bar{\phi} = 0 \tag{2.2.7b}$$

Here we observe that $\bar{\phi}^T \mathbf{M}\, \phi = \phi^T \mathbf{M}\, \bar{\phi}$, $\bar{\phi}^T \mathbf{C}\, \phi = \phi^T \mathbf{C}\, \bar{\phi}$ and $\bar{\phi}^T \mathbf{K}\, \phi = \phi^T \mathbf{K}\, \bar{\phi}$ are merely three real-valued scalars. The α and $\bar{\alpha}$ are simply the solutions to a quadratic equation of the form given by Eq.(2.2.1) with the three scalars as coefficients. Therefore, the definition of $\bar{\phi}^T \mathbf{M}\, \phi$, $\bar{\phi}^T \mathbf{C}\, \phi$ and $\bar{\phi}^T \mathbf{K}\, \phi$ as the *modal mass*, *damping* and *stiffness* of this underdamped mode is justified. Other modal quantities associated with this mode, such as critical damping, damping ratio, undamped frequency and damped frequency, can be easily constructed from the modal mass, damping, and stiffness. For the purpose of discussion, we call Eq.(2.2.7) *damped modal equation* associated with (α, ϕ) and $(\bar{\alpha}, \bar{\phi})$, although it should be emphasized that these damped modal equations do not form a set of independent SDOF systems as in the analysis of an undamped system because the eigenvectors of the damped system do not uncouple the equation of motion.

Remark 2.2.1 If we set the damping matrix $\mathbf{C}$ of a damped system equal to zero and call the resulting system the *corresponding undamped system*, then the modal mass and stiffness of the damped system will be different from those of the corresponding undamped system in general. Consequently, the undamped frequencies of the damped system are different from the frequencies of the corresponding undamped system. Hence, one must be careful to avoid this ambiguity. □

For a real pair eigensolutions (β, ψ) and $(\hat{\beta}, \hat{\psi})$, we can perform a similar manipulation to obtain

$$\beta^2\, \hat{\psi}^T \mathbf{M}\, \psi + \beta\, \hat{\psi}^T \mathbf{C}\, \psi + \hat{\psi}^T \mathbf{K}\, \psi = 0 \tag{2.2.8a}$$

and

$$\hat{\beta}^2\, \psi^T \mathbf{M}\, \hat{\psi} + \hat{\beta}\, \psi^T \mathbf{C}\, \hat{\psi} + \psi^T \mathbf{K}\, \hat{\psi} = 0 \tag{2.2.8b}$$

It follows from a similar argument that $\hat{\psi}^{\mathrm{T}}\, \mathbf{M}\, \psi = \psi^{\mathrm{T}}\, \mathbf{M}\, \hat{\psi}$, $\hat{\psi}^{\mathrm{T}}\, \mathbf{C}\, \psi = \psi^{\mathrm{T}}\, \mathbf{C}\, \hat{\psi}$, and $\hat{\psi}^{\mathrm{T}}\, \mathbf{K}\, \psi = \psi^{\mathrm{T}}\, \mathbf{K}\, \hat{\psi}$ are the *modal mass, damping,* and *stiffness* respectively for this overdamped mode and Eq.(2.2.8) is the damped modal equation of the system associated with (β, ψ) and $(\hat{\beta}, \hat{\psi})$.

Remark 2.2.2 If one applies the decoupling procedure used in the analysis of an undamped dynamic system, the following equation will be obtained

$$\lambda^2\, \psi^{\mathrm{T}}\, \mathbf{M}\, \psi + \lambda\, \psi^{\mathrm{T}}\, \mathbf{C}\, \psi + \psi^{\mathrm{T}}\, \mathbf{K}\, \psi = 0 \qquad (2.2.9)$$

Note that one root of the equation is β while the other is not an eigenvalue of the system. A similar conclusion is reached if ψ is replaced by $\hat{\psi}$ in the equation. Therefore, neither $\psi^{\mathrm{T}}\mathbf{M}\psi$ nor $\hat{\psi}^{\mathrm{T}}\mathbf{M}\hat{\psi}$ can be called modal mass; neither $\psi^{\mathrm{T}}\mathbf{C}\psi$ nor $\hat{\psi}^{\mathrm{T}}\mathbf{C}\hat{\psi}$ can be called modal damping; neither $\psi^{\mathrm{T}}\mathbf{K}\psi$ nor $\hat{\psi}^{\mathrm{T}}\mathbf{K}\hat{\psi}$ can be called modal stiffness; and Eq.(2.2.9) is not a damped modal equation. □

Proportionally damped system. When the damping of the system is proportional, every pair of eigenvectors, both complex conjugate pairs and real pairs, degenerates into a real multiple vector. That is, all $\phi_{\mathrm{I}j}$ are zero so that all $\overline{\phi}_j$ are equal to ϕ_j; and all $\hat{\psi}_j$ coincide with ψ_j. Therefore, there are only n independent real eigenvectors, i.e., $\mathbf{w}_1, \mathbf{w}_2, \ldots, \mathbf{w}_n$. These eigenvectors are the same as those obtained by solving $\lambda^2\, \mathbf{M}\, \mathbf{w} = \mathbf{K}\, \mathbf{w}$. That is, the eigenvectors of a proportionally damped system coincide with the eigenvectors of the corresponding undamped system. Since both $\mathbf{M}$ and $\mathbf{K}$ are symmetric, these eigenvectors are orthogonal with respect to $\mathbf{M}$ and $\mathbf{K}$ and also with respect to $\mathbf{C}$ because of proportionality. In other words, we have for i and j from 1 to n

$$\mathbf{w}_i^{\mathrm{T}}\, \mathbf{M}\, \mathbf{w}_j = \delta_{ij}\, m_j \qquad (2.2.10a)$$

$$\mathbf{w}_i^{\mathrm{T}}\, \mathbf{C}\, \mathbf{w}_j = \delta_{ij}\, c_j \qquad (2.2.10b)$$

$$\mathbf{w}_i^{\mathrm{T}}\, \mathbf{K}\, \mathbf{w}_j = \delta_{ij}\, k_j \qquad (2.2.10c)$$

where m_j, c_j and k_j are the modal mass, damping and stiffness of the j^{th} mode in consideration. If we substitute $\mathbf{w}_j$ for $\mathbf{w}$ into $(\lambda^2 \mathbf{M} + \lambda \mathbf{C} + \mathbf{K})\mathbf{w} = \mathbf{0}$; i.e., we consider the system vibrating in the j^{th} mode, then we can pre-multiply the systems of equation by $\mathbf{w}_j^{\mathrm{T}}$ to obtain the j^{th} modal equation

$$m_j\lambda^2 + c_j\lambda + k_j = 0 \tag{2.2.11}$$

which is of the form given by Eq.(2.2.1). Notice that the undamped frequencies of this proportionally damped system are the same as the frequencies of the corresponding undamped system. This is because the modal mass and stiffness of the proportionally damped system are the same as those of the corresponding undamped system. Due to this property, we can solve a proportionally damped system by the simplified method, where we analyze the corresponding undamped system first to obtain the modal mass and stiffness and then add an arbitrary amount of modal damping or the equivalent damping ratio into the solution process.

Example 2.1 : A test problem is demonstrated here to show the solution of a damped system. The system is a 3 DOF mass-damper-spring system as shown in Figure 2.1. The mass, damping, and stiffness matrices are represented by

$$\mathbf{M} = \begin{bmatrix} 1 & 0 & 0 \\ 0 & 1 & 0 \\ 0 & 0 & 1 \end{bmatrix}$$

$$\mathbf{C} = \begin{bmatrix} 8 & -5 & 0 \\ -5 & 10 & -5 \\ 0 & -5 & 8 \end{bmatrix} \cdot 10$$

$$\mathbf{K} = \begin{bmatrix} 2 & -1 & 0 \\ -1 & 2 & -1 \\ 0 & -1 & 2 \end{bmatrix} \cdot 10^3$$

The eigenvalues and eigenvectors are

$$\begin{bmatrix} \alpha_{R1} & \alpha_{I1} \\ \alpha_{R2} & \alpha_{I2} \\ \beta_1 & \hat{\beta}_1 \end{bmatrix} = \begin{bmatrix} -0.95179046d+01 & -0.22557552d+02 \\ -0.40000000d+02 & -0.20000000d+02 \\ -0.24438497d+02 & -0.13652569d+03 \end{bmatrix}$$

$$[\,\phi_{R1}\ \phi_{I1}\ \phi_{R2}\ \phi_{I2}\ \psi_1\ \hat{\psi}_1\,] =$$

0.7726e+00	-0.7974e-01	-0.1000e+01	0.1672e-13	-0.3456e+00	-0.5996e+00
0.1000e+01	0.0000e+00	0.6887e-13	0.4185e-13	0.1000e+01	0.1000e+01
0.7726e+00	-0.7974e-01	0.1000e+01	0.6939e-17	-0.3456e+00	-0.5996e+00

We can plot the components of an eigenvector on a complex plane with the *x*-axis as the real axis and the *y*-axis as the imaginary axis. This plot, known as a *phasor* diagram, shows immediately how much phase difference there is among the components in the damped mode. For example, the components of an eigenvector of a proportionally damped system are either in-phase or 180 degree out-of-phase; therefore, the phasor is only a straight line. Figure 2.2 shows the phasors of the two underdamped modes of the 3 DOF damped system. Note that the second pair of eigenvectors are real; therefore, the phasor of the second mode is a straight line. This indicates that the second mode is actually a proportionally damped mode, which is due to the special symmetry of the system. In general, the phasors of a damped system will not be straight lines.

To check whether the eigenvectors diagonalize **M**, **C** or **K**, we form the following weighted inner products

$$[\,\phi_{R1}\ \phi_{I1}\ \phi_{R2}\ \phi_{I2}\ \psi_1\ \hat{\psi}_1\,]^T\,\mathbf{M}\,[\,\phi_{R1}\ \phi_{I1}\ \phi_{R2}\ \phi_{I2}\ \psi_1\ \hat{\psi}_1\,] =$$

0.2194e+01	-0.1232e+00	0.1073e-12	0.5477e-13	0.4660e+00	0.7354e-01
-0.1232e+00	0.1272e-01	0.3959e-14	-0.1334e-14	0.5512e-01	0.9562e-01
0.1073e-12	0.3959e-14	0.2000e+01	-0.1672e-13	0.9902e-13	0.4621e-12
0.5477e-13	-0.1334e-14	-0.1672e-13	0.2031e-26	0.3607e-13	0.3182e-13
0.4660e+00	0.5512e-01	0.9902e-13	0.3607e-13	0.1239e+01	0.1414e+01
0.7354e-01	0.9562e-01	0.4621e-12	0.3182e-13	0.1414e+01	0.1719e+01

$$[\,\phi_{R1}\ \phi_{I1}\ \phi_{R2}\ \phi_{I2}\ \psi_1\ \hat{\psi}_1\,]^T\, \mathbf{C}\, [\,\phi_{R1}\ \phi_{I1}\ \phi_{R2}\ \phi_{I2}\ \psi_1\ \hat{\psi}_1\,] =$$

0.4099e+02	-0.1883e+01	0.1781e-11	0.1149e-11	0.1458e+02	0.8583e+01
-0.1883e+01	0.1017e+01	0.8660e-12	0.2270e-12	0.1238e+02	0.1562e+02
0.1783e-11	0.8659e-12	0.1600e+03	-0.1337e-11	0.8823e-11	0.3962e-10
0.1149e-11	0.2270e-12	-0.1337e-11	0.1275e-24	0.4332e-11	0.5055e-11
0.1458e+02	0.1238e+02	0.8823e-11	0.4332e-11	0.1882e+03	0.2277e+03
0.8583e+01	0.1562e+02	0.3962e-10	0.5055e-11	0.2277e+03	0.2774e+03

$$[\,\phi_{R1}\ \phi_{I1}\ \phi_{R2}\ \phi_{I2}\ \psi_1\ \hat{\psi}_1\,]^T\, \mathbf{K}\, [\,\phi_{R1}\ \phi_{I1}\ \phi_{R2}\ \phi_{I2}\ \psi_1\ \hat{\psi}_1\,] =$$

0.1297e+04	-0.8695e+02	0.5105e-10	0.2815e-10	0.7801e+02	-0.1989e+03
-0.8695e+02	0.2543e+02	0.1890e-10	0.4006e-11	0.2697e+03	0.3507e+03
0.5102e-10	0.1890e-10	0.4000e+04	-0.3343e-10	0.1885e-09	0.9497e-09
0.2815e-10	0.4006e-11	-0.3343e-10	0.2661e-23	0.8433e-10	0.9708e-10
0.7801e+02	0.2697e+03	0.1885e-09	0.8433e-10	0.3860e+04	0.4719e+04
-0.1989e+03	0.3507e+03	0.9497e-09	0.9708e-10	0.4719e+04	0.5836e+04

It is readily seen that none of **M**, **C** and **K** is diagonalized by the eigenvectors. From the above weighted inner products, we also can calculate the weighted inner product between eigenvectors. For example,

$$\begin{aligned}
&\psi_1^T\, \mathbf{K}\, \phi_1 \\
&= \psi_1^T\, \mathbf{K}\, [\phi_{R1} + \phi_{I1}\, i^*] \\
&= (\psi_1^T\, \mathbf{K}\, \phi_{R1}) + (\psi_1^T\, \mathbf{K}\, \phi_{I1})\, i^* \\
&= 78.01 + 269.7\, i^*
\end{aligned}$$

In this way, we can obtain the modal mass, damping and stiffness of a particular mode and verify that the solutions of the modal equation are indeed the eigenvalues of the corresponding mode. □

From the above discussion and the example, it is clear that the modal quantities, which characterize the motion of a damped system, can still be constructed from the **M**, **C**, **K** matrices and their eigenvectors. But these eigenvectors are not orthogonal to one another with respect to the **M**, **C** or **K** of a generally damped system. The fact that a n degrees of freedom system can only have exactly n independent vectors to span the whole space should rule out the possibility that these $2n$ eigenvectors can be orthogonal to one another with respect to **M**, **C** or **K**. Accordingly, the equation of motion of a damped system cannot be decoupled by its eigenvectors. To decouple the equations of motion, another approach, described in the next section, is needed.

2.3 Reduced form of the equation of motion

The solution $\mathbf{q}(t)$ of Eq.(1.1.1) can be interpreted geometrically by conceiving an n-dimensional Euclidean space with $q_1, \ldots, q_n$ as axes. This space, known as the *configuration space*, is not very convenient for a geometric representation of the motion because a given point in the configuration space is not enough to define the state of the system uniquely. If we use the generalized velocities $\dot{\mathbf{q}}(t)$ as a set of auxiliary variables, the motion can be described in a $2n$-dimensional Euclidean space spanned by $q_1, \ldots, q_n, \dot{q}_1, \ldots, \dot{q}_n$ known as the *state space*. The vector

$$\mathbf{x}(t) = \begin{Bmatrix} \mathbf{q}(t) \\ \dot{\mathbf{q}}(t) \end{Bmatrix} \tag{2.3.1}$$

is thus called a *state vector* and the tip of this vector traces a *trajectory* in the state space, depicting the manner in which the solution evolves with time. The advantage of this representation in the state space is that two trajectories never intersect, so that a given point in the state space corresponds to a unique trajectory.

From a computational point of view, it is also convenient to use the state vector representation. In particular, by combining Eq.(1.1.1) with the matrix identity

$$\mathbf{M}\,\dot{\mathbf{q}}(t) - \mathbf{M}\,\dot{\mathbf{q}}(t) = \mathbf{0} \tag{2.3.2}$$

we have

$$\begin{bmatrix} \mathbf{C} & \mathbf{M} \\ \mathbf{M} & \mathbf{0} \end{bmatrix} \begin{Bmatrix} \dot{\mathbf{q}}(t) \\ \ddot{\mathbf{q}}(t) \end{Bmatrix} - \begin{bmatrix} -\mathbf{K} & \mathbf{0} \\ \mathbf{0} & \mathbf{M} \end{bmatrix} \begin{Bmatrix} \mathbf{q}(t) \\ \dot{\mathbf{q}}(t) \end{Bmatrix} = \begin{Bmatrix} \mathbf{f}(t) \\ \mathbf{0} \end{Bmatrix} \tag{2.3.3}$$

or alternatively, by combining Eq.(1.1.1) with the matrix identity

$$\mathbf{K}\,\dot{\mathbf{q}}(t) - \mathbf{K}\,\dot{\mathbf{q}}(t) = \mathbf{0} \tag{2.3.4}$$

we have

$$\begin{bmatrix} \mathbf{K} & \mathbf{0} \\ \mathbf{0} & -\mathbf{M} \end{bmatrix} \begin{Bmatrix} \dot{\mathbf{q}}(t) \\ \ddot{\mathbf{q}}(t) \end{Bmatrix} - \begin{bmatrix} \mathbf{0} & \mathbf{K} \\ \mathbf{K} & \mathbf{C} \end{bmatrix} \begin{Bmatrix} \mathbf{q}(t) \\ \dot{\mathbf{q}}(t) \end{Bmatrix} = \begin{Bmatrix} \mathbf{0} \\ -\mathbf{f}(t) \end{Bmatrix} \tag{2.3.5}$$

Note that both Eq.(2.3.3) and Eq.(2.3.5) can be represented by the following linear system

$$\mathbf{A}\,\dot{\mathbf{x}}(t) - \mathbf{B}\,\mathbf{x}(t) = \mathbf{y}(t) \tag{2.3.6}$$

That is, using a state vector approach, we can reduce a system of n second-order equations to a system of $2n$ first-order equations. Accordingly, Eq.(2.3.3) or (2.3.5) is referred to as the *reduced* form of Eq.(1.1.1). Note that if **M**, **C** and **K** are symmetric; then **A** and **B** are also symmetric although neither is positive-definite.

The homogeneous form of the reduced equation of motion is simply

$$\mathbf{A}\,\dot{\mathbf{x}}(t) - \mathbf{B}\,\mathbf{x}(t) = \mathbf{0} \tag{2.3.7}$$

and its solution is of the form

$$\mathbf{x}\,(t) = e^{\lambda t}\,\mathbf{z} \tag{2.3.8}$$

To relate this solution to the solution given by Eq.(2.1.2), we substitute $\mathbf{q}(t) = e^{\lambda t}\,\mathbf{w}$ and $\dot{\mathbf{q}}(t) = e^{\lambda t}\,\lambda\mathbf{w}$ into Eq.(2.3.1) to obtain

$$\mathbf{x}(t) = \begin{Bmatrix} \mathbf{q}(t) \\ \dot{\mathbf{q}}(t) \end{Bmatrix} = e^{\lambda t} \begin{Bmatrix} \mathbf{w} \\ \lambda\mathbf{w} \end{Bmatrix} \tag{2.3.9}$$

Thus, the λ in Eq.(2.3.8) is the same as the λ in Eq.(2.1.2) and the $\mathbf{z}$ is related to the $\mathbf{w}$ by

$$\mathbf{z} = \begin{Bmatrix} \mathbf{w} \\ \lambda \mathbf{w} \end{Bmatrix} \tag{2.3.10}$$

Substituting the solution given by Eq.(2.3.8) into $\mathbf{A}\,\dot{\mathbf{x}}(t) - \mathbf{B}\,\mathbf{x}(t) = \mathbf{0}$, we obtain the following characteristic equation

$$\lambda\,\mathbf{A}\,\mathbf{z} = \mathbf{B}\,\mathbf{z} \tag{2.3.11}$$

which represents a linear generalized eigenproblem. The solution to this equation can be found using a QZ algorithm. The software package RGG from the EISPACK library [E1] can be used to perform this task. It is also possible to arrange the associated eigenproblem in standard form. If Eq.(2.3.11) originates from Eq.(2.3.3), we form $\mathbf{B}^{-1}\,\mathbf{A}\,\mathbf{z} = \dfrac{1}{\lambda}\mathbf{z}$, i.e.,

$$\begin{bmatrix} -\mathbf{K}^{-1}\mathbf{C} & -\mathbf{K}^{-1}\mathbf{M} \\ \mathbf{I} & \mathbf{0} \end{bmatrix} \mathbf{z} = \frac{1}{\lambda}\mathbf{z} \tag{2.3.12}$$

where we have assumed that $\mathbf{K}$ is nonsingular. The case where $\mathbf{K}$ is singular will be considered in Section 3.1. If Eq.(2.3.11) originates from Eq.(2.3.5), we form $\mathbf{A}^{-1}\,\mathbf{B}\,\mathbf{z} = \lambda\,\mathbf{z}$, i.e.,

$$\begin{bmatrix} \mathbf{0} & \mathbf{I} \\ -\mathbf{M}^{-1}\mathbf{K} & -\mathbf{M}^{-1}\mathbf{C} \end{bmatrix} \mathbf{z} = \lambda\,\mathbf{z} \tag{2.3.13}$$

Eq.(2.3.12), which uses the inverse of the stiffness matrix, is called the KI form; while Eq.(2.3.13), which uses the inverse of mass matrix, is called the MI form. The KI form and MI form are equivalent and either can be used to solve for the eigensolutions by a QR algorithm. The software package RG from the EISPACK library [E1] can be used for this purpose. Note that the KI form can readily be used to find the least dominant eigenpair of the system by the vector iteration method;

therefore, the matrix in Eq.(2.3.12), which plays a role similar to the dynamic matrix $\mathbf{K}^{-1}\mathbf{M}$ does in the analysis of an undamped system, is called the *damped dynamic matrix* and is represented by $\mathbf{D}$ for use in the subsequent discussion.

The λ's obtained from solving $\lambda\, \mathbf{A}\, \mathbf{z} = \mathbf{B}\, \mathbf{z}$ are the same as the λ's obtained from solving $(\lambda^2 \mathbf{M} + \lambda\, \mathbf{C} + \mathbf{K})\, \mathbf{w} = \mathbf{0}$, so they can still be arranged as in Eq.(2.1.5). The $\mathbf{z}$'s are related to the $\mathbf{w}$'s as given by Eq.(2.3.10). We can express them as the following :

$$\boldsymbol{\Phi}_1 , \bar{\boldsymbol{\Phi}}_1 , \ldots , \boldsymbol{\Phi}_{nc} , \bar{\boldsymbol{\Phi}}_{nc} , \boldsymbol{\Psi}_1 , \hat{\boldsymbol{\Psi}}_1 , \ldots , \boldsymbol{\Psi}_{nr} , \hat{\boldsymbol{\Psi}}_{nr} \qquad (2.3.14)$$

with

$$\boldsymbol{\Phi}_j = \boldsymbol{\Phi}_{\mathrm{R}j} + \boldsymbol{\Phi}_{\mathrm{I}j}\, \mathrm{i}^* \qquad \bar{\boldsymbol{\Phi}}_j = \boldsymbol{\Phi}_{\mathrm{R}j} - \boldsymbol{\Phi}_{\mathrm{I}j}\, \mathrm{i}^* \qquad (2.3.15)$$

where a direct substitution would give

$$\boldsymbol{\Phi}_{\mathrm{R}j} = \begin{Bmatrix} \boldsymbol{\phi}_{\mathrm{R}j} \\ \alpha_{\mathrm{R}j} \boldsymbol{\phi}_{\mathrm{R}j} - \alpha_{\mathrm{I}j} \boldsymbol{\phi}_{\mathrm{I}j} \end{Bmatrix} \qquad \boldsymbol{\Phi}_{\mathrm{I}j} = \begin{Bmatrix} \boldsymbol{\phi}_{\mathrm{I}j} \\ \alpha_{\mathrm{R}j} \boldsymbol{\phi}_{\mathrm{I}j} + \alpha_{\mathrm{I}j} \boldsymbol{\phi}_{\mathrm{R}j} \end{Bmatrix} (2.3.16)$$

and

$$\boldsymbol{\Psi}_j = \begin{Bmatrix} \boldsymbol{\psi}_j \\ \beta_j \boldsymbol{\psi}_j \end{Bmatrix} \qquad \hat{\boldsymbol{\Psi}}_j = \begin{Bmatrix} \hat{\boldsymbol{\psi}}_j \\ \hat{\beta}_j \hat{\boldsymbol{\psi}}_j \end{Bmatrix} \qquad (2.3.17)$$

2.4 Orthogonality properties

Since both $\mathbf{A}$ and $\mathbf{B}$ are symmetric due to the way we reduce the second-order system into a first-order system, we have the desirable property that the eigenvectors are orthogonal with respect to both $\mathbf{A}$ and $\mathbf{B}$. More precisely, for any two eigenvectors $\mathbf{z}_j$ and $\mathbf{z}_k$ whose associated eigenvalues are different, we have

$$\mathbf{z}_j^{\mathrm{T}}\, \mathbf{A}\, \mathbf{z}_k = 0 \qquad \text{and} \qquad \mathbf{z}_j^{\mathrm{T}}\, \mathbf{B}\, \mathbf{z}_k = 0 \qquad (2.4.1)$$

Here, we notice that neither is a *proper* orthogonality relation because $\mathbf{A}$ and $\mathbf{B}$ are indefinite so that $\mathbf{u}^{\mathrm{T}}\, \mathbf{A}\, \mathbf{u} = 0$ for some nonzero vectors $\mathbf{u}$, i.e., $\mathbf{u}$ is orthogonal to itself.

The eigenvectors associated with underdamped modes are complex. To avoid the complex arithmetic, we express the orthogonality relationships in terms of the real and imaginary parts of the complex eigenvectors. Introducing the different eigenvectors into the first of Eq.(2.4.1), we obtain the following possible conditions

$$(\boldsymbol{\Phi}_{\mathrm{R}j} + \boldsymbol{\Phi}_{\mathrm{I}j}\, \mathrm{i}^*)^{\mathrm{T}} \mathbf{A} (\boldsymbol{\Phi}_{\mathrm{R}k} + \boldsymbol{\Phi}_{\mathrm{I}k}\, \mathrm{i}^*) = 0 \tag{2.4.2}$$

$$(\boldsymbol{\Phi}_{\mathrm{R}j} - \boldsymbol{\Phi}_{\mathrm{I}j}\, \mathrm{i}^*)^{\mathrm{T}} \mathbf{A} (\boldsymbol{\Phi}_{\mathrm{R}k} + \boldsymbol{\Phi}_{\mathrm{I}k}\, \mathrm{i}^*) = 0 \tag{2.4.3}$$

$$\boldsymbol{\Psi}_j^{\mathrm{T}} \mathbf{A} (\boldsymbol{\Phi}_{\mathrm{R}k} + \boldsymbol{\Phi}_{\mathrm{I}k}\, \mathrm{i}^*) = 0 \tag{2.4.4}$$

$$\hat{\boldsymbol{\Psi}}_j^{\mathrm{T}} \mathbf{A} (\boldsymbol{\Phi}_{\mathrm{R}k} + \boldsymbol{\Phi}_{\mathrm{I}k}\, \mathrm{i}^*) = 0 \tag{2.4.5}$$

Solving Eqs.(2.4.2) and (2.4.3) simultaneously and noting that both real and imaginary parts must vanish separately, we obtain

$$\boldsymbol{\Phi}_{\mathrm{R}j}^{\mathrm{T}} \mathbf{A} \boldsymbol{\Phi}_{\mathrm{R}k} = 0 \qquad \boldsymbol{\Phi}_{\mathrm{I}j}^{\mathrm{T}} \mathbf{A} \boldsymbol{\Phi}_{\mathrm{I}k} = 0 \tag{2.4.6}$$

$$\boldsymbol{\Phi}_{\mathrm{R}j}^{\mathrm{T}} \mathbf{A} \boldsymbol{\Phi}_{\mathrm{I}k} = 0 \qquad \boldsymbol{\Phi}_{\mathrm{I}j}^{\mathrm{T}} \mathbf{A} \boldsymbol{\Phi}_{\mathrm{R}k} = 0 \tag{2.4.7}$$

Similarly, we obtain from Eq.(2.4.4) and Eq.(2.4.5)

$$\boldsymbol{\Psi}_j^{\mathrm{T}} \mathbf{A} \boldsymbol{\Phi}_{\mathrm{R}k} = 0 \qquad \boldsymbol{\Psi}_j^{\mathrm{T}} \mathbf{A} \boldsymbol{\Phi}_{\mathrm{I}k} = 0 \tag{2.4.8}$$

$$\hat{\boldsymbol{\Psi}}_j^{\mathrm{T}} \mathbf{A} \boldsymbol{\Phi}_{\mathrm{R}k} = 0 \qquad \hat{\boldsymbol{\Psi}}_j^{\mathrm{T}} \mathbf{A} \boldsymbol{\Phi}_{\mathrm{I}k} = 0 \tag{2.4.9}$$

Eqs.(2.4.6), (2.4.7), (2.4.8) and (2.4.9) express the orthogonality property of the eigenvectors in terms of their real and imaginary parts. These relationships are developed with **A** as the weighting matrix. It is clear that the same relationships hold if we replace **A** by **B** as the weighting matrix.

Scaling of eigenvectors. We assume that the eigenvectors of the system considered is such that $\mathbf{z}_j^{\mathrm{T}} \mathbf{A}\, \mathbf{z}_j \neq 0$. For convenience, we scale the eigenvectors such that

$$\mathbf{z}_j^{\mathrm{T}} \mathbf{A}\, \mathbf{z}_j = 1 \qquad \mathbf{z}_j^{\mathrm{T}} \mathbf{B}\, \mathbf{z}_j = \lambda_j \tag{2.4.10}$$

For overdamped modes, it simply is

$$\boldsymbol{\Psi}_j^{\mathrm{T}} \mathbf{A} \boldsymbol{\Psi}_j = 1 \qquad \boldsymbol{\Psi}_j^{\mathrm{T}} \mathbf{B} \boldsymbol{\Psi}_j = \beta_j \tag{2.4.11}$$

Since neither **A** or **B** is positive-definite, it is not always possible to obtain Eq.(2.4.11) using real vectors. As a result, we may use the following alternative to avoid pure imaginary vectors.

$$\boldsymbol{\Psi}_j^{\mathrm{T}} \mathbf{A} \boldsymbol{\Psi}_j = \delta_j \qquad \boldsymbol{\Psi}_j^{\mathrm{T}} \mathbf{B} \boldsymbol{\Psi}_j = \delta_j \, \beta_j \tag{2.4.12}$$

where δ_j is either 1 or -1.

For underdamped modes, it is possible to simplify the expression in terms of the real and imaginary parts of the complex eigenvectors using $\boldsymbol{\Phi}_{\mathrm{R}j} \mathrm{i}^* + \boldsymbol{\Phi}_{\mathrm{I}j}$ to substitute for $\mathbf{z}_j$ in Eq.(2.4.10) and expanding it :

$$\boldsymbol{\Phi}_{\mathrm{R}j}^{\mathrm{T}} \mathbf{A} \boldsymbol{\Phi}_{\mathrm{R}j} - \boldsymbol{\Phi}_{\mathrm{I}j}^{\mathrm{T}} \mathbf{A} \boldsymbol{\Phi}_{\mathrm{I}j} = 1 \tag{2.4.13}$$

$$\boldsymbol{\Phi}_{\mathrm{R}j}^{\mathrm{T}} \mathbf{A} \boldsymbol{\Phi}_{\mathrm{I}j} + \boldsymbol{\Phi}_{\mathrm{I}j}^{\mathrm{T}} \mathbf{A} \boldsymbol{\Phi}_{\mathrm{R}j} = 0 \tag{2.4.14}$$

and

$$\boldsymbol{\Phi}_{\mathrm{R}j}^{\mathrm{T}} \mathbf{B} \boldsymbol{\Phi}_{\mathrm{R}j} - \boldsymbol{\Phi}_{\mathrm{I}j}^{\mathrm{T}} \mathbf{B} \boldsymbol{\Phi}_{\mathrm{I}j} = \alpha_{\mathrm{R}j} \tag{2.4.15}$$

$$\boldsymbol{\Phi}_{\mathrm{R}j}^{\mathrm{T}} \mathbf{B} \boldsymbol{\Phi}_{\mathrm{I}j} + \boldsymbol{\Phi}_{\mathrm{I}j}^{\mathrm{T}} \mathbf{B} \boldsymbol{\Phi}_{\mathrm{R}j} = \alpha_{\mathrm{I}j} \tag{2.4.16}$$

Nevertheless, recall that $\boldsymbol{\Phi}_j$ and $\overline{\boldsymbol{\Phi}}_j$ are orthogonal; i.e.,

$$(\boldsymbol{\Phi}_{\mathrm{R}j} - \boldsymbol{\Phi}_{\mathrm{I}j} \, \mathrm{i}^*)^{\mathrm{T}} \mathbf{A} (\boldsymbol{\Phi}_{\mathrm{R}j} + \boldsymbol{\Phi}_{\mathrm{I}j} \, \mathrm{i}^*) = 0 \tag{2.4.17}$$

$$(\boldsymbol{\Phi}_{\mathrm{R}j} - \boldsymbol{\Phi}_{\mathrm{I}j} \, \mathrm{i}^*)^{\mathrm{T}} \mathbf{B} (\boldsymbol{\Phi}_{\mathrm{R}j} + \boldsymbol{\Phi}_{\mathrm{I}j} \, \mathrm{i}^*) = 0 \tag{2.4.18}$$

and thus expanding Eq.(2.4.17) and Eq.(2.4.18), we obtain

$$\boldsymbol{\Phi}_{\mathrm{R}j}^{\mathrm{T}} \mathbf{A} \boldsymbol{\Phi}_{\mathrm{R}j} + \boldsymbol{\Phi}_{\mathrm{I}j}^{\mathrm{T}} \mathbf{A} \boldsymbol{\Phi}_{\mathrm{I}j} = 0 \tag{2.4.19}$$

$$\boldsymbol{\Phi}_{\mathrm{R}j}^{\mathrm{T}} \mathbf{B} \boldsymbol{\Phi}_{\mathrm{R}j} + \boldsymbol{\Phi}_{\mathrm{I}j}^{\mathrm{T}} \mathbf{B} \boldsymbol{\Phi}_{\mathrm{I}j} = 0 \tag{2.4.20}$$

Solving Eq.(2.4.13) and Eq.(2.4.19) simultaneously gives

$$\boldsymbol{\Phi}_{\mathrm{R}j}^{\mathrm{T}} \mathbf{A} \boldsymbol{\Phi}_{\mathrm{R}j} = \frac{1}{2} \qquad \boldsymbol{\Phi}_{\mathrm{I}j}^{\mathrm{T}} \mathbf{A} \boldsymbol{\Phi}_{\mathrm{I}j} = -\frac{1}{2} \tag{2.4.21}$$

while Eq.(2.4.14) itself gives

$$\Phi_{Rj}^{T}\,\mathbf{A}\,\Phi_{Ij} = \Phi_{Ij}^{T}\,\mathbf{A}\,\Phi_{Rj} = 0 \qquad (2.4.22)$$

A similar manipulation yields

$$\Phi_{Rj}^{T}\,\mathbf{B}\,\Phi_{Rj} = \frac{1}{2}\alpha_{Rj} \qquad \Phi_{Ij}^{T}\,\mathbf{B}\,\Phi_{Ij} = -\frac{1}{2}\alpha_{Rj} \qquad (2.4.23)$$

$$\Phi_{Rj}^{T}\,\mathbf{B}\,\Phi_{Ij} = \Phi_{Ij}^{T}\,\mathbf{B}\,\Phi_{Rj} = \frac{1}{2}\alpha_{Ij} \qquad (2.4.24)$$

These formulae of normalization and the aforementioned orthogonality properties are useful in solving for the eigenpairs of the system. For example, we may have the following during the solution.

$$[\,\Phi_{Rp}\,\Phi_{Ip}\,\Phi_{Rq}\,\Phi_{Iq}\,\Psi_r\,\hat{\Psi}_r\,\Psi_s\,\hat{\Psi}_s\,]^{T}\,\mathbf{A}\,[\,\Phi_{Rp}\,\Phi_{Ip}\,\Phi_{Rq}\,\Phi_{Iq}\,\Psi_r\,\hat{\Psi}_r\,\Psi_s\,\hat{\Psi}_s\,] =$$

$$\begin{bmatrix} 0.5 & 0 & 0 & 0 & 0 & 0 & 0 & 0 \\ 0 & -0.5 & 0 & 0 & 0 & 0 & 0 & 0 \\ 0 & 0 & 0.5 & 0 & 0 & 0 & 0 & 0 \\ 0 & 0 & 0 & -0.5 & 0 & 0 & 0 & 0 \\ 0 & 0 & 0 & 0 & \delta_r & 0 & 0 & 0 \\ 0 & 0 & 0 & 0 & 0 & \hat{\delta}_r & 0 & 0 \\ 0 & 0 & 0 & 0 & 0 & 0 & \delta_s & 0 \\ 0 & 0 & 0 & 0 & 0 & 0 & 0 & \hat{\delta}_s \end{bmatrix} \qquad (2.4.25)$$

$$[\,\Phi_{Rp}\,\Phi_{Ip}\,\Phi_{Rq}\,\Phi_{Iq}\,\Psi_r\,\hat{\Psi}_r\,\Psi_s\,\hat{\Psi}_s\,]^{T}\,\mathbf{B}\,[\,\Phi_{Rp}\,\Phi_{Ip}\,\Phi_{Rq}\,\Phi_{Iq}\,\Psi_r\,\hat{\Psi}_r\,\Psi_s\,\hat{\Psi}_s\,] =$$

$$\begin{bmatrix} 0.5\alpha_{Rp} & 0.5\alpha_{Ip} & 0 & 0 & 0 & 0 & 0 & 0 \\ 0.5\alpha_{Ip} & -0.5\alpha_{Rp} & 0 & 0 & 0 & 0 & 0 & 0 \\ 0 & 0 & 0.5\alpha_{Rq} & 0.5\alpha_{Iq} & 0 & 0 & 0 & 0 \\ 0 & 0 & 0.5\alpha_{Iq} & -0.5\alpha_{Rq} & 0 & 0 & 0 & 0 \\ 0 & 0 & 0 & 0 & \delta_r\beta_r & 0 & 0 & 0 \\ 0 & 0 & 0 & 0 & 0 & \hat{\delta}_r\hat{\beta}_r & 0 & 0 \\ 0 & 0 & 0 & 0 & 0 & 0 & \delta_s\beta_s & 0 \\ 0 & 0 & 0 & 0 & 0 & 0 & 0 & \hat{\delta}_s\hat{\beta}_s \end{bmatrix} \qquad (2.4.26)$$

Note that we can put all the foregoing formulae together as

$$\mathbf{Z}^{\mathrm{T}}\,\mathbf{A}\,\mathbf{Z} = \boldsymbol{\Delta} \qquad \mathbf{Z}^{\mathrm{T}}\,\mathbf{B}\,\mathbf{Z} = \boldsymbol{\Delta}\,\boldsymbol{\Lambda} \tag{2.4.27}$$

where both Δ and Λ are diagonal matrices and the diagonal element δ_j is 1 for complex λ_j and 1 or -1 for real λ_j. Eq.(2.4.27) represents the orthonormality property and is used in Chapter 6 when Eq.(2.3.6) is decoupled to determine the response of the system.

Example 2.1 : (continued)

The state form of eigenvectors can be scaled to

$$[\ \Phi_{R1}\ \Phi_{I1}\ \Phi_{R2}\ \Phi_{I2}\ \Psi_1\ \hat{\Psi}_1\ ] =$$

0.5747e–01	0.5324e–01	0.7906e–01	0.7906e–01	-0.3059e–01	-0.4328e–01
0.6657e–01	0.7578e–01	-0.2137e–14	-0.8753e–14	0.8850e–01	0.7218e–01
0.5747e–01	0.5324e–01	-0.7906e–01	-0.7906e–01	-0.3059e–01	-0.4328e–01
0.6539e+00	-0.1803e+01	-0.1581e+01	-0.4743e+01	0.7475e+00	0.5909e+01
0.1076e+01	-0.2223e+01	-0.8197e–13	0.3764e–12	-0.2163e+01	-0.9854e+01
0.6539e+00	-0.1803e+01	0.1581e+01	0.4743e+01	0.7475e+00	0.5909e+01

The orthogonality property can be verified by forming the following weighted inner products.

$$[\ \Phi_{R1}\ \Phi_{I1}\ \Phi_{R2}\ \Phi_{I2}\ \Psi_1\ \hat{\Psi}_1\ ]^{\mathrm{T}}\,\mathbf{A}\,[\ \Phi_{R1}\ \Phi_{I1}\ \Phi_{R2}\ \Phi_{I2}\ \Psi_1\ \hat{\Psi}_1\ ] =$$

0.5000e+00	0.1995e–16	-0.1325e–13	-0.2345e–13	-0.1110e–13	-0.2256e–13
0.2082e–16	-0.5000e+00	-0.4025e–14	0.1662e–13	0.4220e–14	0.4400e–13
-0.1325e–13	-0.4037e–14	0.5000e+00	0.1561e–16	-0.3137e–13	0.7879e–14
-0.2346e–13	0.1662e–13	0.2082e–16	-0.5000e+00	-0.1487e–13	0.1449e–12
-0.1110e–13	0.4221e–14	-0.3137e–13	-0.1487e–13	0.1000e+01	-0.3567e–14
-0.2254e–13	0.4402e–13	0.7883e–14	0.1449e–12	-0.3525e–14	-0.1000e+01

$$[\ \Phi_{R1}\ \Phi_{I1}\ \Phi_{R2}\ \Phi_{I2}\ \Psi_1\ \hat{\Psi}_1\ ]^T\ \mathbf{B}\ [\ \Phi_{R1}\ \Phi_{I1}\ \Phi_{R2}\ \Phi_{I2}\ \Psi_1\ \hat{\Psi}_1\ ] =$$

-0.4759e+01	-0.1128e+02	0.1025e–12	0.8610e–12	0.1763e–12	0.8845e–12
-0.1128e+02	0.4759e+01	0.3789e–12	0.5327e–12	0.1814e–12	-0.1319e–12
0.1023e–12	0.3786e–12	-0.2000e+02	-0.1000e+02	0.9529e–12	0.2790e–11
0.8612e–12	0.5329e–12	-0.1000e+02	0.2000e+02	0.8902e–12	-0.9109e–11
0.1763e–12	0.1814e–12	0.9530e–12	0.8905e–12	-0.2444e+02	-0.5455e–12
0.8848e–12	-0.1319e–12	0.2790e–11	-0.9109e–11	-0.5455e–12	0.1365e+03

2.5 Some examples of a damped system

In this section we show a number of damped dynamic systems which are to be analyzed and solved in subsequent discussion. We describe each of them individually and call them Test Problems. The solution algorithms developed in this study are implemented in the research version of FEAP, a "Finite Element Analysis Program," written by R. L. Taylor (a simplified version of this program is presented in Chapter 24 of [Z1]). The solutions reported herein are performed by the Digital Equipment VAXstation II/GPX computer system where the Ultrix 1.2 operating system and the f77 Fortran compiler are used.

Test Problem 1 : The system is a cantilever beam with a lumped translational viscous-damper attached at the tip. The geometrical configuration and physical properties of the beam are shown in Figure 2.3. The consistent mass is used for matrix **M**. The damping matrix **C** has only one nonzero element representing the magnitude c of the lumped damper. The cantilever beam is divided into 20 equal elements and has 40 degrees of freedom. The associated (**A**, **B**) is of the order 80.

Figure 2.4 shows the eigenvalues of the system for $c = 5$ case and $c = 5000$ case. Note that in $c = 5000$ case the real pair are too large and hence they are not shown in the Figure. Table 2.1 shows the first five eigenvalues of this system. The associated eigenvectors are plotted in Figure 2.5, 2.6 and 2.7 for c equal to 0, 5 and 5000 respectively. For the $c = 0$ case, all eigenvalues are pure imaginary and all eigenvectors are real. This solution can be checked with a theoretical solution. For the $c = 5$ and $c = 5000$ cases, both eigenvalues and eigenvectors are complex. Note the first mode in $c = 0$ case becomes an overdamped mode in the $c = 5$ and $c = 5000$ cases. Hence the first underdamped mode in the damped systems evolves from the second mode of the undamped case. The location of the damper may be an indication why the first mode of the undamped case becomes an overdamped mode in the damped cases. Figure 2.8 shows the phasors of the first three underdamped modes for $c = 5$. It can be seen that the eigenvectors of this damped system are "truly complex". Figure 2.9 shows the phasors of the first three underdamped modes for $c = 5000$. It can be seen that the eigenvectors of this heavily damped system are almost real. This is similar to the situation in an undamped system. The effect of the lumped damper on this beam system is important since it can cause a drastic change in the eigensolutions.

The eigenproblem associated with the damped system can be solved by the RG or RGG routines; the eigenproblem $\omega^2 \mathbf{M} \psi = \mathbf{K} \psi$ associated with the corresponding undamped system can be solved by the RS routine. Table 2.2 shows the CPU time required for the complete solution of this system by RS, RG, and RGG. The RS, RG, RGG routines use the symmetric QL, the QR, the QZ algorithms, respectively, and they are obtained from the EISPACK library [E1]

Test Problem 2 : The system consists of two beams connected by a hinge with rotational viscous-damper. The geometrical configuration and physical properties of the system are shown in Figure 2.10. The boundary condition of the system is that the A's and B in Figure 2.10 are hinges. Just as in Test Problem 1, the consistent mass is used for matrix **M**. The matrix **C** has only four nonzero elements, which represent the lumped rotational damper c. The system is divided into 40 equal elements and has 80 degrees of freedom. The associated (**A**, **B**) is of the order 160.

Since this system is symmetric, there are symmetric modes and anti-symmetric modes. Table 2.3 shows the first eight eigenvalues of the system. All the complex eigenvalues of are plotted in the Figure 2.11. The real pair are too large, so they are not shown in the Figure. We also consider a different boundary condition where there is no restraint; i.e., A's and B in Figure 2.10 are nothing. Under this boundary condition, the system has rigid body modes. We use the shift of origin technique described in Section 3.1 to compute the eigensolutions of the unrestrained system. The eignvectors of the unrestrained system are plotted in Figures 2.12, 2.13, and 2.14 for c equal to 0, 5, and 5000 respectively. The solutions of the undamped system ($c = 0$ case) is the same as the solutions of two adjacent beams obtained separately; that is, 40 modes are associated with the vibration of one beam with the other beam motionless, and the other 40 modes are the other way around. But the solution of the damped systems ($c = 5$ and $c = 5000$ cases) clearly shows that there are actually 40 symmetric and 40 anti-symmetric modes. When the damper is in effect, i.e., damping is not equal to zero, all the symmetric modes become complex modes while all the anti-symmetric modes remain unaffected, i.e., they are still real modes. The physical explanation for damping affecting only the symmetric modes is that there is no relative displacement, hence no relative velocity, around the damper when the system vibrates in the anti-symmetric modes. The last mode of the damped system is an overdamped mode. But, in contrast to the previous problem, this overdamped mode evolves from the highest mode of the corresponding undamped system.

Table 2.4 shows the CPU time required for the complete solution of the system by RG and RGG and the CPU time required for the complete solution of the corresponding undamped system by RS.

Test Problem 3 : This problem is a three dimensional space truss system. There are 44 nodes and the 4 end nodes are fully restrained, as shown in Figure

2.15. Thus, there are 120 degrees of freedom and the associated (**A**, **B**) is of the order 240. All truss bars have the same density and Young's modulus but different damping, as shown in Figure 2.15, resulting in a nonproportionally damped system.

Figure 2.16 shows the complete set of eigenvalues of this system. The CPU time required for the complete solution of this system by RG and RGG is 1788 and 4633 seconds respectively. The CPU time required for the complete solution of the corresponding undamped system by RS is 459 seconds.

Test Problem 4 : This problem is a larger three dimensional space truss system. The typical cell is the same as the typical cell in the last Problem. There are 300 nodes and the 4 end nodes are fully restrained, as shown in Figure 2.17; thus, there are 888 degrees of freedom. All truss bars have the same density and Young's modulus but different damping, resulting in a nonproportionally damped system. The associated (**A**, **B**) is of the order 1776, which is beyond the storage capability of the computer program for the complete solution. Figure 2.18 shows the first twenty eigenvalues of this system, obtained by methods to be discussed later.

From the information on the CPU time required to find the complete solution of these Test Problems, we observe the following.

(1) The RG routine is more efficient than the RGG routine for solving the damped systems listed above. The difference in CPU time spent between the two increases with the size of the problem.

(2) There is a considerable increase of CPU time in solving $\mathbf{D}\,\mathbf{z} = \frac{1}{\lambda}\mathbf{z}$ or $\lambda\,\mathbf{A}\,\mathbf{z} = \mathbf{B}\,\mathbf{z}$ when we change the zero damping matrix **C** to a nonzero one, even though the change is made in just a few elements of matrix **C**, as in Test examples 1 and 2.

(3) It is much more expensive to solve the eigenproblem associated with a damped system than the eigenproblem associated with an undamped system.

Table 2.1 *Eigenvalues of Test problem 1*

mode	$c = 0$	$c = 5$	$c = 5000$
1	$\pm 1.41i^*$	$-0.55,\ -4.83$	$-0.00048,\ 276807.1$
2	$\pm 8.81i^*$	$-1.66 \pm 7.75i^*$	$-0.0023 \pm 6.17i^*$
3	$\pm 24.68i^*$	$-1.89 \pm 24.07i^*$	$-0.0080 \pm 19.99i^*$
4	$\pm 48.36i^*$	$-1.94 \pm 47.92i^*$	$-0.017 \pm 41.70i^*$
5	$\pm 79.96i^*$	$-1.97 \pm 79.61i^*$	$-0.029 \pm 71.32i^*$

Table 2.2 *CPU Time for Test Problem 1*

damping / routine	RS	RG	RGG
$c = 0$	19.2	91.1	161.8
$c = 5$	-	152.5	223.7
$c = 5000$	-	145.8	192.3

Table 2.3 *Eigenvalues of Test problem 2*

mode	$c = 0$	$c = 5$	$c = 5000$
1	$\pm 0.99i^{*}$	$\pm 0.99i^{*}$	$\pm 0.99i^{*}$
2	$\pm 0.99i^{*}$	$-0.10\pm 1.00i^{*}$	$-0.002\pm 1.54i^{*}$
3	$\pm 3.95i^{*}$	$\pm 3.95i^{*}$	$\pm 3.95i^{*}$
4	$\pm 3.95i^{*}$	$-0.39\pm 4.05i^{*}$	$-0.002\pm 5.00i^{*}$
5	$\pm 8.88i^{*}$	$\pm 8.88i^{*}$	$\pm 8.88i^{*}$
6	$\pm 8.88i^{*}$	$-7.93\pm 9.26i^{*}$	$-0.002\pm 10.43i^{*}$
7	$\pm 15.79i^{*}$	$\pm 15.79i^{*}$	$\pm 15.79i^{*}$
8	$\pm 15.79i^{*}$	$-1.18\pm 16.65i^{*}$	$-0.002\pm 17.83i^{*}$

Table 2.4 *CPU Time for Test problem 2*

damping / routine	RS	RG	RGG
$c = 0$	107.2	434.0	646.7
$c = 5$	-	985.8	1500.8
$c = 5000$	-	1149.1	1454.4

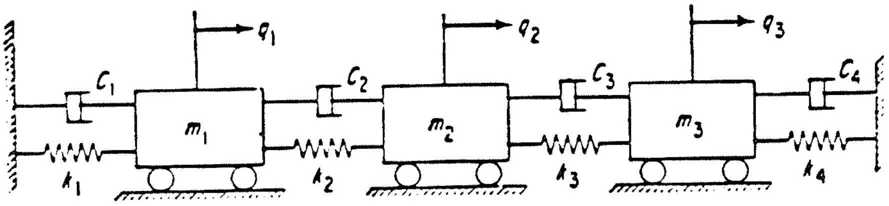

$m_1 = m_2 = m_3 = m_4 = 1.0$

$c_1 = c_4 = 30$

$c_2 = c_3 = 50$

$k_1 = k_2 = k_3 = k_4 = 1000$

Figure 2.1 3 dof damped system

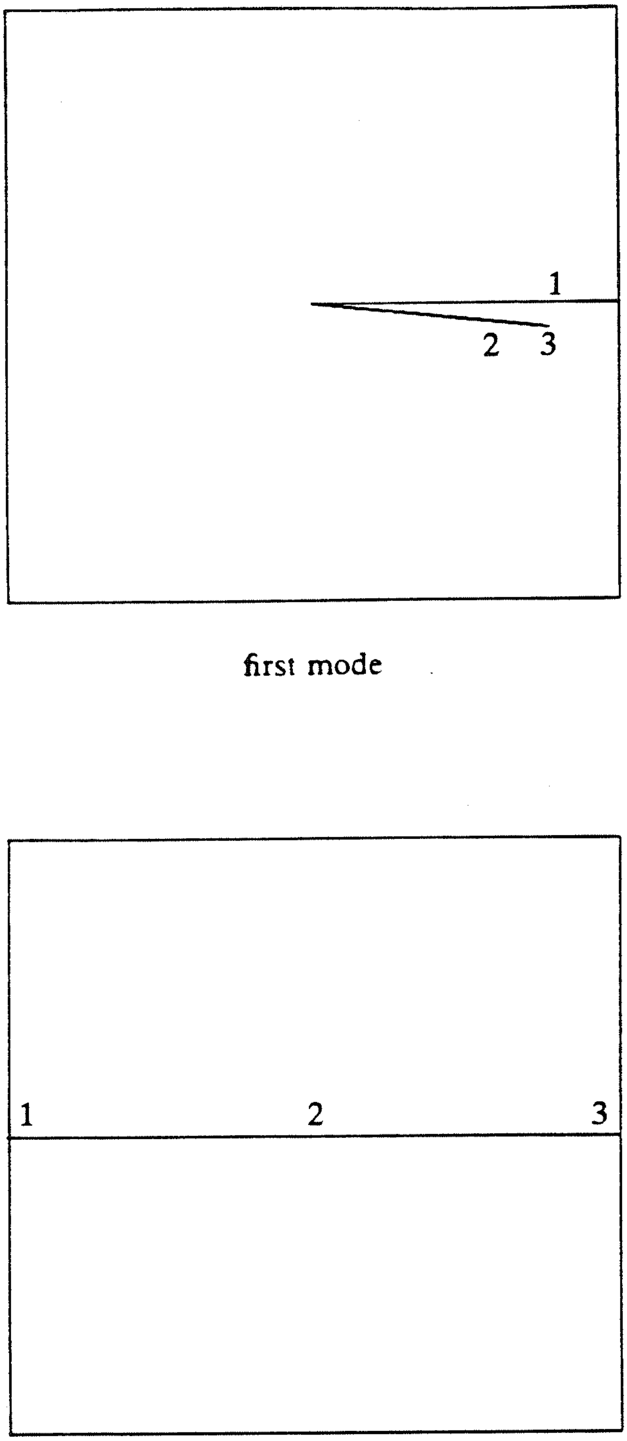

first mode

second mode

Figure 2.2 phasor for the 3 dof system

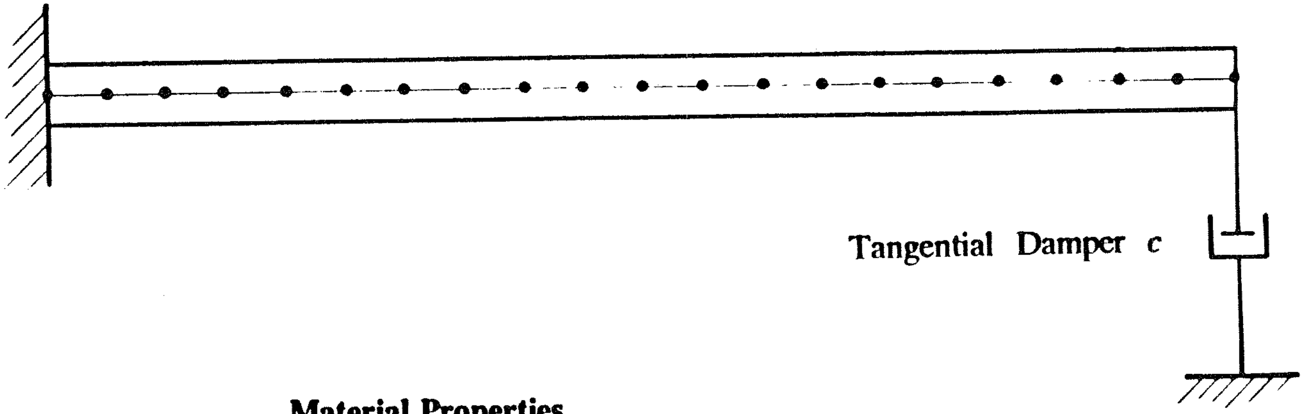

Material Properties

modulus	1000
length	5
density	1
inertia	1
area	1

Figure 2.3 Test Problem 1

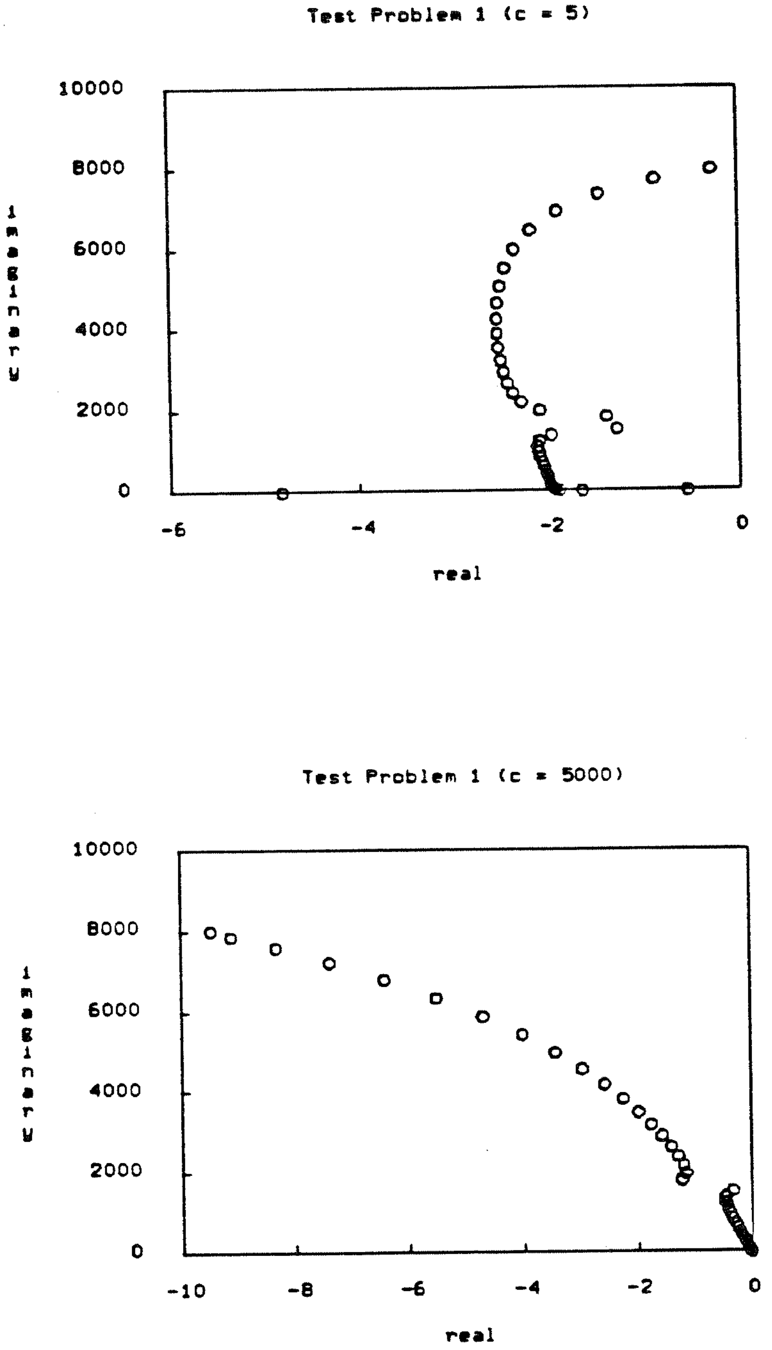

Test Problem 1 (c = 5)

Test Problem 1 (c = 5000)

Figure 2.4 eigenvalues of Test Problem 1

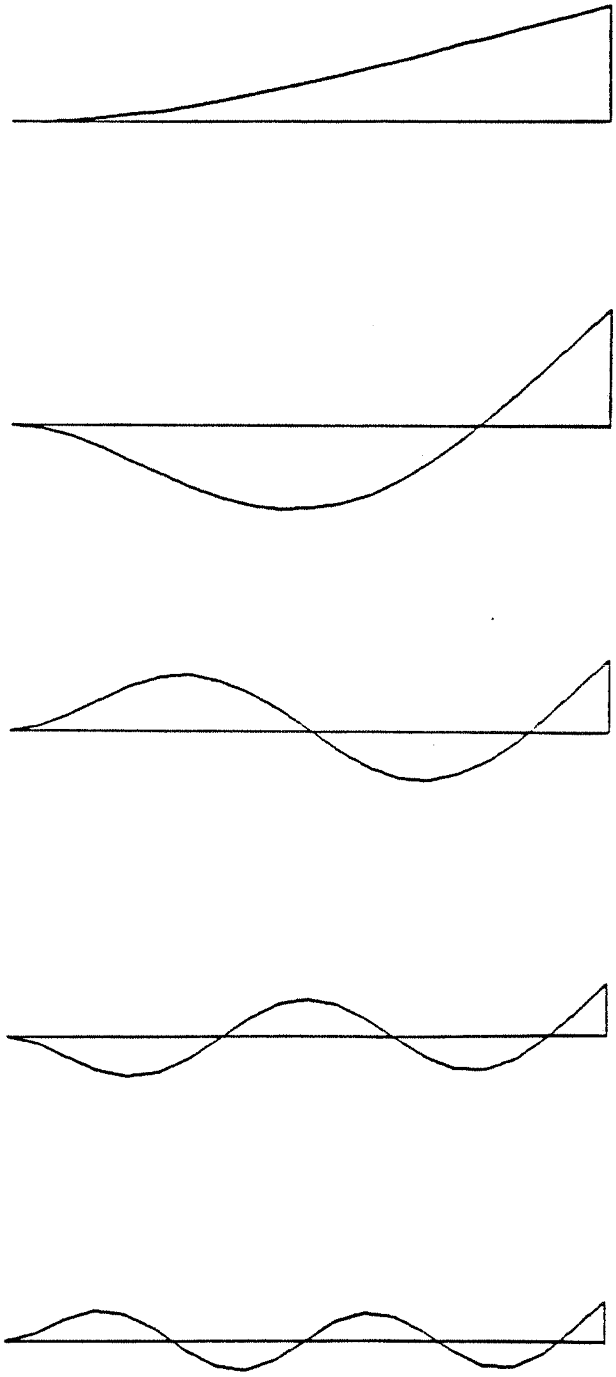

Figure 2.5 eigenvectors of Test Problem 1 (c = 0)

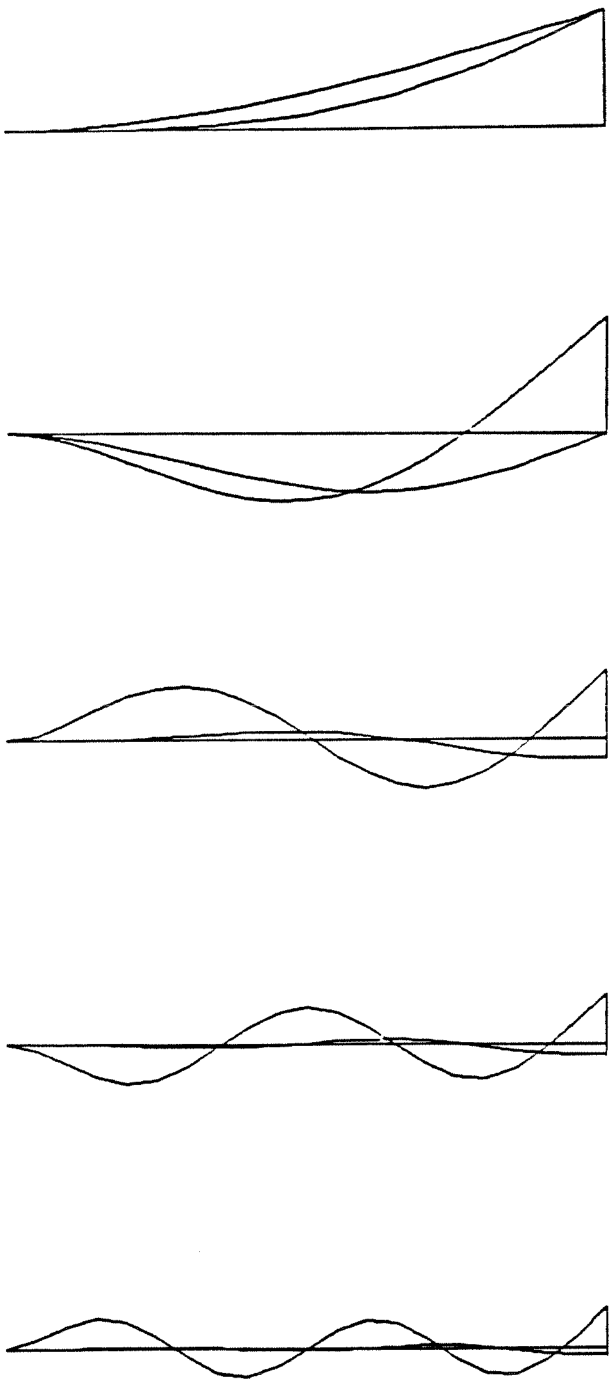

Figure 2.6 eigenvectors of Test Problem 1 (c = 5)

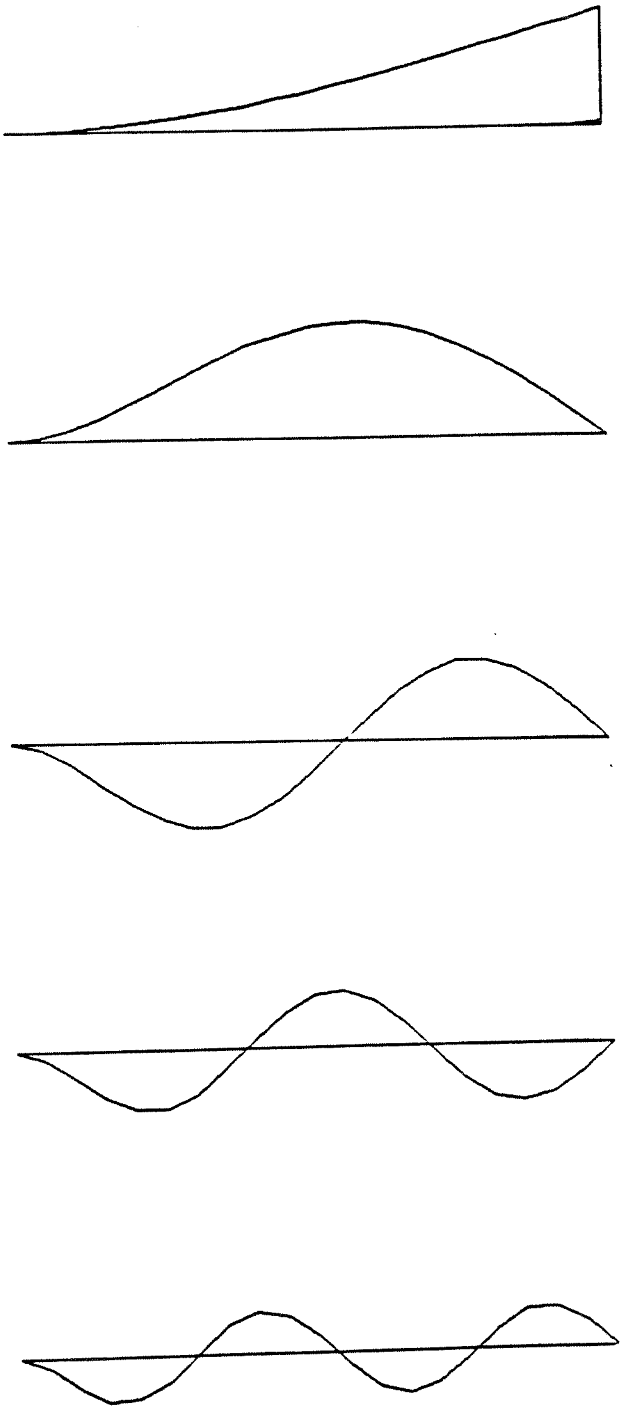

Figure 2.7 eigenvectors of Test Problem 1 (c = 5000)

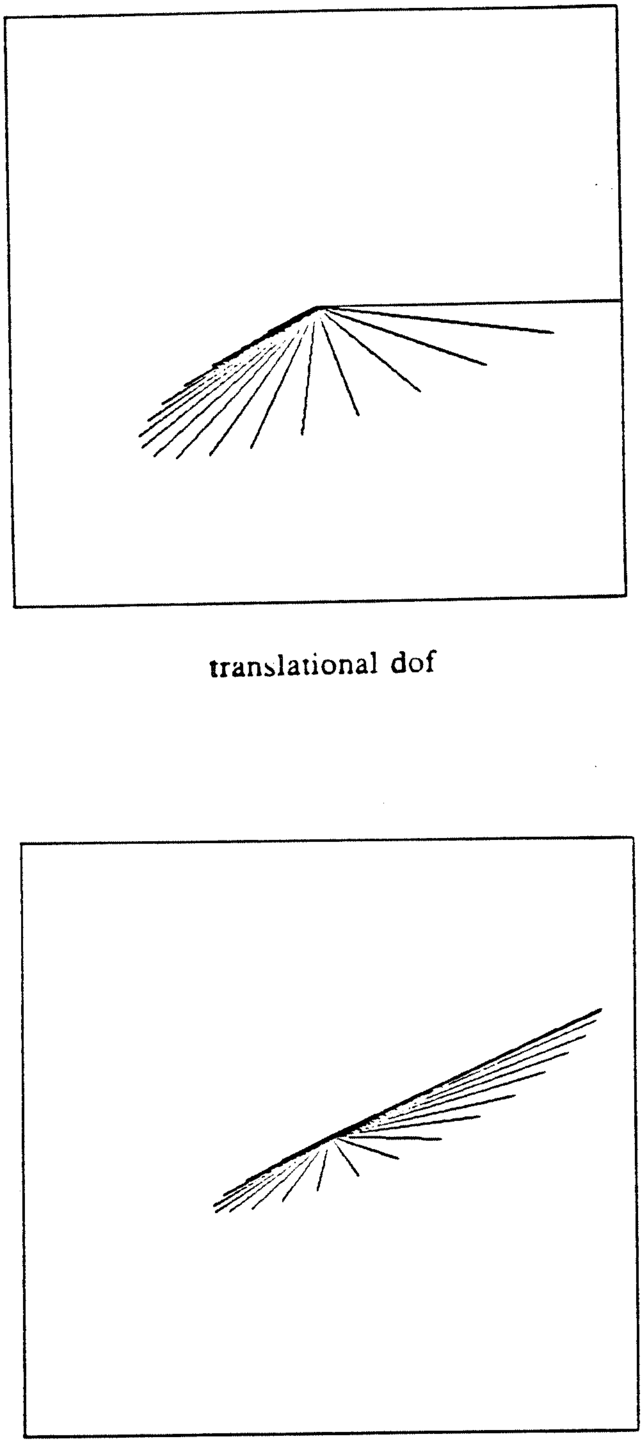

translational dof

rotational dof

Figure 2.8 (a) second mode phasor (c = 5)

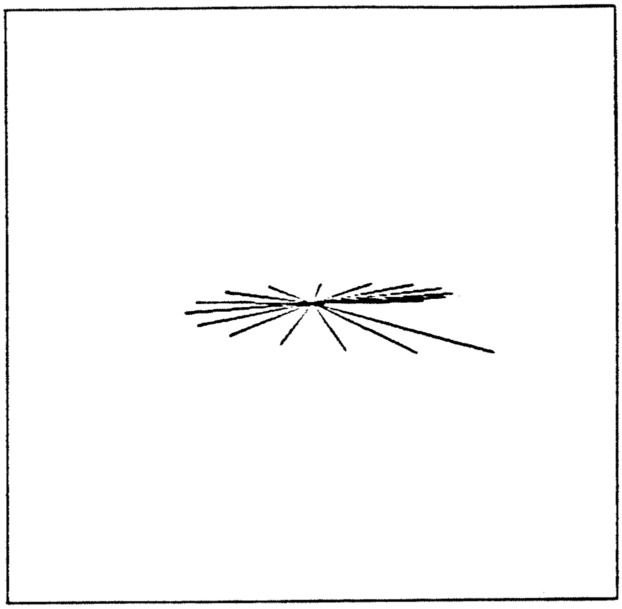

translational dof

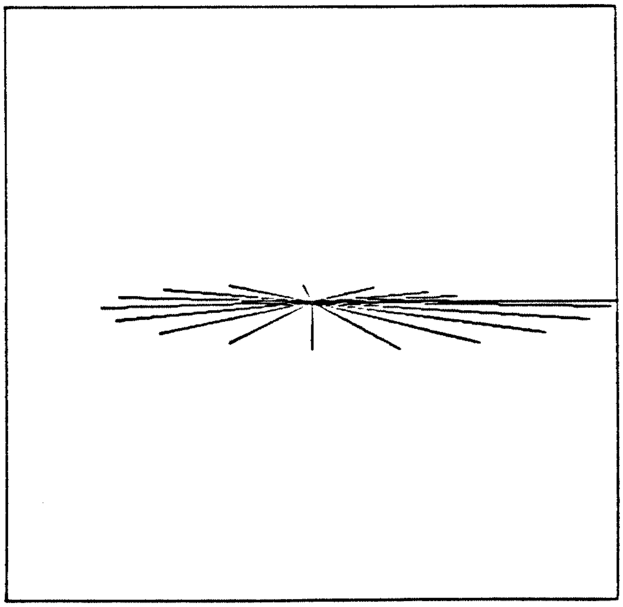

rotational dof

Figure 2.8 (b) third mode phasor (c = 5)

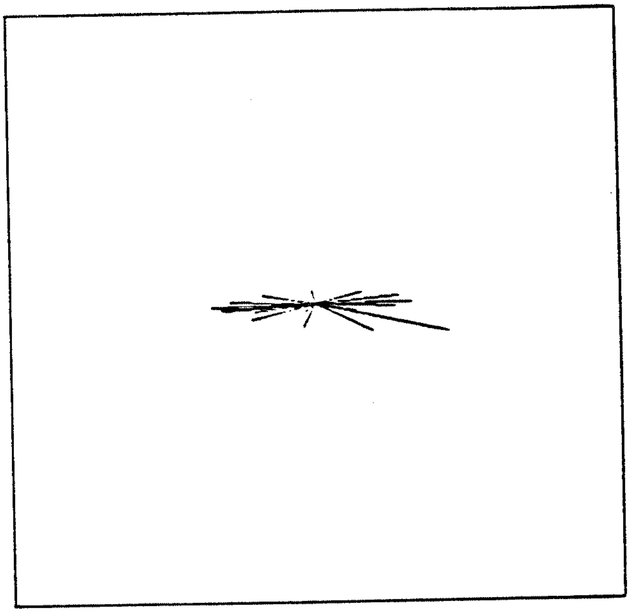

translational dof

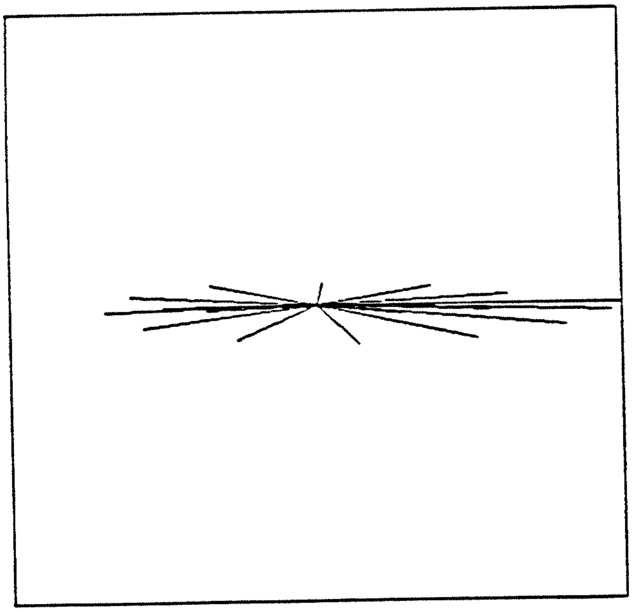

rotational dof

Figure 2.8 (c) fourth mode phasor (c = 5)

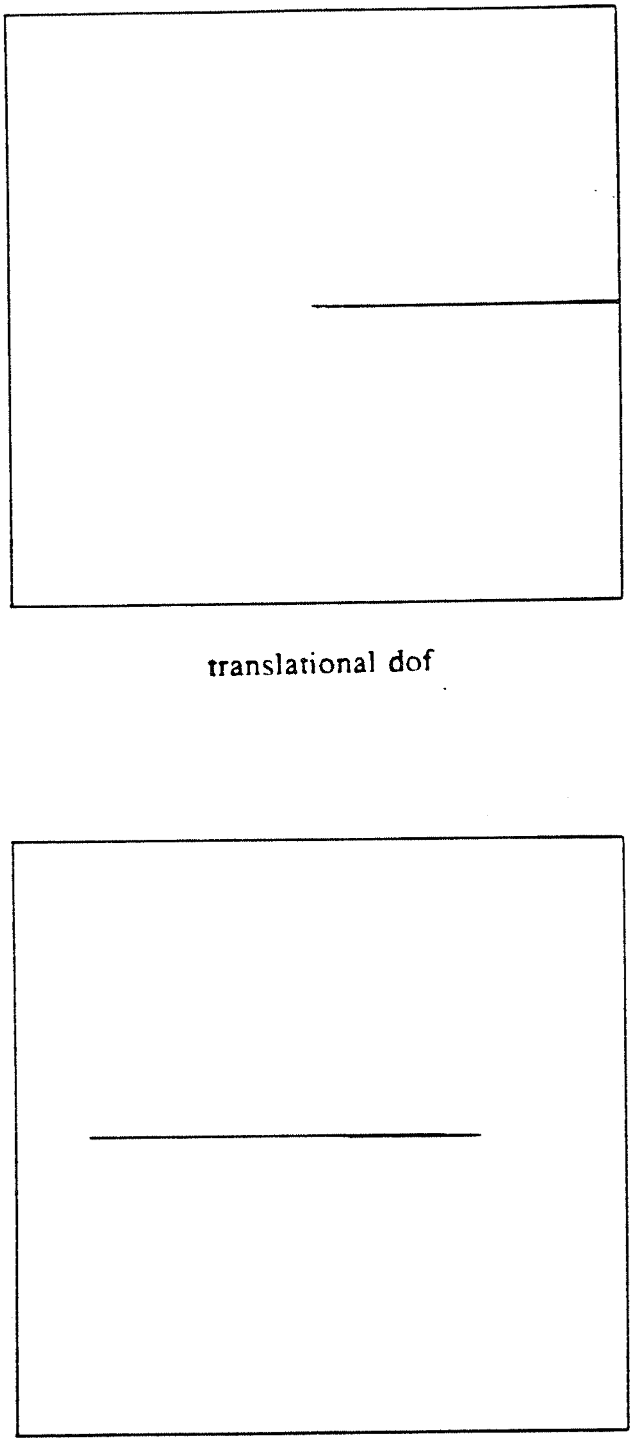

translational dof

rotational dof

Figure 2.9 (a) second mode phasor (c = 5000)

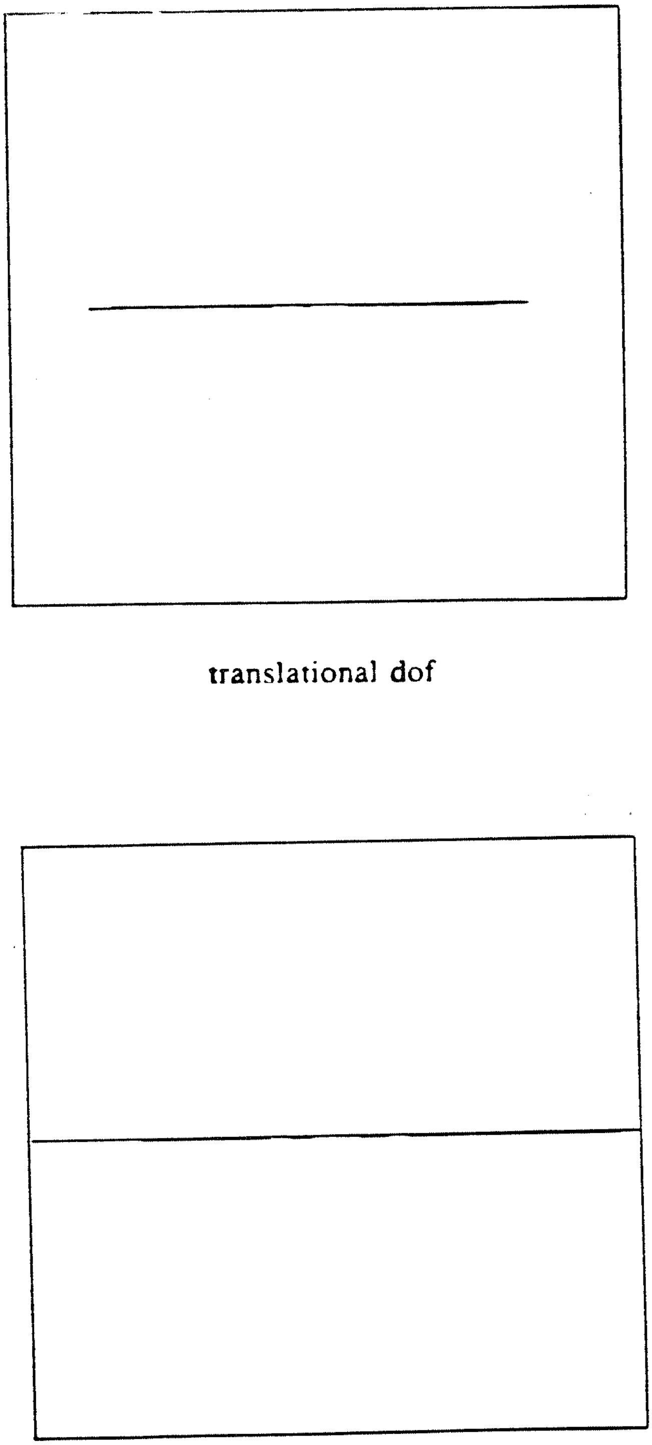

translational dof

rotational dof

Figure 2.9 (b) third mode phasor (c = 5000)

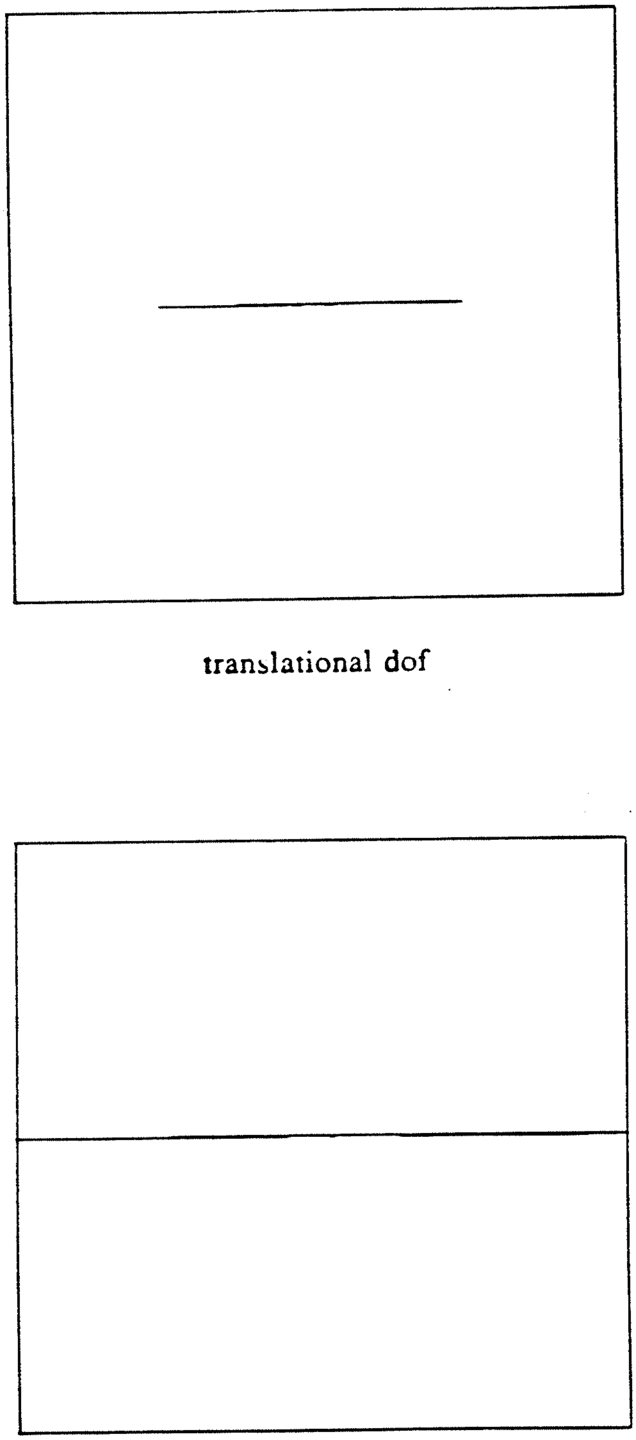

translational dof

rotational dof

Figure 2.9 (c) fourth mode phasor (c = 5000)

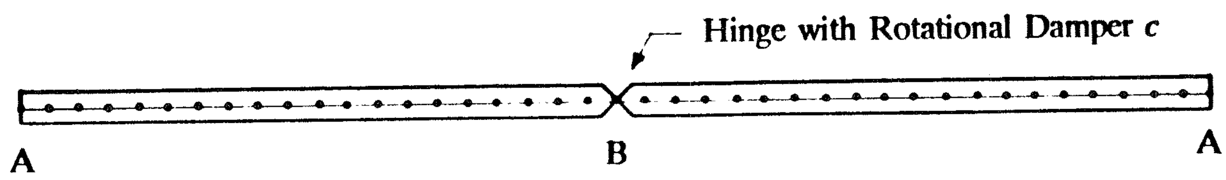

$$M = c\,\Delta\dot{\theta}$$

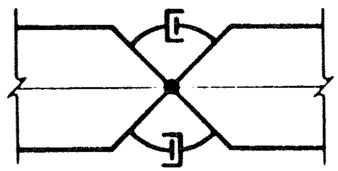

Detail for Rotational Damper

Material Properties

beam	1	2
modulus	1000	1000
length	20	20
density	1	1
inertia	1	1
area	1	1

Figure 2.10 Test Problem 2

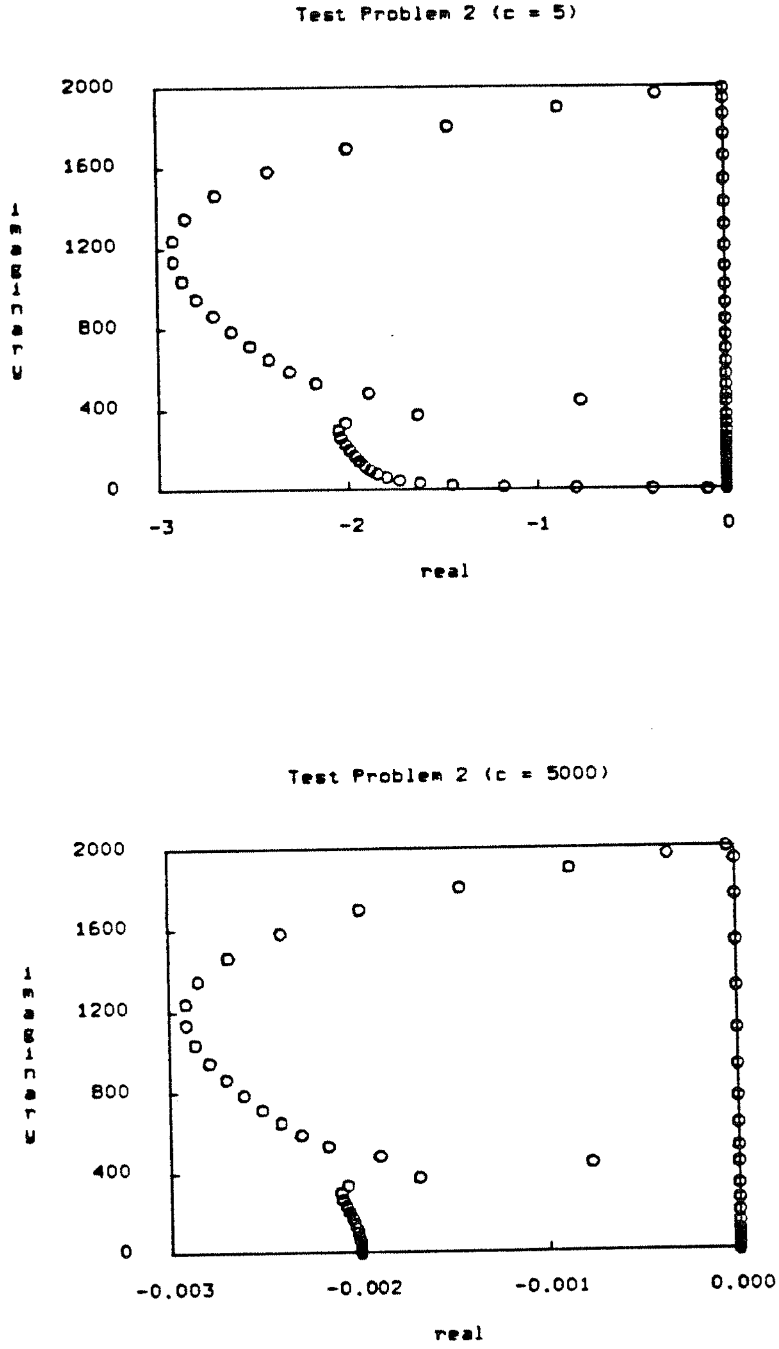

Figure 2.11 eigenvalues of Test Problem 2

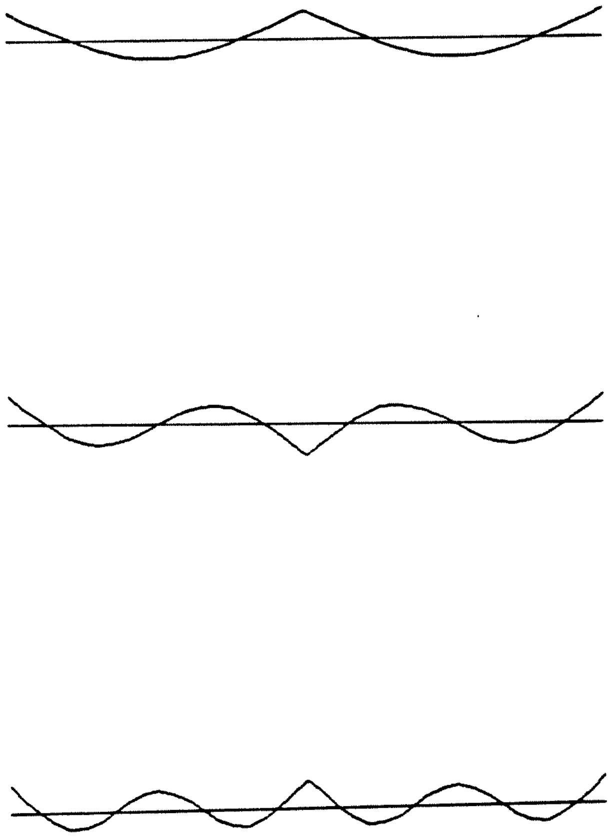

Figure 2.12 (a) eigenvectors of Test Problem 2 symmetric modes (c = 0)

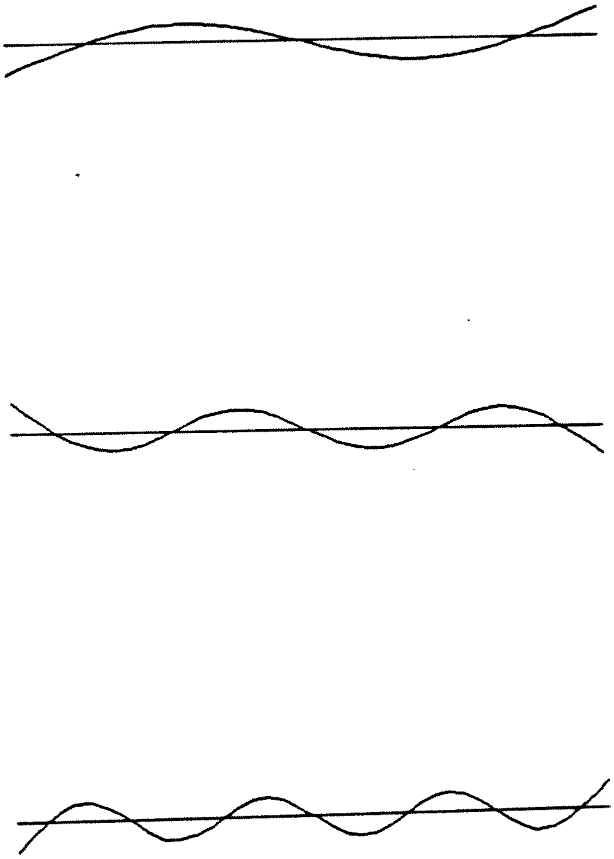

Figure 2.12 (b) eigenvectors of Test Problem 2
anti-symmetric modes (c = 0)

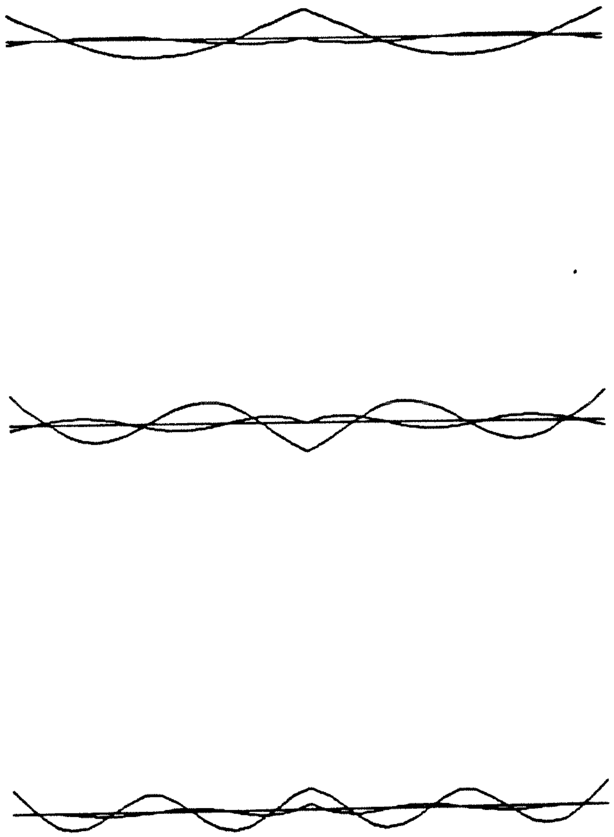

Figure 2.13 eigenvectors of Test Problem 2
symmetric modes (c = 5)

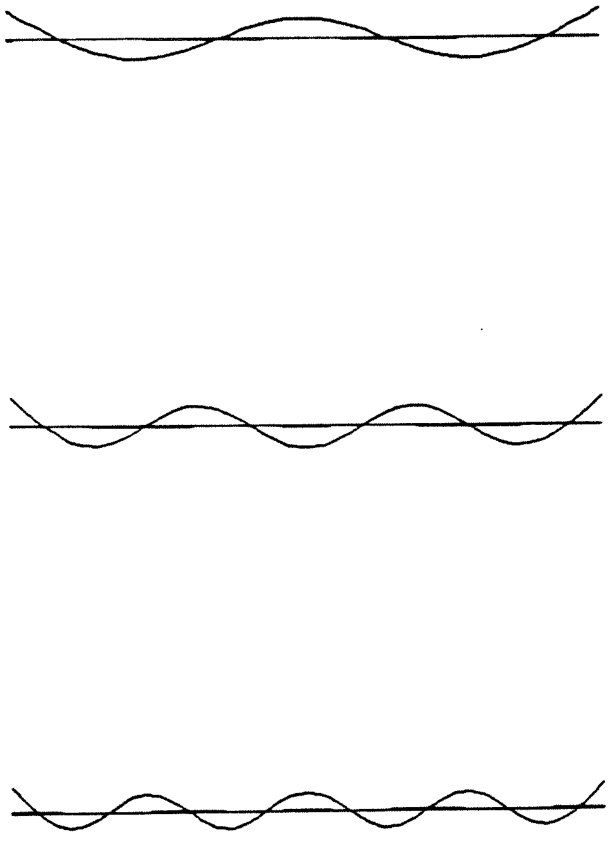

Figure 2.14 eigenvectors of Test Problem 2
symmetric modes (c = 5000)

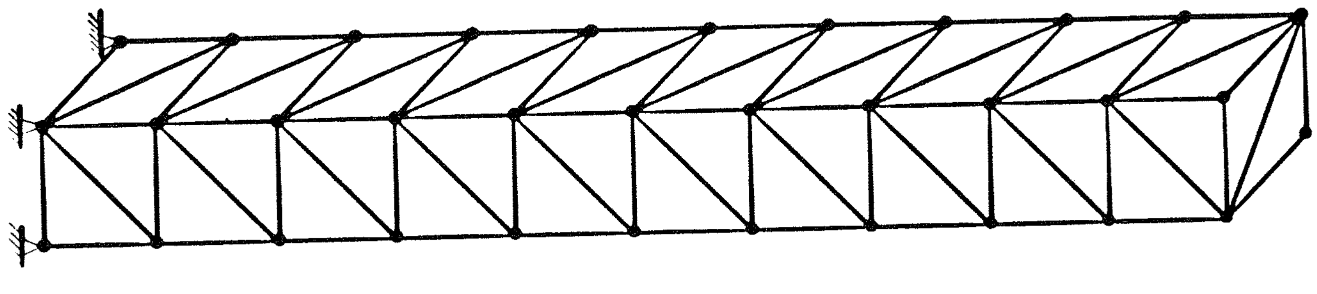

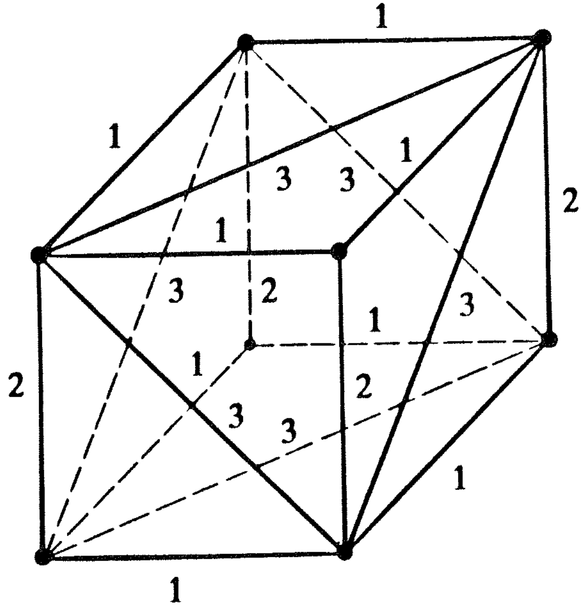

Typical Cell

Material Properties

member	1	2	3
modulus	1	1	1
density	1	1	1
inertia	1	1	1
area	1	1	1
damping	0.5	1.0	2.0

Figure 2.15 Test Problem 3

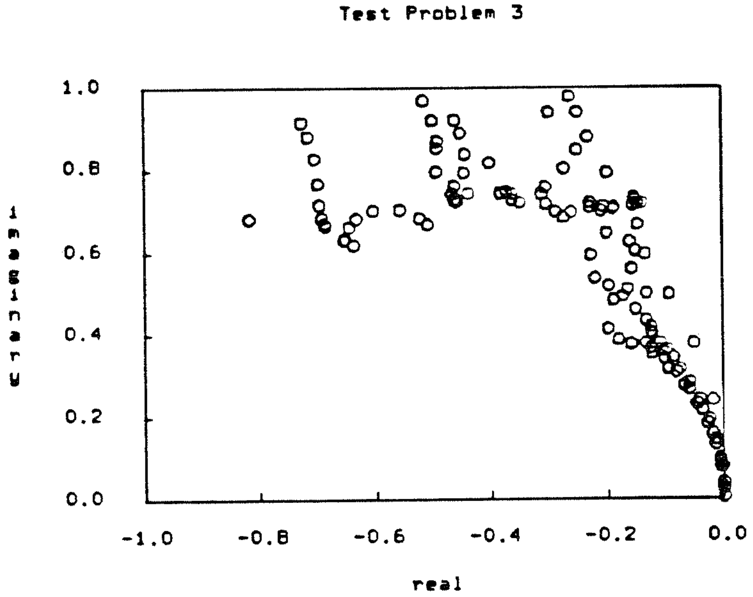

Figure 2.16 eigenvalues of Test Problem 3

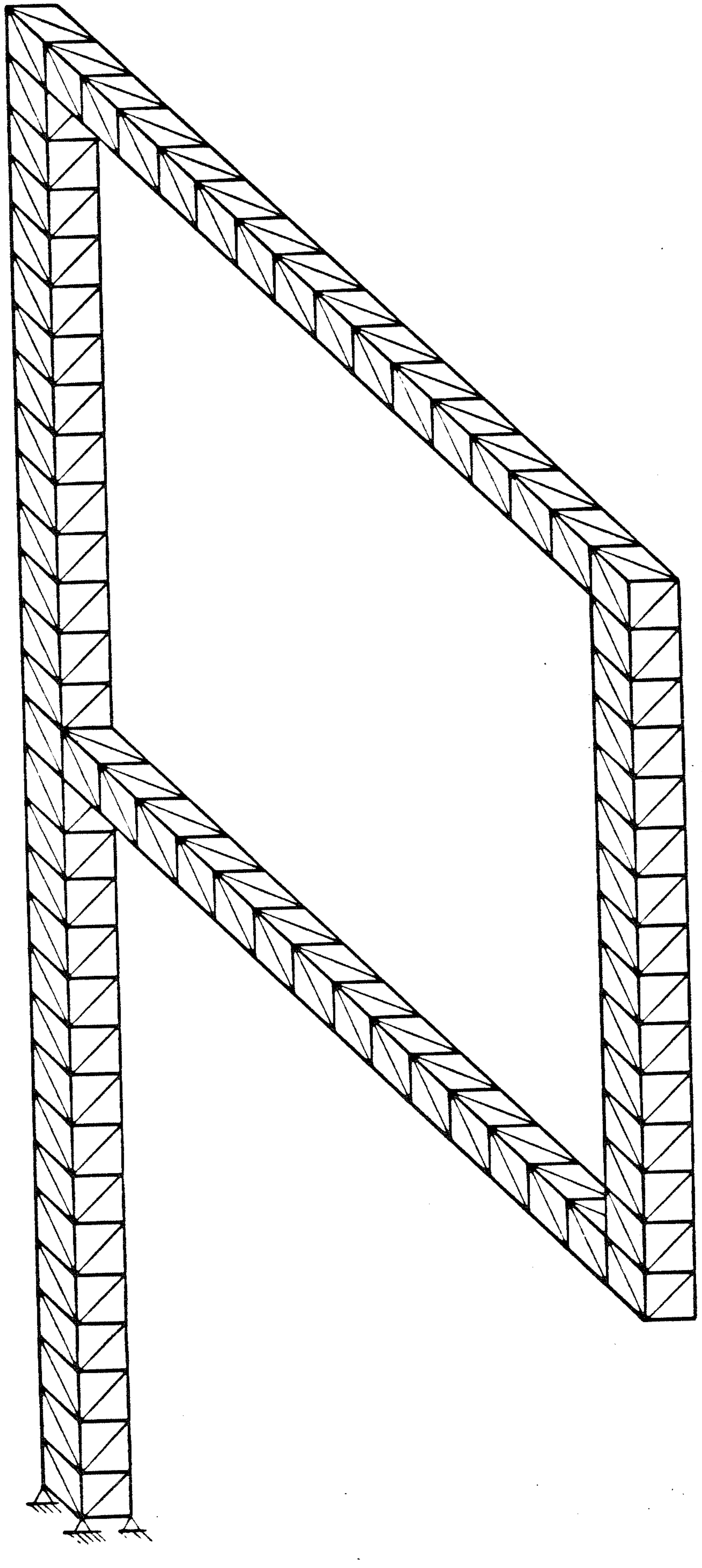

Figure 2.17 Test Problem 4

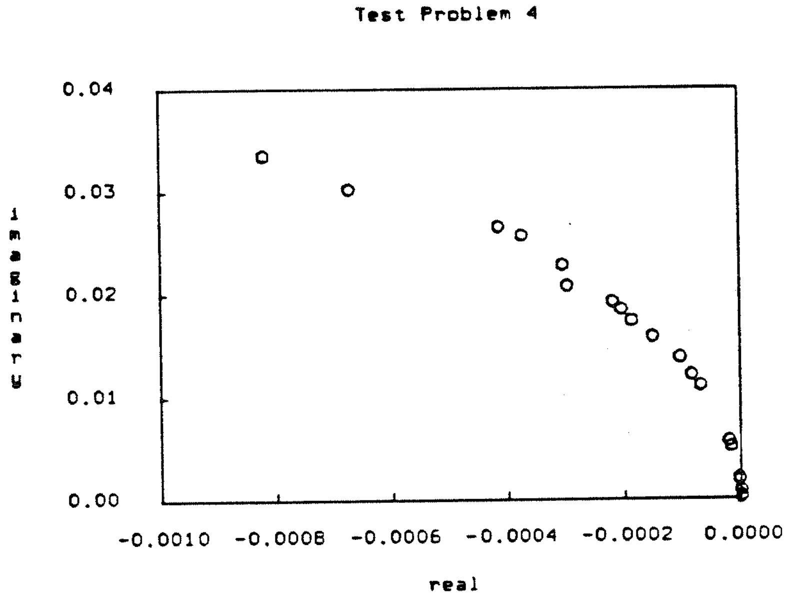

Figure 2.18 eigenvalues of Test Problem 4

Chapter 3
Preliminaries to the Solution of Large Eigenproblems

3.1 Vector iteration method

The vector iteration method may be used to extract the least dominant eigenpair of a damped system from $\mathbf{D}\,\mathbf{z} = \frac{1}{\lambda}\mathbf{z}$. The solution procedure for solving $\mathbf{D}\,\mathbf{z} = \frac{1}{\lambda}\mathbf{z}$ is the same as the one for solving $\mathbf{K}^{-1}\,\mathbf{M}\,\boldsymbol{\psi} = \frac{1}{\omega^2}\boldsymbol{\psi}$, except that there are two least dominant eigenpairs in $\mathbf{D}\,\mathbf{z} = \frac{1}{\lambda}\mathbf{z}$ instead of one. As shown in Chapter 2, the eigensolutions associated with an underdamped mode exist in complex conjugate pairs. Therefore, a pair of eigenvalues with the same modulus are least dominant in $\mathbf{D}\,\mathbf{z} = \frac{1}{\lambda}\mathbf{z}$. The usual iteration procedure will not converge directly to either one of them but rather to their linear combination. This can be explained by the iteration

$$\mathbf{v}^{(k+1)} = \mathbf{D}\,\mathbf{v}^{(k)} \tag{3.1.1}$$

where $\mathbf{v}$ is a real vector, and superscript k, $k+1$ are the iteration number. Here when k is large enough, only the components in the two least dominant eigenvectors will remain and thus $\mathbf{v}^{(k)}$ can be expressed as

$$\mathbf{v}^{(k)} \approx \alpha_1\,\lambda_1^k\,\mathbf{z}_1 + \bar{\alpha}_1\,\bar{\lambda}_1^k\,\bar{\mathbf{z}}_1 \tag{3.1.2}$$

where $(\lambda_1, \mathbf{z}_1)$ is the least dominant eigenpair, $(\bar{\lambda}_1, \bar{\mathbf{z}}_1)$ is its conjugate, α_1 is a constant, and $\bar{\alpha}_1$ is its conjugate.

The standard procedure for determining the complex conjugate eigenpairs in this case is to keep three successive iteration vectors without intermediate normalization, say $\mathbf{v}^{(k)}$, $\mathbf{v}^{(k+1)}$ and $\mathbf{v}^{(k+2)}$. If λ_1 and $\bar{\lambda}_1$ are the roots of the quadratic equation,

$$\lambda^2 + b\,\lambda + c = 0 \tag{3.1.3}$$

it follows that

$$\mathbf{v}^{(k+2)} + b\ \mathbf{v}^{(k+1)} + c\ \mathbf{v}^{(k)} = 0 \tag{3.1.4}$$

This can be verified by substituting Eq.(3.1.2) into Eq.(3.1.4). Note that Eq.(3.1.4) represents a system of $2n$ equations in two unknowns b and c. The unknowns b and c are generally found by solving two arbitrary equations from the set of Eq.(3.1.4), as described in [F2, H1, M1]. A better way to solve for b and c, however, is to find the least square solution of Eq.(3.1.4), as shown in [J1] and [W1]. After b and c are found, λ_1 and $\bar{\lambda_1}$ is obtained by solving Eq.(3.1.3). The corresponding eigenvectors can be calculated from

$$\mathbf{z}_1 \approx \mathbf{v}^{(k+2)} - \bar{\lambda_1}\ \mathbf{v}^{(k+1)} \qquad \bar{\mathbf{z}}_1 \approx \mathbf{v}^{(k+2)} - \lambda_1\ \mathbf{v}^{(k+1)} \tag{3.1.5}$$

From the above discussion, it is apparent that the computation of the complex conjugate eigensolutions of a damped system is more laborious than the computation of the real eigensolutions of an undamped system. Note that the rate of convergence is $\dfrac{\lambda_1}{\lambda_2}$ in solving $\mathbf{D}\ \mathbf{z} = \dfrac{1}{\lambda}\mathbf{z}$ while it is $\dfrac{\omega_1^2}{\omega_2^2}$ in solving $\mathbf{K}^{-1}\ \mathbf{M}\ \psi = \dfrac{1}{\omega^2}\psi$ and that $\mathbf{z}$ is twice the size of ψ. Therefore, the number of operations for solving $\mathbf{D}\ \mathbf{z} = \dfrac{1}{\lambda}\mathbf{z}$ is about 4 times that of solving $\mathbf{K}^{-1}\ \mathbf{M}\ \psi = \dfrac{1}{\omega^2}\psi$ when the vector iteration method is used.

The vector iteration method may only be used to find the least dominant eigenpair. To find other eigenpairs, other technique, such as deflation or shift of origin, needs to be added. The deflation procedure has rather poor numerical stability and requires more effort for higher modes. Hence it is not effective in practice. Detailed accounts can be found in [W1]. Unlike the eigenvalues of an undamped system, the eigenvalues of a damped system are complex in general; therefore, we cannot obtain any desired complex conjugate eigenpair by using only real shift. The use of complex shift, however, changes the associated matrices, which are originally real, into complex ones. Moreover, it does not produce satisfactory results as stated in [W1]. Therefore, we need more suitable methods to solve the eigenproblem associated with a damped system. This is the subject of the subsequent Chapters.

Although we cannot use the shift of origin to extract desired higher modes, we need the technique for the case where the eigensolutions required are centered around a specific point and/or where $\lambda = 0$. For this use, we take the shift into consideration and rewrite the characteristic equation as

$$\begin{gathered}(\lambda - \sigma)^2 \mathbf{M}\,\mathbf{w} + (\lambda - \sigma)\,\mathbf{C}\,\mathbf{w} + \mathbf{K}\,\mathbf{w} + \\ (2\lambda\sigma - \sigma^2)\,\mathbf{M}\,\mathbf{w} + \sigma\,\mathbf{C}\,\mathbf{w} = 0\end{gathered} \tag{3.1.6}$$

where σ represents the desired shift. This can be re-arranged into

$$\begin{gathered}(\lambda - \sigma)^2 \mathbf{M}\,\mathbf{w} + (\lambda - \sigma)(\mathbf{C} + 2\,\sigma\,\mathbf{M})\,\mathbf{w} + \\ (\mathbf{K} + \sigma\,\mathbf{C} + \sigma^2\,\mathbf{M})\,\mathbf{w} = 0\end{gathered} \tag{3.1.7}$$

Notice that the shifted eigenvalue is $\lambda - \sigma$, therefore, the corresponding auxiliary equation is

$$\mathbf{M}(\lambda - \sigma)\,\mathbf{w} - \mathbf{M}(\lambda - \sigma)\,\mathbf{w} = 0 \tag{3.1.8}$$

Combining Eq.(3.1.7) and (3.1.8), we have the shifted form of the reduced eigenproblem as

$$\begin{gathered}(\lambda - \sigma)\begin{bmatrix}(\mathbf{C}+2\sigma\mathbf{M}) & \mathbf{M} \\ \mathbf{M} & \mathbf{0}\end{bmatrix}\begin{bmatrix}\mathbf{w} \\ (\lambda-\sigma)\mathbf{w}\end{bmatrix} = \\ \begin{bmatrix}-\mathbf{K}-\sigma\mathbf{C}-\sigma^2\mathbf{M} & \mathbf{0} \\ \mathbf{0} & \mathbf{M}\end{bmatrix}\begin{bmatrix}\mathbf{w} \\ (\lambda-\sigma)\mathbf{w}\end{bmatrix}\end{gathered} \tag{3.1.9}$$

where the shifted **A** and **B** matrices remain symmetric. Here, we only need to factor the shifted stiffness matrix $\mathbf{K} + \sigma\,\mathbf{C} + \sigma^2\,\mathbf{M}$, which is still in banded form. If we form $(\mathbf{B} - \sigma \mathbf{A}) \mathbf{z} = (\lambda - \sigma) \mathbf{A}\, \mathbf{z}$; then it is necessary to factor, or invert, the entire $(\mathbf{B} - \sigma \mathbf{A})$, which is much more expensive and hence should be avoided.

3.2 Generalized Rayleigh-Ritz method

In the solution of the eigenproblem resulting from an undamped dynamic system, i.e., $\omega^2\, \mathbf{M}\, \psi = \mathbf{K}\, \psi$ the Rayleigh-Ritz method is commonly used to obtain a reduced eigensystem. In this method, the property that the Rayleigh Quotient

$$R(\mathbf{x}) = \frac{\mathbf{x}^{\mathrm{T}}\, \mathbf{K}\, \mathbf{x}}{\mathbf{x}^{\mathrm{T}}\, \mathbf{M}\, \mathbf{x}} \tag{3.2.1}$$

possesses a stationary value in the neighborhood of each eigenvector is used to find the best approximation to the eigenvectors of $(\mathbf{M}, \mathbf{K})$ from the subspace spanned by the trial vectors. In the following, we show that the Rayleigh-Ritz method can be extended to reduce the original eigensystem associated with $(\mathbf{A}, \mathbf{B})$ onto a smaller one. To this end, we start with a brief account of some definitions which are related to subsequent discussion.

A square matrix pencil $(\mathbf{F}, \mathbf{G})$ of order n is called *regular* if $\mathbf{F}$ is non-singular. Such a matrix pencil will have n eigenvalues if they are counted according to their multiplicities. A regular symmetric matrix pencil of order n having n linear independent eigenvectors is called *simple*; otherwise, it is said to be *defective*. An eigenvector $\mathbf{z}$ of a symmetric simple matrix pencil $(\mathbf{F}, \mathbf{G})$ can be scaled such that

$$\mathbf{z}^{\mathrm{T}}\, \mathbf{F}\, \mathbf{z} = 1 \qquad \mathbf{z}^{\mathrm{T}}\, \mathbf{G}\, \mathbf{z} = \lambda \tag{3.2.2}$$

where λ is the eigenvalue associated with $\mathbf{z}$. For this simple matrix pencil, we form the quotient

$$R(\mathbf{z}) = \frac{\mathbf{z}^{\mathrm{T}}\, \mathbf{G}\, \mathbf{z}}{\mathbf{z}^{\mathrm{T}}\, \mathbf{F}\, \mathbf{z}} = \lambda \tag{3.2.3}$$

to demonstrate in the following that it is stationary in the neighborhood of the eigenvector $\mathbf{z}$. To establish that R has such stationary property, we introduce an arbitrary small variation in $\mathbf{z}$ and show that the resulting change in R is zero to the first order of the variation. That is, we consider $R(\mathbf{z}+\delta\mathbf{z})$ with $\delta\mathbf{z}$ being the small variation of an eigenvector $\mathbf{z}$

$$\begin{aligned} R(\mathbf{z}+\delta\mathbf{z}) &= \frac{(\mathbf{z}+\delta\mathbf{z})^{\mathrm{T}}\,\mathbf{G}\,(\mathbf{z}+\delta\mathbf{z})}{(\mathbf{z}+\delta\mathbf{z})^{\mathrm{T}}\,\mathbf{F}\,(\mathbf{z}+\delta\mathbf{z})} \\ &= R(\mathbf{z}) + \frac{(\mathbf{z}+\delta\mathbf{z})^{\mathrm{T}}\,\mathbf{G}\,(\mathbf{z}+\delta\mathbf{z})}{(\mathbf{z}+\delta\mathbf{z})^{\mathrm{T}}\,\mathbf{F}\,(\mathbf{z}+\delta\mathbf{z})} - \lambda\,\frac{(\mathbf{z}+\delta\mathbf{z})^{\mathrm{T}}\,\mathbf{F}\,(\mathbf{z}+\delta\mathbf{z})}{(\mathbf{z}+\delta\mathbf{z})^{\mathrm{T}}\,\mathbf{F}\,(\mathbf{z}+\delta\mathbf{z})} \\ &= R(\mathbf{z}) + \frac{(\mathbf{z}+\delta\mathbf{z})^{\mathrm{T}}\,(\mathbf{G}-\lambda\mathbf{F})\,(\mathbf{z}+\delta\mathbf{z})}{(\mathbf{z}+\delta\mathbf{z})^{\mathrm{T}}\,\mathbf{F}\,(\mathbf{z}+\delta\mathbf{z})} \qquad (3.2.4) \\ &= R(\mathbf{z}) + \frac{(\mathbf{z}+2\delta\mathbf{z})^{\mathrm{T}}\,(\mathbf{G}-\lambda\mathbf{F})\,\mathbf{z} + (\delta\mathbf{z})^{\mathrm{T}}\,(\mathbf{G}-\lambda\mathbf{F})\,\delta\mathbf{z}}{(\mathbf{z}+\delta\mathbf{z})^{\mathrm{T}}\,\mathbf{F}\,(\mathbf{z}+\delta\mathbf{z})} \\ &= R(\mathbf{z}) + \frac{(\delta\mathbf{z})^{\mathrm{T}}\,(\mathbf{G}-\lambda\mathbf{F})\,\delta\mathbf{z}}{(\mathbf{z}+\delta\mathbf{z})^{\mathrm{T}}\,\mathbf{F}\,(\mathbf{z}+\delta\mathbf{z})} \end{aligned}$$

where the equalities $\mathbf{z}^{\mathrm{T}}\,(\mathbf{G}-\lambda\mathbf{F})\,(\delta\mathbf{z}) = (\delta\mathbf{z})^{\mathrm{T}}\,(\mathbf{G}-\lambda\mathbf{F})\,\mathbf{z}$ and $(\mathbf{G}-\lambda\mathbf{F})\,\mathbf{z} = \mathbf{0}$ have been used. Note that the numerator in the last line of the preceding equation is equal to a term of second order in $\delta\mathbf{z}$. Since $\mathbf{z}^{\mathrm{T}}\,\mathbf{F}\,\mathbf{z} = 1$ and the $\delta\mathbf{z}$ is small, one can reasonably assume that the denominator is not zero. This shows that $R(\mathbf{z}+\delta\mathbf{z})$ is equal to $R(\mathbf{z})$ plus a second order term in $\delta\mathbf{z}$. That is, the first variation of the quotient R vanishes and, accordingly, R is stationary.

We now turn to the matrix pencil $(\mathbf{A}, \mathbf{B})$ obtained from the quadratic eigenproblem to examine the conditions under which the matrix pencil is simple. To determine whether $\mathbf{A}$ is singular, we compute the determinant of the matrix $\mathbf{A}$ as follows :

$$\begin{aligned} det\,\mathbf{A} &= det\begin{bmatrix} \mathbf{C} & \mathbf{M} \\ \mathbf{M} & \mathbf{0} \end{bmatrix} \\ &= (-1)^n\, det\begin{bmatrix} \mathbf{M} & \mathbf{0} \\ \mathbf{C} & \mathbf{M} \end{bmatrix} \qquad (3.2.5) \\ &= (-1)^n\,(\,det\,\mathbf{M}\,)^2 \end{aligned}$$

This result shows that det**A** does not depend on the elements of matrix **C** and that **A** is non-singular if **M** is non-singular. That is, the condition that **M** is non-singular is sufficient for the matrix pencil (**A**, **B**) to be regular. This and the assumption that the associated eigenproblem of the dynamic system considered has a full set of eigenvectors ensure that (**A**, **B**) is a simple matrix pencil. Therefore, the quotient

$$R(\mathbf{y}) = \frac{\mathbf{y}^{\mathrm{T}}\,\mathbf{B}\,\mathbf{y}}{\mathbf{y}^{\mathrm{T}}\,\mathbf{A}\,\mathbf{y}} \tag{3.2.6}$$

is stationary when **y** is in the neighborhood of the eigenvectors of (**A**, **B**).

Now, we can generalize the Rayleigh-Ritz method to obtain an approximation to the eigensolutions of (**A**, **B**) from a set of trial vectors. For this purpose, we consider an n by m matrix ($m \leq n$)

$$\mathbf{Q} = [\ \mathbf{q}_1\,\mathbf{q}_2\,\mathbf{q}_3 \cdot \cdot \cdot \cdot\ \mathbf{q}_m\ ] \tag{3.2.7}$$

which contains m trial vectors approximating the eigenvectors of (**A**, **B**). We look for the linear combinations of the $\mathbf{q}_i$ which give the best approximations to the eigenvectors. In other words, we want to find a vector **s** of dimension m such that $\mathbf{y} = \mathbf{Q}\,\mathbf{s}$ is the best approximation to the eigenvector from the subspace spanned by **Q**. To achieve this, we form the quotient

$$R(\mathbf{s}) = \frac{\mathbf{s}^{\mathrm{T}}\,\mathbf{Q}^{\mathrm{T}}\,\mathbf{B}\,\mathbf{Q}\,\mathbf{s}}{\mathbf{s}^{\mathrm{T}}\,\mathbf{Q}^{\mathrm{T}}\,\mathbf{A}\,\mathbf{Q}\,\mathbf{s}} \tag{3.2.8}$$

The best approximation **y** is obtained by invoking the property that the Rayleigh quotient $R(\mathbf{s})$ is stationary. The necessary condition for $R(\mathbf{s})$ to be stationary is that the vector **s** satisfy

$$\mathbf{A}^{*}\,\mathbf{s}\,\theta = \mathbf{B}^{*}\,\mathbf{s} \tag{3.2.9}$$

where $\mathbf{A}^{*}$ and $\mathbf{B}^{*}$ are m by m projected matrices given by

$$\mathbf{A}^{*} = \mathbf{Q}^{\mathrm{T}}\,\mathbf{A}\,\mathbf{Q} \qquad\qquad \mathbf{B}^{*} = \mathbf{Q}^{\mathrm{T}}\,\mathbf{B}\,\mathbf{Q} \tag{3.2.10}$$

The solution of Eq.(3.2.9) yields $\theta_1 , \ldots , \theta_m$, which are the Ritz values, and

$\mathbf{s}_1, \ldots, \mathbf{s}_m$, which are the parameters used to form the Ritz vectors $\mathbf{Y} = [\,\mathbf{y}_1, \ldots, \mathbf{y}_m\,]$ by the relation $\mathbf{y}_j = \mathbf{Q}\,\mathbf{s}_j$. These Ritz pairs $(\theta_j, \mathbf{y}_j)$ are the best approximations to the eigenpairs sought from the subspace spanned by the trial vectors $\mathbf{Q}$.

In essence, we have shown that the Rayleigh-Ritz method can be extended to the indefinite matrix pencil $(\mathbf{A}, \mathbf{B})$. From a set of trial vectors, the optimal combinations that approximate the eigensolutions of the original problem can be obtained through the solution of a reduced problem. This reduction technique makes the partial solution of a large eigenproblem feasible.

3.3 Projection method

In recent research on solving large sparse eigenproblems, the projection method has attracted much attention. In this section, we briefly review the general framework of the projection method and then describe how it can be used to solve the eigenproblem associated with a damped system.

Consider two subspaces L and K of the solution space, referred to as the right and the left *admissible space* respectively, and assume that they have the same dimensions. The projection method consists in approximating an exact eigenvector $\mathbf{u}$, by a vector $\tilde{\mathbf{u}}$ in subspace K, by requiring that the residual vector of $\tilde{\mathbf{u}}$ satisfy the Petrov-Galerkin condition, i.e., the residual vector of $\tilde{\mathbf{u}}$ is orthogonal to subspace L. When L = K we say that the method is an *orthogonal* projection method; otherwise, we say that the method is an *oblique* projection method. We choose the orthogonal projection method because it is simpler and requires less work than the oblique projection method.

The orthogonal projection method applied to solving $\lambda\,\mathbf{A}\,\mathbf{z} = \mathbf{B}\,\mathbf{z}$ seeks an approximate eigenvalue θ and its associated vector $\mathbf{y}$, which belongs to the subspace K, such that the following Galerkin condition is satisfied :

$$\theta \mathbf{A}\,\mathbf{y} - \mathbf{B}\,\mathbf{y} \perp \mathrm{K} \tag{3.3.1}$$

Let **Q** be an arbitrary orthogonal basis of K; then we can replace the preceding equation by

$$\mathbf{Q}^{\mathrm{T}} (\theta \mathbf{A}\,\mathbf{y} - \mathbf{B}\,\mathbf{y}) = \mathbf{0} \tag{3.3.2}$$

The fact that **y** is in the subspace of K implies that **y** = **Q s**, where **s** represents a set of free parameters. The choice of these free parameters in **s** is made to satisfy the Galerkin condition Eq.(3.3.2), that is, **s** is the solution of

$$\mathbf{Q}^{\mathrm{T}} (\theta \mathbf{A}\,\mathbf{Q} - \mathbf{B}\,\mathbf{Q})\, \mathbf{s} = \mathbf{0} \tag{3.3.3}$$

This expression is identical with Eq.(3.2.11) obtained from the generalized Rayleigh-Ritz approximation to the same problem. While the Rayleigh-Ritz method is restricted to those (**A**, **B**) which satisfy the condition of being simple matrix pencil, the projection method does not have this limitation. From this point of view the projection method, which analyzes the problem geometrically, is advantageous when compared to the generalized Rayleigh-Ritz method.

The important feature that makes the projection method work is obviously that the exact eigenvector is well approximated by some vectors of the subspace K. It is then desirable to estimate *a priori* the distance between the exact eigenvector and the subspace of approximation. A rigorous treatment of this matter involves detailed mathematical proof and remains to be investigated.

As it turns out, most methods for solving large sparse symmetric eigensystems can be formulated in terms of the orthogonal projection method. Among them, the two methods we will discuss later are the subspace iteration method and the Lanczos method. The major difference between them is that the dimension of the subspace of approximation K is fixed in the subspace iteration method while the dimension of K is increased by one at every step in the Lanczos method. The strategy of the subspace iteration method is to adjust gradually the subspace K of fixed dimension until it leads to in the required eigenvectors' direction. The strategy of the Lanczos method is to expand gradually the dimension of K until it contains the subspace spanned by all the required eigenvectors.

Chapter 4
Subspace Iteration Method

4.1 Consideration for complex eigenpairs

The subspace iteration method is recognized as an efficient method to extract the least dominant set of eigenpairs of an undamped system represented by $\omega^2 \mathbf{M} \psi = \mathbf{K} \psi$; therefore, it is desirable to extend this method to solve for the least dominant set of eigenpairs of a damped system represented by $\lambda \mathbf{A} \mathbf{z} = \mathbf{B} \mathbf{z}$. Theoretically, solving $\lambda \mathbf{A} \mathbf{z} = \mathbf{B} \mathbf{z}$ is the same as solving $\omega^2 \mathbf{M} \psi = \mathbf{K} \psi$; however, the former is computationally more complicated than the latter since in general the solutions of $\lambda \mathbf{A} \mathbf{z} = \mathbf{B} \mathbf{z}$ are complex while the solutions of $\omega^2 \mathbf{M} \psi = \mathbf{K} \psi$ are real. Due to the similarity in the two formulations, the conventional subspace iteration algorithm may be used to compute the eigenpairs of a damped system. For use in subsequent discussion, the essential steps in the subspace iteration method are summarized in Box 4.1.

We now show what is obtained during the iteration process, considering that the solutions generally are complex-valued. Assuming we have performed many iterations and have almost eliminated the undesirable higher mode components in **U**, we start the next iteration to further improve **U**. The first step is to solve for a new set of vectors **V** from

$$\mathbf{B}\,\mathbf{V} = \mathbf{A}\,\mathbf{U} \tag{4.1.1}$$

where **U** contains the approximate eigenvectors from the previous iteration and can be arranged as the following :

$$\mathbf{U} = [\, \mathbf{a}_1 + \mathbf{b}_1 i^* ,\, \mathbf{a}_1 - \mathbf{b}_1 i^* ,\, \mathbf{a}_2 + \mathbf{b}_2 i^* ,\, \mathbf{a}_2 - \mathbf{b}_2 i^* ,\, \ldots ,\, \mathbf{d}_1 ,\, \mathbf{d}_2 ,\, \ldots \,] \tag{4.1.2}$$

Since both **A** and **B** are real, **V** will have the same form as **U**; accordingly,

$$\mathbf{V} = [\, \mathbf{r}_1 + \mathbf{s}_1 i^* ,\, \mathbf{r}_1 - \mathbf{s}_1 i^* ,\, \mathbf{r}_2 + \mathbf{s}_2 i^* ,\, \mathbf{r}_2 - \mathbf{s}_2 i^* ,\, \ldots ,\, \mathbf{t}_1 ,\, \mathbf{t}_2 ,\, \ldots \,] \tag{4.1.3}$$

Box 4.1 *Subspace Iteration Method*

For k = 1, 2, 3, ... , until satisfied

1. Iterate from E_k to E_{k+1} :

$$\mathbf{B}\,\mathbf{V} = \mathbf{A}\,\mathbf{U}$$

2. Find the projections of the operators **B** and **A** onto E_{k+1} :

$$\mathbf{G} = \mathbf{V}^{\mathrm{T}}\,\mathbf{B}\,\mathbf{V} \qquad \mathbf{H} = \mathbf{V}^{\mathrm{T}}\,\mathbf{A}\,\mathbf{V}$$

3. Solve the projected eigensystem :

$$\mathbf{G}\,\mathbf{X} = \mathbf{H}\,\mathbf{X}\,\mathbf{\Theta}$$

4. Form an improved approximation to the eigenvectors :

$$\tilde{\mathbf{U}} = \mathbf{V}\,\mathbf{X}$$

5. Scale $\tilde{\mathbf{U}}$ and take $\tilde{\mathbf{U}}$ as **U** for the next iteration or, if the convergence criterion is satisfied, exit.

Then, provided that the approximating vectors **U** are not orthogonal to one of the required eigenvectors, we have

$$\mathbf{\Theta} \to \Lambda \quad \text{and} \quad \mathbf{U} \to \mathbf{Z} \quad \text{as} \quad k \to \infty$$

The second step is to form projection matrices **G** and **H** by

$$\mathbf{G} = \mathbf{V}^{\mathrm{T}}\,\mathbf{B}\,\mathbf{V} \qquad \text{and} \qquad \mathbf{H} = \mathbf{V}^{\mathrm{T}}\,\mathbf{A}\,\mathbf{V} \tag{4.1.4}$$

The matrices **G** and **H** have a special structure due to the way we arrange the matrices **U** and **V**. To show this structure, we partition **G** into the following 4 sub-matrices

$$\mathbf{G} = \begin{bmatrix} \mathbf{G}_{cc} & \mathbf{G}_{rc} \\ \mathbf{G}_{cr} & \mathbf{G}_{rr} \end{bmatrix} \tag{4.1.5}$$

where $\mathbf{G}_{cc}$ is constructed entirely from complex vectors, $\mathbf{G}_{cr}$ is constructed from complex vectors and real vectors, $\mathbf{G}_{rc}$ is the transpose of $\mathbf{G}_{cr}$, and $\mathbf{G}_{rr}$ is constructed entirely from real vectors. If we further partition $\mathbf{G}_{cc}$ into 2 by 2 submatrices which correspond to complex conjugate pairs of vectors, then all submatrices have the following structure

$$\begin{bmatrix} (\mathbf{r}_i^{\mathrm{T}}\mathbf{B}\mathbf{r}_j - \mathbf{s}_i^{\mathrm{T}}\mathbf{B}\mathbf{s}_j) + (\mathbf{r}_i^{\mathrm{T}}\mathbf{B}\mathbf{s}_j + \mathbf{s}_i^{\mathrm{T}}\mathbf{B}\mathbf{r}_j)\mathrm{i}^* & (\mathbf{r}_i^{\mathrm{T}}\mathbf{B}\mathbf{r}_j + \mathbf{s}_i^{\mathrm{T}}\mathbf{B}\mathbf{s}_j) - (\mathbf{r}_i^{\mathrm{T}}\mathbf{B}\mathbf{s}_j - \mathbf{s}_i^{\mathrm{T}}\mathbf{B}\mathbf{r}_j)\mathrm{i}^* \\ (\mathbf{r}_i^{\mathrm{T}}\mathbf{B}\mathbf{r}_j + \mathbf{s}_i^{\mathrm{T}}\mathbf{B}\mathbf{s}_j) + (\mathbf{r}_i^{\mathrm{T}}\mathbf{B}\mathbf{s}_j - \mathbf{s}_i^{\mathrm{T}}\mathbf{B}\mathbf{r}_j)\mathrm{i}^* & (\mathbf{r}_i^{\mathrm{T}}\mathbf{B}\mathbf{r}_j - \mathbf{s}_i^{\mathrm{T}}\mathbf{B}\mathbf{s}_j) - (\mathbf{r}_i^{\mathrm{T}}\mathbf{B}\mathbf{s}_j + \mathbf{s}_i^{\mathrm{T}}\mathbf{B}\mathbf{r}_j)\mathrm{i}^* \end{bmatrix}$$

We can also partition $\mathbf{G}_{cr}$ into 2 by 1 submatrices which correspond to complex conjugate pairs. All submatrices have the following structure

$$\begin{bmatrix} (\mathbf{r}_i^{\mathrm{T}}\mathbf{B}\mathbf{t}_j) + (\mathbf{s}_i^{\mathrm{T}}\mathbf{B}\mathbf{t}_j)\mathrm{i}^* \\ (\mathbf{r}_i^{\mathrm{T}}\mathbf{B}\mathbf{t}_j) - (\mathbf{s}_i^{\mathrm{T}}\mathbf{B}\mathbf{t}_j)\mathrm{i}^* \end{bmatrix}$$

$\mathbf{G}_{rr}$ has elements of the following form

$$\mathbf{t}_i^{\mathrm{T}}\mathbf{B}\mathbf{t}_j$$

Similarly, **H** has the same form as **G** except that **B** is replaced by **A** in the above formulae. The third step is to solve the projected eigensystem

$$\mathbf{G}\,\mathbf{X} = \mathbf{H}\,\mathbf{X}\,\boldsymbol{\Theta} \qquad (4.1.6)$$

where $\boldsymbol{\Theta}$ and **X** are eigenvalues and eigenvectors of the projected system. The last step is to find the improved approximation to the eigenvectors of the original system by

$$\tilde{\mathbf{U}} = \mathbf{V}\,\mathbf{X} \qquad (4.1.7)$$

where $\tilde{\mathbf{U}}$ is scaled to give **U** for a new iteration. This procedure is continued until a specified convergence criterion is fulfilled; then we have $\boldsymbol{\Theta}$ and **U** as the required eigensolutions.

It is clear from the foregoing discussion that if **U** contains complex vectors then all the **V**, **G** and **H** will become complex. This implies that when the subspace iteration method is applied to solve $\lambda\ \mathbf{A}\ \mathbf{z} = \mathbf{B}\ \mathbf{z}$, we must use complex arithmetic. The use of complex arithmetic not only requires more storage space but also more computational effort. Moreover, a solution system that can handle complex matrices is required for the solution of the projected eigensystem. To save storage space and computational effort, it is desirable to modify the algorithm to avoid the complex arithmetic. To this end, we make the following modification in the subspace iteration method when solving $\lambda \mathbf{A} \mathbf{z} = \mathbf{B} \mathbf{z}$. Note that all the information of a complex conjugate pair of vectors is contained in the real and imaginary parts of each complex vector. During the iteration process, we use the real and imaginary parts of a complex vector to replace the pair of complex conjugate vectors and retain the real vectors without modification. That is, we use

$$\mathbf{U}^* = [\, \mathbf{a}_1 \,, \mathbf{b}_1 \,, \mathbf{a}_2 \,, \mathbf{b}_2 \,, \ldots, \mathbf{d}_1 \,, \mathbf{d}_2 \,, \ldots \,] \qquad (4.1.8)$$

instead of $\mathbf{U}$ in the iteration process. As a result of this substitution, $\mathbf{V}^*$ becomes

$$\mathbf{V}^* = [\, \mathbf{r}_1 \,, \mathbf{s}_1 \,, \mathbf{r}_2 \,, \mathbf{s}_2 \,, \ldots, \mathbf{t}_1 \,, \mathbf{t}_2 \,, \ldots \,] \qquad (4.1.9)$$

and the modified projection matrices $\mathbf{G}^*$ and $\mathbf{H}^*$ can be obtained by Eq.(4.1.4) with $\mathbf{V}$ replaced by $\mathbf{V}^*$. We partition the matrix $\mathbf{G}^*$ as before. The 2 by 2 submatrices of $\mathbf{G}^*_{cc}$ now become

$$\begin{bmatrix} \mathbf{r}_i^{\mathrm{T}}\mathbf{B}\mathbf{r}_j & \mathbf{r}_i^{\mathrm{T}}\mathbf{B}\mathbf{s}_j \\ \mathbf{s}_i^{\mathrm{T}}\mathbf{B}\mathbf{r}_j & \mathbf{s}_i^{\mathrm{T}}\mathbf{B}\mathbf{s}_j \end{bmatrix}$$

The 2 by 1 submatrices of $\mathbf{G}^*_{cr}$ now become

$$\begin{bmatrix} \mathbf{r}_i^{\mathrm{T}}\mathbf{B}\mathbf{t}_j \\ \mathbf{s}_i^{\mathrm{T}}\mathbf{B}\mathbf{t}_j \end{bmatrix}$$

The submatrix $\mathbf{G}^*_{rr}$ remains unchanged and thus is equal to $\mathbf{G}_{rr}$. The matrix $\mathbf{H}^*$ is identical to $\mathbf{G}^*$ with $\mathbf{B}$ replaced by $\mathbf{A}$. We note that three quarters of the computational effort and half of the storage space can be eliminated by forming $\mathbf{G}^*_{cc}$ instead of $\mathbf{G}_{cc}$, and half of the computational effort and the storage space can be eliminated by forming $\mathbf{G}^*_{rc}$ and $\mathbf{G}^*_{cr}$ instead of $\mathbf{G}_{rc}$ and $\mathbf{G}_{cr}$.

The question which remains is the following : what is the relation between the solution obtained from using these modified matrices, which are distinguished by superscript *, and the solution obtained from using the original matrices? The answer is in the following theorem.

Theorem : If the $\mathbf{G}^*$ and $\mathbf{H}^*$ are formed according to the above procedure and the modified eigensystem is represented by $\mathbf{G}^* \mathbf{X}^* = \mathbf{H}^* \mathbf{X}^* \boldsymbol{\Theta}^*$; then we have $\Theta^* = \boldsymbol{\Theta}$ and $\mathbf{X}^* = \mathbf{N}\,\mathbf{X}$, where N is the transformation matrix defined in the proof.

Proof : Any complex conjugate pair of numbers can be *factored* into its components and units in the following way

$$[\, \alpha+\beta i \quad \alpha-\beta i \,] = [\, \alpha \quad \beta \,]\ \mathbf{L} \tag{4.1.10}$$

where **L** contains the real and imaginary unit and can be found to be

$$\mathbf{L} = \begin{bmatrix} 1 & 1 \\ i & -i \end{bmatrix} \tag{4.1.11}$$

Using this factorization, we can relate the original iteration vectors to the modified iteration vectors by

$$\mathbf{U} = \mathbf{U}^*\,\mathbf{N} \qquad \text{and} \qquad \mathbf{V} = \mathbf{V}^*\,\mathbf{N} \tag{4.1.12}$$

where N is made up of the **L** in the first nc 2 by 2 diagonal blocks, $2nr$ unities along the rest of the diagonal, and zero everywhere else. From this formulation, the relationship between the original projected matrices and the modified projected matrices is

$$\mathbf{G} = \mathbf{N}^T\,\mathbf{G}^*\,\mathbf{N} \qquad \text{and} \qquad \mathbf{H} = \mathbf{N}^T\,\mathbf{H}^*\,\mathbf{N} \tag{4.1.13}$$

This indicates that $\mathbf{G}^*$ and $\mathbf{H}^*$ are obtained by an *equivalent transformation* from **G** and **H** respectively and they have the same transformation matrix **N**. Therefore, the two *pencils* $(\mathbf{G}^*, \mathbf{H}^*)$ and $(\mathbf{G}, \mathbf{H})$ are *equivalent*. We substitute Eq.(4.1.13) into $\mathbf{G}\,\mathbf{X} = \mathbf{H}\,\mathbf{X}\,\boldsymbol{\Theta}$ to obtain

$$\mathbf{N}^T\,\mathbf{G}^*\,\mathbf{N}\,\mathbf{X} = \mathbf{N}^T\,\mathbf{H}^*\,\mathbf{N}\,\mathbf{X}\,\boldsymbol{\Theta} \tag{4.1.14}$$

Since N^T is non-singular, we can premultiply Eq.(4.1.14) by $(N^T)^{-1}$ to obtain

$$\mathbf{G}^* \ (\mathbf{N}\,\mathbf{X}) = \mathbf{H}^* \ (\mathbf{N}\,\mathbf{X})\, \mathbf{\Theta} \qquad (4.1.15)$$

This concludes the proof. □

To find the modified improved vectors $\bar{\mathbf{U}}^*$ we substitute $\mathbf{N}\,\mathbf{X}$ for $\mathbf{X}^*$ in $\bar{\mathbf{U}}^* = \mathbf{V}^*\,\mathbf{X}^*$ and obtain $\bar{\mathbf{U}}^* = \mathbf{V}^*\,\mathbf{N}\,\mathbf{X} = \mathbf{V}\,\mathbf{X}$, which is equal to $\bar{\mathbf{U}}$. This indicates that the same result will be obtained by using $\mathbf{U}^*$ as by using $\mathbf{U}$. That is, the modified iteration vectors $\mathbf{U}^*$ have been transformed back by the algorithm itself after one complete cycle of subspace iteration and no inverse transformation is required to bring $\mathbf{U}^*$ back to $\mathbf{U}$.

The main features of the above discussion can be summarized as follows. To use the procedure described in Box 4.1, we can take $\mathbf{U}^*$ as the iteration vectors to reduce computational effort and storage space. Both $\mathbf{U}^*$, $\mathbf{V}^*$ are real-valued and hence only real arithmetic is required in the iteration process. Moreover, $\mathbf{G}^*$ and $\mathbf{H}^*$ are also real and thus the solution of the projected eigensystem $\mathbf{G}^*\,\mathbf{X}^* = \mathbf{H}^*\,\mathbf{X}^*\,\mathbf{\Theta}^*$ can be performed using a QZ algorithm, which is available from the EISPACK library.

4.2 Practical implementation

The theoretical aspects of solving for the eigenpairs of a damped system by the subspace iteration method have been described in the previous section. In this section, we consider practical implementation of the method and present a computation algorithm.

We used **A** and **B** instead of **M**, **C** and **K** in the discussion of the theoretical properties. In practical implementation, however, to minimize storage requirements both **A** and **B** are not formed explicitly. To work directly with the matrices **M**, **C**, and **K**, we partition the iteration matrices **U** and **V** equally into upper and lower parts as

$$\mathbf{U} = \begin{bmatrix} \mathbf{U}_u \\ \mathbf{U}_l \end{bmatrix} \qquad \mathbf{V} = \begin{bmatrix} \mathbf{V}_u \\ \mathbf{V}_l \end{bmatrix} \tag{4.2.1}$$

A result which follows immediately from this partitioning method is that after the solution of the equation $\mathbf{B}\ \mathbf{V} = \mathbf{A}\ \mathbf{U}$ we have

$$\mathbf{M}\ \mathbf{V}_l = \mathbf{M}\ \mathbf{U}_u \quad \text{or} \quad \mathbf{V}_l = \mathbf{U}_u \tag{4.2.2}$$

That is, the lower part of **V** is just the upper part of **U**. Therefore, it is not necessary to factor, or invert, **M**. This is because the lower part of matrices **A** and **B** comes from an identity equation, as already shown in Chapter 2.

As in any iteration method, we need a criterion to judge whether the solution has converged to within a prescribed tolerance during iterations. Let $\lambda_j = \lambda_{Rj} + \lambda_{Ij} i^*$, $\lambda_{j+1} = \lambda_{Rj+1} + \lambda_{Ij+1} i^*$ be the approximates found in two consecutive iterations, then the criterion for convergence is defined as

$$\sqrt{(\Delta_R)^2 + (\Delta_I)^2} \leq tol \tag{4.2.3}$$

where *tol* represents a prescribed tolerance and

$$\Delta_R = 1.0 - \frac{\lambda_{Rj}}{\lambda_{Rj+1}} \tag{4.2.4a}$$

$$\Delta_I = 1.0 - \frac{\lambda_{Ij}}{\lambda_{Ij+1}} \tag{4.2.4b}$$

This criterion also works for real eigenvalues.

As the following section will demonstrate, it takes much more effort to solve the projected eigenproblem of a damped system than to solve a projected eigenproblem of an undamped system, since the solution of a damped system are complex while the solutions of an undamped system are real. Therefore, the projected eigensystem is formed and solved every two iterations instead of every iteration. This strategy also will make the rate of convergence in solving a damped system of the same order as the rate of convergence in solving the corresponding undamped system. For example when the damping matrix is null, then the number of iterations required to obtain the solutions of $\lambda\ \mathbf{A}\ \mathbf{z} = \mathbf{B}\ \mathbf{z}$ by the above strategy is almost the same as the number of iterations required to obtain the solutions of $\omega^2\ \mathbf{M}\ \psi = \mathbf{K}\ \psi$ by the conventional subspace algorithm.

We summarize the above discussion and present the CSUBSP algorithm for extracting eigenpairs of a damped system in Box 4.2. From Box 4.2 we can see that one iteration using m vectors requires the following number of operations

$$\begin{gathered} 4m\,\mu(\mathbf{M}) + 2m\,\mu(\mathbf{C}) + 2m\,\nu(\mathbf{K}) \\ 4nm^2 + 5nm + 3m \qquad (4.2.5) \\ cost(\mathrm{RGG}) \end{gathered}$$

where $\mu(\mathbf{M})$ and $\mu(\mathbf{C})$ represent the number of operations to form $\mathbf{M}\ \mathbf{x}$ and $\mathbf{C}\ \mathbf{x}$, respectively, and $\nu(\mathbf{K})$ represents the number of operations to solve $\mathbf{K}\ \mathbf{y} = \mathbf{x}$ for typical n-vectors $\mathbf{x}$ and $\mathbf{y}$. In Box 4.2 and in the above discussion, an iteration vector means either a complex conjugate pair of vectors or a real pair of vectors. Therefore, m iteration vectors contain $2m$ columns of component vectors, which will become m pairs of Ritz vectors (some in complex conjugate pairs and others in real pairs) at the end of the iteration process. Recall that the number of operations required to perform one iteration by a conventional subspace iteration algorithm, such as SUBSP in FEAP, to solve $\omega^2\ \mathbf{M}\ \psi = \mathbf{K}\ \psi$ is

$$\begin{gathered} q\mu(\mathbf{M}) + q\nu(\mathbf{K}) \\ 2nq^2 + 4nq + q \qquad (4.2.6) \\ cost(\mathrm{QL}) \end{gathered}$$

where q is the number of iteration vectors used. Let us assume that the same number of iteration vectors is used to solve a damped system and its corresponding undamped system, that is $m = 2q$; then we see that the number of operations per iteration required by CSUBSP is much larger than the number of operations required by SUBSP. The ratio between the two numbers of operations ranges from 4 to more than 8 depending upon the *cost*(RGG) relative to the *cost*(QL), $\mu(\mathbf{M})$ and $\mu(\mathbf{C})$ relative to $\nu(\mathbf{K})$, and the ratio of q to n. That is, using CSUBSP to extract a few eigenpairs of a damped system requires at least four times as much effort as using SUBSP to extract the same number of eigenpairs of the corresponding undamped system. This will be shown explicitly by examples in the following section.

For a given number of iteration vectors, the number of iterations required to achieve convergence by the subspace iteration method depends on how close the starting space is to the subspace spanned by the required eigenvectors. The closer the starting space, the fewer the number of iterations and hence the less the computer CPU time needed to obtain solutions. The starting vectors used to obtain the solutions of the examples in the next section are constructed by evenly distributing n unities on $2m$ columns of vectors with zeroes at other entries. This type of starting vectors is basically the same as that currently used by SUBSP in FEAP. This choice of starting vectors may not be optimal; other choices, based on previous experience and on the characteristics of the system to be solved, may be more desirable. As the examples in Chapter 2 demonstrate, an eigenvector of a damped system contains real and imaginary parts or, if put in another way, contains an amplitude and a phase angle. Therefore, it is much more difficult to predict good starting vectors of a damped system than of an undamped system.

4.3 Numerical examples

In this section, we present several examples to show the capability of the subspace iteration algorithm CSUBSP to find the eigensolutions of damped systems.

To examine the effect of different types of damping matrices, we solve two groups of problems : (1) beam structures with lumped damping, as described in Test Problems 1 and 2 and (2) truss structures with distributed damping, as described in Test Problems 3 and 4. The following are used as the criteria for comparison :

(1) the number of vectors required and the number of the guard vectors used during the iteration process,

(2) the number of iterations performed to get the required number of eigenvalues within a prescribed tolerance, which is set to be 10^{-12} for the following examples,

(3) CPU time used by RGG to solve the reduced eigensystem $\mathbf{G} \mathbf{X} = \mathbf{H} \mathbf{X} \mathbf{\Theta}$, and

(4) total CPU time to solve the problem.

We also present the results of the corresponding undamped system solved by the conventional subspace iteration algorithm SUBSP to show explicitly how much more effort is required to solve a damped system than to solve the corresponding undamped system.

In the first group of problems, we consider three cases (1) c = 0, (2) c = 5 and (3) c = 5000 to examine how the lumped damping will affect the convergence rate of the algorithm. Table 4.1 and Table 4.2 summarize the results obtained for Test Problem 1 by CSUBSP and SUBSP, respectively. Similarly, Table 4.3 and Table 4.4 summarize the results obtained for Test Problem 2 by CSUBSP and SUBSP, respectively. From the results shown in Table 4.1 to Table 4.4, we observe the following.

(1) The solution for a damped system with null damping by CSUBSP requires almost the same number of iterations as the solution of the corresponding undamped system by SUBSP. This implies that for undamped systems the starting vectors used in CSUBSP are as good as those used in SUBSP. But when the damping coefficient c is not equal to zero, the CSUBSP takes more

iterations to converge to the required solutions.

(2) It is difficult to decide how many guard vectors should be used to achieve minimum CPU time, especially when damping is present.

(3) The CPU time spent on using RGG is significantly greater than the CPU time spent on using QL, even in these relatively small problems.

From these two examples we can perceive an important feature pertaining to the solution of a quadratic eigenproblem. In Chapter 2 we showed that eigenvalues of a damped system appear in pairs. For underdamped modes, α_j and $\bar{\alpha}_j$ appear simultaneously. For overdamped modes, β_j and $\hat{\beta}_j$ appear simultaneously. In heavily damped systems, such as the systems where c = 5000 in the above examples, the modulus of the primary eigenvalue β_1 can be very small while the modulus of the secondary eigenvalue $\hat{\beta}_1$ can be very large. But they are tied together; i.e., during the subspace iteration process, we cannot have one without having the other. As a result, convergence of the primary eigenvalue is fast during the iteration process while convergence of the secondary eigenvalue is slow. Sometimes, the secondary eigenvalue may not converge at all if it exceeds all the eigenvalues associated with those eigenvectors which span the subspace under consideration. Fortunately, large secondary eigenvalues can be ignored in computing the response of the structure. This will be shown in Chapter 6.

In the second group of problems, we assume that the system has distributed damping. Hence, each truss member may have different damping which results in a damping matrix with the same banded structure as the stiffness matrix. Table 4.5 and Table 4.6 summarize the results obtained for Test Problem 3 by CSUBSP and SUBSP, respectively. Similarly, Table 4.7 and Table 4.8 summarize the results obtained for Test Problem 4 by CSUBSP and SUBSP, respectively. From the results shown in Table 4.5 to Table 4.8, we observe the following.

(1) Since the damping is relatively small, we need only approximately the same number of iterations to solve the damped system using CSUBSP and the corresponding undamped system using SUBSP.

(2) The optimum number of guard vectors is the same for the damped system and the corresponding undamped system in both examples considered. This is because the mode shapes of a lightly damped system do not change much from the mode shapes of the corresponding undamped system.

(3) While the CPU time spent on using QL is about 23% and 5% of the total CPU time spent to solve Test Problem 3 and 4, respectively, the CPU time spent on using RGG is about 54% and 21% of the total CPU time spent to solve Test Problem 3 and 4, respectively.

From the discussion of the results from the Test Problems, it is apparent that CSUBSP is quite expensive compared to SUBSP. Although it is possible to modify the algorithm so that RG, instead of RGG, may be used to solve the projected eigenproblem, the large number of iterations required to achieve convergence cannot be reduced unless an improved set of starting vectors is used. Therefore, the subspace iteration method is not an efficient method to extract a least dominate set of eigenpairs of a general problem except where only a few (say two or three) iterations are required to achieve convergence.

Box 4.2 *Subspace Iteration Algorithm for Damped Systems*

INITIAL CALCULATIONS :	OPERATION COUNT
1. Factorize $\mathbf{K}$	$\frac{1}{2}nb^2$
2. Select starting iteration vectors $\mathbf{U}$	
$\mathbf{U} = \begin{bmatrix} \mathbf{U}_u \\ \mathbf{U}_l \end{bmatrix} =$ random vectors	
SUBSPACE ITERATIONS : For i = 1,2...	OPERATION COUNT
1. Form $\mathbf{A}\,\mathbf{U} = \mathbf{W}$	
$\mathbf{W}_u = \mathbf{C}\,\mathbf{U}_u + \mathbf{M}\,\mathbf{U}_l\ ,\ \mathbf{W}_l = \mathbf{M}\,\mathbf{U}_u$	$m\,\mu(\mathrm{C}) + 2m\,\mu(\mathrm{M})$
2. Form $\mathbf{V}$	
$\mathbf{V}_u = -\,\mathbf{K}^{-1}\,\mathbf{W}_u\ ,\ \mathbf{V}_l = \mathbf{U}_u$	$m\,\nu(\mathrm{K})$
3. Scale $\mathbf{V}$ such that for j from 1 to m	
$\mid \mathbf{v}_j^{\mathrm{T}}\,\mathbf{B}\,\mathbf{v}_j \mid\ = 1.0$	$3nm$
4. Form $\mathbf{A}\,\mathbf{V} = \underline{\mathbf{U}}$	
$\underline{\mathbf{U}_u} = \mathbf{C}\,\mathbf{V}_u + \mathbf{M}\,\mathbf{V}_l\ ,\ \underline{\mathbf{U}_l} = \mathbf{M}\,\mathbf{V}_u$	$m\,\mu(\mathrm{C}) + 2m\,\mu(\mathrm{M})$
5. Form projected matrices	
$\mathbf{G} = \mathbf{V}_u^{\mathrm{T}}\,\mathbf{W}_u + \mathbf{V}_l^{\mathrm{T}}\,\mathbf{W}_l$	$nm\,(m+1)$
$\mathbf{H} = \mathbf{V}_u^{\mathrm{T}}\,\underline{\mathbf{U}_u} + \mathbf{V}_l^{\mathrm{T}}\,\underline{\mathbf{U}_l}$	$nm\,(m+1)$
6. Solve the projected eigenproblem	
$\mathbf{H}\,\mathbf{X} = \mathbf{G}\,\mathbf{X}\,\mathbf{\Lambda}^{-1}$	*cost* (RGG)
7. Check for convergence	
If $\sqrt{(\Delta_{\mathrm{R}})^2 + (\Delta_{\mathrm{I}})^2} \leq tol$, exit.	$5m$
8. Form new iteration vectors $\mathbf{U}$	
$\mathbf{W}_u = \underline{\mathbf{U}_u}\,\mathbf{X}$	nm^2
$\mathbf{U}_u = -\,\mathbf{K}^{-1}\,\mathbf{W}_u$	$m\,\nu(\mathrm{K})$
$\mathbf{U}_l = \mathbf{V}_u\,\mathbf{X}$	nm^2
FINAL CALCULATIONS :	OPERATION COUNT
1. Form eigenvectors $\mathbf{U}$	
$\mathbf{U}_u = \mathbf{V}_u\,\mathbf{X}\ ,\ \mathbf{U}_l = \mathbf{V}_l\,\mathbf{X}$	$2nm^2$

Table 4.1 *Test Problem 1 by CSUBSP*

damping	no. of vectors & guard vectors	no. of iterations	CPU time for RGG	total CPU time
c = 0	4,1	9	8.4	25.5
	4,2	8	12.0	31.0
	4,3	7	16.0	36.3
	4,4	5	17.3	34.6
c = 5	4,1	19	16.9	52.0
	4,2	12	17.5	45.9
	4,3	10	22.6	51.4
	4,4	6	19.4	40.2
c = 5000	4,1	19	17.4	52.6
	4,2	12	18.3	46.5
	4,3	10	23.3	52.1
	4,4	7	23.9	48.1

Table 4.2 *Test Problem 1 by SUBSP*

no. of vectors & guard vectors	no. of iterations	CPU time for QL	total CPU time
4,1	10	0.5	4.3
4,2	8	0.7	4.5
4,3	7	0.9	5.0
4,4	5	0.9	4.6

Table 4.3 *Test Problem 2 by CSUBSP*

damping	no. of vectors & guard vectors	no. of iterations	CPU time for RGG	total CPU time
c = 0	8,2	10	38.2	123.3
	8,4	9	80.5	184.9
	8,6	9	94.1	219.0
	8,8	6	93.5	194.8
c = 5	8,2	17	116.4	268.7
	8,4	10	117.0	233.1
	8,6	9	160.2	291.0
	8,8	7	186.7	310.5
c = 5000	8,2	17	110.2	263.3
	8,4	10	105.4	221.5
	8,6	9	145.2	276.5
	8,8	7	165.5	289.5

Table 4.4 *Test Problem 2 by SUBSP*

no. of vectors & guard vectors	no. of iterations	CPU time for QL	total CPU time
8,2	11	2.7	17.4
8,4	9	3.6	19.5
8,6	9	5.5	24.7
8,8	6	5.0	21.2

Table 4.5 *Test Problem 3 by CSUBSP*

no. of vectors & guard vectors	no. of iterations	CPU time for RGG	total CPU time
12,2	23	421.9	977.0
12,4	18	483.2	1012.9
12,6	21	794.2	1534.2
12,8	18	919.4	1665.4
12,10	13	880.8	1503.5
12,12	11	948.4	1551.8

Table 4.6 *Test Problem 3 by SUBSP*

no. of vectors & guard vectors	no. of iterations	CPU time for QL	total CPU time
12,2	25	16.9	98.7
12,4	20	19.3	99.5
12,6	21	27.9	128.4
12,8	21	36.9	157.2
12,10	13	29.8	118.5
12,12	12	35.2	130.8

Table 4.7 *Test Problem 4 by CSUBSP*

no. of vectors & guard vectors	no. of iterations	CPU time for RGG	total CPU time
20,2	48	2928.2	24855.6
20,4	35	2778.9	20992.8
20,6	29	2896.6	20123.3
20,8	22	2740.6	17394.0
20,10	18	2745.8	16122.8
20,12	18	3321.9	18138.8
20,14	12	2614.5	13431.2
20,16	15	3874.7	18829.2
20,18	12	3641.1	16691.6
20,20	12	4227.0	18405.6

Table 4.8 *Test Problem 4 by SUBSP*

no. of vectors & guard vectors	no. of iterations	CPU time for QL	total CPU time
20,2	43	95.7	2842.4
20,4	36	101.2	2749.2
20,6	28	98.3	2401.7
20,8	23	97.7	2232.8
20,10	18	91.1	1953.5
20,12	15	91.0	1799.1
20,14	13	95.9	1752.2
20,16	15	126.6	2195.3
20,18	12	119.2	1938.2
20,20	11	125.6	1948.6

Chapter 5
Lanczos Method

5.1 Lanczos algorithm for damped systems

The Lanczos algorithm was introduced in 1950 as an efficient method to extract some eigenvalues and associated eigenvectors of a symmetric standard eigenproblem. It can also be used to solve $\omega^2 \mathbf{M} \psi = \mathbf{K} \psi$, since this generalized eigenproblem can be transformed into a standard one which is still symmetric. However, we can avoid the transformation by working directly with $\mathbf{K}_\sigma^{-1} \mathbf{M} \psi = \frac{1}{\omega^2} \psi$ where $\mathbf{K}_\sigma = \mathbf{K} - \sigma \mathbf{M}$ and σ is a shift. Although $\mathbf{K}_\sigma^{-1} \mathbf{M}$ is not symmetric, it is self-adjoint with respect to the $\mathbf{M}$ inner product defined by $(\mathbf{u}, \mathbf{v})_\mathbf{M} = \mathbf{v}^T \mathbf{M} \mathbf{u}$ (see [N3] for details). Given a starting vector, the Lanczos algorithm generates a sequence of vectors which are $\mathbf{M}$-orthonormal to each other. These vectors, known as Lanczos vectors, are used in the Rayleigh-Ritz procedure to transform the original system into a smaller symmetric tridiagonal system. The solutions of the reduced tridiagonal system can be obtained easily and inexpensively. In addition, usually almost half of the solutions obtained are very good approximates to the eigenpairs. These advantages make the Lanczos algorithm a favorable method for the solution of large eigenproblems.

Both matrices of the pencil $(\mathbf{A}, \mathbf{B})$ associated with a damped system are indefinite. Therefore, the weighted inner-product of a vector is not necessarily positive, as stated in Chapter 2. Except for this *improper* inner-product, the rest of the Lanczos algorithm for solving $\omega^2 \mathbf{M} \psi = \mathbf{K} \psi$ may be applied to solving $\lambda \mathbf{A} \mathbf{z} = \mathbf{B} \mathbf{z}$. To deduce an algorithm for solving $\lambda \mathbf{A} \mathbf{z} = \mathbf{B} \mathbf{z}$, we proceed by induction as follows. Assuming that the first j Lanczos vectors $(\mathbf{q}_1, \mathbf{q}_2, \ldots, \mathbf{q}_j)$ have been found, we describe how to construct the next Lanczos vector. Here, we require that the $\mathbf{q}_{j+1}$ satisfy the condition $\mathbf{q}_{j+1}^T \mathbf{A} \mathbf{q}_i = 0$ for all i from 1 to j; that is, the new

Lanczos vector is **A**-orthogonal to all the previous Lanczos vectors. To obtain $\mathbf{q}_{j+1}$, a preliminary vector $\bar{\mathbf{q}}_{j+1}$ is first calculated from the previous vector $\mathbf{q}_j$ as in the Krylov sequence.

$$\bar{\mathbf{q}}_{j+1} = \mathbf{B}^{-1}\,\mathbf{A}\,\mathbf{q}_j \tag{5.1.1}$$

In general, this preliminary vector can be expressed as a linear combination of all the previous Lanczos vectors and a residual vector; namely,

$$\bar{\mathbf{q}}_{j+1} = \hat{\mathbf{q}}_{j+1} + \alpha_j \mathbf{q}_j + \beta_{j-1}\mathbf{q}_{j-1} + \epsilon_{j-2}\mathbf{q}_{j-2} + \cdots \tag{5.1.2}$$

where $\hat{\mathbf{q}}_{j+1}$ is the residual vector, which is **A**-orthogonal to all previous Lanczos vectors, and α_j, β_{j-1}, ϵ_{j-2}, . . . are the components of $\bar{\mathbf{q}}_{j+1}$ in the directions of the previous Lanczos vectors. These component coefficients can be evaluated by imposing the condition of **A**-orthogonality among the Lanczos vectors. Thus, pre-multiplying both sides of Eq.(5.1.2) by $\mathbf{q}_j^T\,\mathbf{A}$, we obtain

$$\begin{aligned}\mathbf{q}_j^T\,\mathbf{A}\,\bar{\mathbf{q}}_{j+1} = \mathbf{q}_j^T\,\mathbf{A}\,\hat{\mathbf{q}}_{j+1} + \alpha_j \mathbf{q}_j^T\,\mathbf{A}\,\mathbf{q}_j\, + \\ \beta_{j-1}\mathbf{q}_j^T\,\mathbf{A}\,\mathbf{q}_{j-1} + \epsilon_{j-2}\mathbf{q}_j^T\,\mathbf{A}\,\mathbf{q}_{j-2} + \cdots\end{aligned} \tag{5.1.3}$$

Here the first term on the right-hand side vanishes due to **A**-orthogonality, and all terms after the second vanish for the same reason. Hence, the component of $\bar{\mathbf{q}}_{j+1}$ along $\mathbf{q}_j$ can be readily obtained through

$$\alpha_j = \frac{\mathbf{q}_j^T\,\mathbf{A}\,\bar{\mathbf{q}}_{j+1}}{\mathbf{q}_j^T\,\mathbf{A}\,\mathbf{q}_j} \tag{5.1.4}$$

The component of $\bar{\mathbf{q}}_{j+1}$ along $\mathbf{q}_{j-1}$ may be found similarly by pre-multiplying Eq.(5.1.2) by $\mathbf{q}_{j-1}^T\mathbf{A}$. In this case all terms except the third vanish due to **A**-orthogonality, so we have

$$\beta_{j-1} = \frac{\mathbf{q}_{j-1}^T\,\mathbf{A}\,\bar{\mathbf{q}}_{j+1}}{\mathbf{q}_{j-1}^T\,\mathbf{A}\,\mathbf{q}_{j-1}} \tag{5.1.5}$$

Similarly, the component of $\mathbf{q}_{j-2}$ contained in $\bar{\mathbf{q}}_{j+1}$ is found to be

$$\epsilon_{j-2} = \frac{\mathbf{q}_{j-2}^{\mathrm{T}} \mathbf{A} \bar{\mathbf{q}}_{j+1}}{\mathbf{q}_{j-2}^{\mathrm{T}} \mathbf{A} \mathbf{q}_{j-2}} \tag{5.1.6}$$

Making use of Eq.(5.1.1) and the fact that the transpose of a scalar and the scalar are identical, we obtain

$$\begin{aligned} \mathbf{q}_{j-2}^{\mathrm{T}} \mathbf{A} \bar{\mathbf{q}}_{j+1} &= \mathbf{q}_{j-2}^{\mathrm{T}} \mathbf{A} \mathbf{B}^{-1} \mathbf{A} \mathbf{q}_{j} \\ &= \mathbf{q}_{j}^{\mathrm{T}} \mathbf{A} \mathbf{B}^{-1} \mathbf{A} \mathbf{q}_{j-2} \\ &= \mathbf{q}_{j}^{\mathrm{T}} \mathbf{A} \bar{\mathbf{q}}_{j-1} \end{aligned} \tag{5.1.7}$$

Next, expanding $\bar{\mathbf{q}}_{j-1}$ in terms of the preceding Lanczos vectors and the residual vector $\hat{\mathbf{q}}_{j-1}$ as in Eq.(5.1.2), we obtain

$$\mathbf{q}_{j}^{\mathrm{T}} \mathbf{A} \bar{\mathbf{q}}_{j-1} = \mathbf{q}_{j}^{\mathrm{T}} \mathbf{A} \left(\hat{\mathbf{q}}_{j-1} + \alpha_{j-2}\mathbf{q}_{j-2} + \beta_{j-3}\mathbf{q}_{j-3} + \epsilon_{j-4}\mathbf{q}_{j-4} + \ldots\right. \tag{5.1.8}$$

Since all terms on the right hand side vanish due to the **A**-orthogonality, we achieve the anticipated result $\epsilon_{j-2} = 0$. A similar manipulation could be applied to Eq.(5.1.2) to demonstrate that all further terms in the expansion of $\bar{\mathbf{q}}_{j+1}$ vanish. In other words, $\bar{\mathbf{q}}_{j+1}$ can be expressed as the combination of only the previous two Lanczos vectors and the residual vector. Therefore, we can combine Eq.(5.1.1) and Eq.(5.1.2) to give the recurrence formula for deriving the residual vector $\hat{\mathbf{q}}_{j+1}$ as

$$\hat{\mathbf{q}}_{j+1} = \mathbf{B}^{-1} \mathbf{A} \mathbf{q}_{j} - \alpha_{j} \mathbf{q}_{j} - \beta_{j-1} \mathbf{q}_{j-1} \tag{5.1.9}$$

with α_j and β_{j-1} given in Eq.(5.1.4) and Eq.(5.1.5) respectively. The new Lanczos vector is then obtained simply by scaling the residual vector $\hat{\mathbf{q}}_{j+1}$, i.e.,

$$\mathbf{q}_{j+1} = \frac{\hat{\mathbf{q}}_{j+1}}{\gamma_{j+1}} \tag{5.1.10}$$

where γ_{j+1} is the *pseudo length* of $\hat{\mathbf{q}}_{j+1}$ and is defined as

$$\gamma_{j+1} = \sqrt{(\delta_{j+1} \hat{\mathbf{q}}_{j+1}^{\mathrm{T}} \mathbf{A} \hat{\mathbf{q}}_{j+1})} \tag{5.1.11}$$

with $\delta_{j+1} = sgn\ (\hat{\mathbf{q}}_{j+1}^T\ \mathbf{A}\ \hat{\mathbf{q}}_{j+1})$. Here we use an extra array $\boldsymbol{\delta}$ to store the pseudo length of the Lanczos vectors, which is normalized to be 1 or -1.

In the above derivation, we assumed that γ_{j+1} is not equal to zero. Although in practice it is highly improbable that a zero γ_{j+1} is encountered; we still include the discussion of this situation for the completeness of the proposed algorithm. For the indefinite matrix pencil under consideration, there are two possible alternatives when γ_{j+1} is equal to zero : (1) $\hat{\mathbf{q}}_{j+1}$ is equal to zero, or (2) $\hat{\mathbf{q}}_{j+1}$ is not equal to zero. If the first case occurs, which means that we have captured an *invariant subspace* [P1], every Ritz pair is an exact eigenpair of the original system. If the second case occurs, which implies that we have unfortunately chosen an unlucky starting vector, we can simply start the procedure over by choosing another starting vector.

An algorithm for computing the Lanczos vectors is summarized in Box 5.1, showing that only $14n + 2\mu(\mathbf{M}) + \mu(\mathbf{C}) + \nu(\mathbf{K})$ multiplications are required to generate each new Lanczos vector, where $\mu(\mathbf{M})$, $\mu(\mathbf{C})$ represents the number of operations to compute $\mathbf{M}\ \mathbf{x}$, $\mathbf{C}\ \mathbf{x}$, respectively, and $\nu(\mathbf{K})$ represents the number of operations to solve $\mathbf{K}\ \mathbf{y} = \mathbf{x}$ for typical n-vectors $\mathbf{x}$, $\mathbf{y}$. The algorithm can take full advantage of the symmetry and sparsity of the matrices **M**, **C**, and **K** and does not even need to explicitly form matrices **A** and **B**.

5.2 Orthogonality between Lanczos vectors

The algorithm presented above involves orthogonalization against only the two preceding vectors at each step. In finite precision arithmetic, inevitable rounding errors in computation will generate vectors that are not orthogonal to each other. To be precise about the loss of orthogonality between Lanczos vectors, we measure orthogonality between $\mathbf{q}_j$ and $\mathbf{q}_k$ by

$$\eta_{j\,k} = \mathbf{q}_j^T\ \mathbf{A}\ \mathbf{q}_k \tag{5.2.1}$$

The $\eta_{j\,k}$ are equal to zero for all $k < j$ and $|\eta_{j\,j}|$ is equal to 1 if the **q**'s are orthonormal. In finite precision arithmetic, we might expect these $|\eta_{j\,k}|$ to be at ϵ level, where ϵ is the machine round-off error unit. The output from a simple Lanczos run, however, shows that the computed η's are much larger than ϵ and can even be of the order 1. This loss of orthogonality is unfortunately widespread. To illustrate the loss in orthogonality, we run the simple Lanczos algorithm on Test Problem 1. The beam structure shown in Figure 2.3 is divided into five equal segments and has 10 degrees of freedom. The simple Lanczos algorithm is used to generate 20 Lanczos vectors which is the order of (**A**, **B**). We then show in Figure 5.1 the quantities $\log_{10} (|\eta_{i\,j} - \delta_{ij}\,\delta_j|/\epsilon)$ rounded to the next integer, with δ_{ij} being the Kronecker delta function. In exact arithmetic, all these quantities should be zero.

Figure 5.1 shows that the orthogonality relation starts to fail at an early stage of the calculation and the growth of η's appears to follow a regular pattern. We may simulate this pattern in the following way. To include the effect induced by rounding errors, we change the three-term recurrence formula Eq.(5.1.9) into

$$\gamma_{j+1}\,\mathbf{q}_{j+1} = \mathbf{B}^{-1}\,\mathbf{A}\,\mathbf{q}_j - \alpha_j\,\mathbf{q}_j - \beta_{j-1}\,\mathbf{q}_{j-1} + \mathbf{f}_{j+1} \qquad (5.2.2)$$

where the n-vector $\mathbf{f}_{j+1}$ accounts for rounding errors introduced during the step and $\alpha's$, $\beta's$, $\gamma's$ and $\mathbf{q}'s$ denote the computed quantities. Pre-multiplying Eq.(5.2.2) by $\mathbf{q}_k^{\mathrm{T}}\,\mathbf{A}$ and using the definition in Eq.(5.2.1), we obtain

$$\gamma_{j+1}\,\eta_{j+1\,k} = \mathbf{q}_k^{\mathrm{T}}\,\mathbf{A}\,\mathbf{B}^{-1}\,\mathbf{A}\,\mathbf{q}_j - \alpha_j\,\eta_{j\,k} - \beta_{j-1}\,\eta_{j-1\,k} + \mathbf{q}_k^{\mathrm{T}}\,\mathbf{A}\,\mathbf{f}_{j+1} (5.2.3)$$

Interchanging the index j and k of Eq.(5.2.3) we obtain a similar expansion :

$$\gamma_{k+1}\,\eta_{k+1\,j} = \mathbf{q}_j^{\mathrm{T}}\,\mathbf{A}\,\mathbf{B}^{-1}\,\mathbf{A}\,\mathbf{q}_k - \alpha_k\,\eta_{k\,j} - \beta_{k-1}\,\eta_{k-1\,j} + \mathbf{q}_j^{\mathrm{T}}\,\mathbf{A}\,\mathbf{f}_{k+1} (5.2.4)$$

From the symmetry of $\mathbf{A}\,\mathbf{B}^{-1}\,\mathbf{A}$, the first term on the right-hand side of Eq.(5.2.3) and (5.2.4) are equal and therefore can be eliminated by subtraction, resulting in

$$\gamma_{j+1}\,\eta_{j+1\,k} = \gamma_{k+1}\eta_{j\,k+1} + (\alpha_k - \alpha_j)\eta_{j\,k} + \qquad (5.2.5)$$

Figure 5.1 $\log_{10} (\frac{|\eta_{i\,j} - \delta_{ij}\,\delta_j\,|}{\epsilon})$

row/col	1	2	3	4	5	6	7	8	9	10	11	12	13	14	15	16	17	18	19	20
1	0	1	0	1	3	4	7	8	11	13	15	16	15	12	10	12	13	14	15	15
2		0	1	0	2	3	5	7	9	11	14	15	14	11	11	13	14	15	17	17
3			0	1	2	2	4	6	8	10	13	14	13	10	11	13	15	16	17	16
4				0	1	1	3	4	7	9	11	12	11	11	12	14	15	16	16	16
5					0	1	2	3	5	7	10	11	9	10	11	13	14	15	15	15
6						0	1	1	4	6	8	9	8	10	11	13	14	15	15	15
7							0	1	2	4	6	7	6	8	9	12	13	14	14	14
8								0	2	1	5	5	6	8	9	11	12	13	14	14
9									0	1	2	3	4	6	7	9	11	12	12	12
10										0	2	1	3	5	6	8	10	11	12	12
11											0	0	1	3	4	7	8	10	13	13
12												0	0	1	4	7	9	11	14	14
13													0	2	2	6	8	10	13	13
14														0	1	2	5	7	10	10
15			Symmetric												0	2	2	5	8	8
16																0	1	1	5	4
17																	0	1	3	4
18																		1	3	3
19																			1	2
20																				1

$$\beta_{k-1}\eta_{j\,k-1} - \beta_{j-1}\eta_{j-1\,k} + \mathbf{q}_k^T\,\mathbf{A}\,\mathbf{f}_{j+1} - \mathbf{q}_j^T\,\mathbf{A}\,\mathbf{f}_{k+1}$$

The last two terms of Eq.(5.2.5) are due to unknown local rounding errors which are assumed to be at round-off level. We can denote them simply by a number $\psi_{j+1\,k}$. Thus, we achieve a recurrence that governs the evolution of the $\eta_{j+1\,k}$

$$\gamma_{j+1}\,\eta_{j+1\,k} = \gamma_{k+1}\,\eta_{j\,k+1} + (\alpha_k - \alpha_j)\,\eta_{j\,k} + \tag{5.2.6}$$

$$\beta_{k-1}\eta_{j\,k-1} - \beta_{j-1}\eta_{j-1\,k} + \psi_{j+1\,k}$$

This recurrence can also be expressed compactly in vector form as

$$\gamma_{j+1}\,\eta_{j+1} = \mathbf{T}\,\eta_j - \alpha_j\eta_j - \beta_{j-1}\eta_{j-1} + \psi_{j+1} \tag{5.2.7}$$

where $\eta_{j+1\,k}$ and $\psi_{j+1\,k}$ are the elements of $\boldsymbol{\eta}_{j+1}$ and $\boldsymbol{\psi}_{j+1}$, respectively, and **T** is a tri-diagonal matrix defined in Eq.(5.3.2). This formula states that $\boldsymbol{\eta}_{j+1}$ is some combination of $\boldsymbol{\eta}_j$ and $\boldsymbol{\eta}_{j-1}$ plus the contamination from round-off $\boldsymbol{\psi}_{j+1}$ occurring at this step. The loss of orthogonality therefore can be viewed as the result of an amplification of each local error after its introduction into the computation. This statement is consistent with the phenomenon observed in Figure 5.1.

Full re-orthogonalization. To maintain all the $\eta_{j+1\,k}$'s at round-off level, a full re-orthogonalization (FRO) scheme can be adopted which performs the explicit orthogonalization of $\mathbf{q}_{j+1}$ against all the previous $\mathbf{q}'s$. To this end, we add the following Gram-Schmidt orthogonalization step after the three-term recurrence step to force $\hat{\mathbf{q}}_{j+1}$ to be orthogonal to $\mathbf{q}_1, \ldots, \mathbf{q}_j$ up to the round-off level

$$\mathbf{p}_{j+1} = \mathbf{A}\,\hat{\mathbf{q}}_{j+1}$$

$$\hat{\mathbf{q}}_{j+1} \leftarrow \hat{\mathbf{q}}_{j+1} - \sum_{i=1}^{j} \delta_i\, \mathbf{q}_i\, (\mathbf{q}_i^{\mathrm{T}}\, \mathbf{p}_{j+1}) \qquad (5.2.8)$$

where $\delta_i = \mathbf{q}_i^{\mathrm{T}}\,\mathbf{A}\,\mathbf{q}_i$ is 1 or -1. During the summation, the vector $\mathbf{p}_{j+1}$ is not changed to avoid extra $2\mu(\mathbf{M}) + \mu(\mathbf{C})$ multiplication of $\hat{\mathbf{q}}_{j+1}$ by **A**. This modification can bring all the η's to the round-off level, however an extra $4jn$ multiplication is added to the original cost. This additional cost is not small compared to the cost of performing the three-term recurrence. Indeed, this cost will become dominant after some steps depending on the costs $\mu(\mathbf{M})$, $\mu(\mathbf{C})$ and $\nu(\mathbf{K})$ relative to n.

Partial re-orthogonalization. The FRO scheme just discussed aims at keeping all the η's at ϵ level, where ϵ is the machine round-off error unit. However, current research [P1, P2] shows that semi-orthogonality; i.e., maintaining all the η's at $\sqrt{\epsilon}$ level, between Lanczos vectors generated by $\mathbf{K}^{-1}\,\mathbf{M}$ is sufficient to achieve the eigensolutions of (**M**, **K**) within the desired accuracy. Following this direction, we examine whether semi-orthogonality is enough to achieve satisfactory eigensolutions for (**A**, **B**). To this end, we monitor the η_{j+1} when computing a new vector $\mathbf{q}_{j+1}$. As soon as any component of the η_{j+1} reaches $\sqrt{\epsilon}$ a full Gram-Schmidt sweep is done. In this way, re-orthogonalization is performed for only some **q**'s, rather than for every **q**'s. Therefore, this scheme is called partial re-orthogonalization (PRO). To determine whether re-orthogonalization is required, we need to know all the elements in η_{j+1}. Forming η_{j+1} explicitly requires $2jn$ multiplications, which is actually half the cost of the re-orthogonalization process. Thus, for economic reasons, we use an estimated η_{j+1}, represented by Eq.(5.2.7), to determine whether re-orthogonalization is required. The unknown vector ψ_{j+1} in Eq.(5.2.7) can be replaced by appropriately chosen random numbers, which are based on a statistical study to reflect the effect of round-off [S2, S3]. Accordingly, we use the following recurrence in the algorithm to estimate the level of orthogonality.

$$\eta_{j+1} = \frac{1}{\gamma_{j+1}} [\, \mathbf{T}\, \eta_j - \alpha_j \eta_j - \beta_{j-1} \eta_{j-1} + \psi_{j+1} \,] \tag{5.2.9}$$

This formula holds for $j+1 \geq 3$ and starts by assuming that $\eta_{1\,1} = \delta_1$, $\eta_{2\,1} = \psi_{2\,1}$ and $\eta_{2\,2} = \delta_2$.

5.3 Reduction to tri-diagonal system

After m steps, we have the Lanczos vectors $\mathbf{Q} = [\mathbf{q}_1, \ldots, \mathbf{q}_m]$ satisfying the matrix form of the three-term recurrence formula :

$$\gamma_{m+1}\, \mathbf{q}_{m+1}\, e_m^{\mathrm{T}} = \mathbf{B}^{-1}\, \mathbf{A}\, \mathbf{Q} - \mathbf{Q}\, \mathbf{T} \tag{5.3.1}$$

where $e_m^{\mathrm{T}} = (0\ 0\ \ldots\ 0\ 1)$ and **T** is a tri-diagonal matrix of the coefficients from the three-term recurrence

$$\mathbf{T} = \begin{bmatrix} \alpha_1 & \beta_1 & & & & \\ \gamma_2 & \alpha_2 & \beta_2 & & & \\ & \cdot & \cdot & \cdot & & \\ & & \cdot & \cdot & \cdot & \\ & & & \gamma_{m-1} & \alpha_{m-1} & \beta_{m-1} \\ & & & & \gamma_m & \alpha_m \end{bmatrix} \tag{5.3.2}$$

These Lanczos vectors are A-orthogonal; i.e., they satisfy

$$\mathbf{Q}^T \mathbf{A} \mathbf{Q} = \mathbf{\Delta} \tag{5.3.3}$$

where Δ is the diagonal matrix with diagonal elements δ_i, which is either 1 or -1. After pre-multiplying Eq. (5.3.1) by $\mathbf{Q}^T \mathbf{A}$, using Eq.(5.3.3) we can obtain

$$\mathbf{Q}^T \mathbf{A} \mathbf{B}^{-1} \mathbf{A} \mathbf{Q} = \mathbf{\Delta T} \tag{5.3.4}$$

Now, we choose the span of the set of Lanczos vectors, $\mathbf{Q}$, as the admissible space and apply the projection method described in Chapter 3 to obtain a reduced eigenproblem. Let (Θ^{-1}, $\mathbf{Y}$) be the approximates to the eigenpairs. We require that the residual vectors be $\mathbf{A}$-orthogonal to the admissible space, that is,

$$\mathbf{Q}^T \mathbf{A} (\mathbf{B}^{-1} \mathbf{A} \mathbf{Y} - \mathbf{Y} \Theta^{-1}) = \mathbf{0} \tag{5.3.5}$$

From this relation and $\mathbf{Y} = \mathbf{Q} \mathbf{S}$, it follows that

$$\mathbf{\Delta} \mathbf{T} \mathbf{S} - \mathbf{\Delta} \mathbf{S} \boldsymbol{\Theta}^{-1} = \mathbf{0} \tag{5.3.6}$$

or equivalently

$$\mathbf{T} \mathbf{S} = \mathbf{S} \boldsymbol{\Theta}^{-1} \tag{5.3.7}$$

which is a standard eigenproblem. For the moment, we construct the complex eigensolutions of this reduced problem by a QR algorithm, which is readily available in the EISPACK library [E1]. It is believed that a better algorithm can be developed to take advantage of the fact that $\mathbf{T}$ is tri-diagonal. After the solution of this reduced problem the Ritz values are contained in $\boldsymbol{\Theta}$ and the Ritz vectors $\mathbf{Y} = [\mathrm{y}_1 , \ldots , \mathrm{y}_m]$ are given by $\mathbf{Y} = \mathbf{Q} \mathbf{S}$. To make the Ritz vectors satisfy

$| \mathbf{y}_j^T \mathbf{A} \mathbf{y}_j | = 1$, we can scale the $\mathbf{s}_j$ such that $| \mathbf{s}_j^T \Delta \mathbf{s}_j | = 1$ for $j = 1, \ldots, m$. These Ritz pairs are the approximates to the least dominant eigenpairs of the original system (**A**, **B**). To measure the quality of this approximation, we form the residual vectors given by

$$\mathbf{r}_i = \mathbf{B}^{-1} \mathbf{A} \mathbf{y}_i - \mathbf{y}_i \frac{1}{\theta_i} \tag{5.3.8}$$

The three-term recurrence formula can be used to simplify the computation of these residual vectors. Post-multiplying Eq.(5.3.1) by $\mathbf{s}_i$ leads to

$$\gamma_{m+1} \mathbf{q}_{m+1} e_m^T \mathbf{s}_i = \mathbf{B}^{-1} \mathbf{A} \mathbf{Q} \mathbf{s}_i - \mathbf{Q} \mathbf{T} \mathbf{s}_i \tag{5.3.9}$$

Making use of $\mathbf{T} \mathbf{s}_i = \mathbf{s}_i \frac{1}{\theta_i}$ and $\mathbf{Q} \mathbf{s}_i = \mathbf{y}_i$, we obtain

$$\mathbf{B}^{-1} \mathbf{A} \mathbf{y}_i - \mathbf{y}_i \frac{1}{\theta_i} = \gamma_{m+1} \mathbf{q}_{m+1} \mathbf{s}_i(m) \tag{5.3.10}$$

where $s_i(m)$ represents the m^{th} element of the vector $\mathbf{s}_i$. That is, the residual vector can be obtained simply from

$$\mathbf{r}_i = \gamma_{m+1} \mathbf{q}_{m+1} s_i(m) \tag{5.3.11}$$

and its inner product can accordingly be obtained from

$$\mathbf{r}_i^T \mathbf{A} \mathbf{r}_i = \delta_{m+1} \gamma_{m+1} s_i(m) \tag{5.3.12}$$

where in general $s_i(m)$ is a complex number. Note that all δ_{m+1}, γ_{m+1} and $s_i(m)$ are readily available from the Lanczos algorithm and therefore no extra computational effort is required to form the quantity $\mathbf{r}_i^T \mathbf{A} \mathbf{r}_i$. Since $\mathbf{r}_i = \mathbf{0}$ corresponds to an exact solution, we can measure the quality of the approximate solution by examining the magnitude of the components of $\mathbf{r}_i$. Since $\mathbf{r}_i^T \mathbf{A} \mathbf{r}_i = 0$ does not necessarily imply $\mathbf{r}_i = \mathbf{0}$, we have to be cautious about the use of $\mathbf{r}_i^T \mathbf{A} \mathbf{r}_i$ as a measure of how good the approximation is.

5.4 Numerical examples

In this section we use the Lanczos algorithm with the re-orthogonalization scheme described in the previous sections to find the complex eigenpairs of damped dynamic systems. To test the effectiveness of the developed algorithm, we first run the Lanczos algorithm with FRO on Test Problems 1 and 2, with different lumped damping coefficients, up to the size of the problem even though the algorithm is not intended for the complete solution of an eigenproblem. Tables 5.1 and 5.2 show the results obtained from solving Test Problems 1 and 2, respectively. From the solution of these two groups of problems, we observe the following.

(1) The last residual norm of each case is at the round-off level, which implies that the computed Lanczos vectors have spanned the whole solution space as expected. This desirable result exhibits the robustness of the developed algorithm. The Ritz pairs obtained from solving the resulting tri-diagonal system are all accurate eigensolutions as can be verified with the solutions obtained by RG or RGG shown in Chapter 2.

(2) The solution of the tri-diagonal system takes much more CPU time than the generation of the Lanczos vectors. The tri-diagonal matrix is very close to the 2 by 2 block diagonal form from which the eigenvalues can be readily read out, as shown in Eq.(2.4.25) and Eq.(2.4.26). Therefore, a more efficient algorithm than the QR algorithm is desired to take advantage of the tri-diagonality of the matrix **T**.

(3) In general, the starting vector for the Lanczos algorithm may be chosen arbitrarily. However, if the starting vector is orthogonal to any of the eigenvectors of (**A**, **B**), all the Lanczos vectors will also be orthogonal to these eigenvectors. In practice, round-off errors eventually will introduce components along these eigenvectors; however, this comes slowly and the convergence to these eigenvectors is deferred. Therefore, we need to avoid the possibility of the starting

vector being orthogonal to the wanted eigenvectors of the system. Since the structural system in Test Problem 2 is symmetric, there will be anti-symmetric modes as well as symmetric modes. If a symmetric starting vector is used, such as (1, 1, . . . , 1), all the Lanczos vectors will be symmetric. Accordingly, all the anti-symmetric modes of the structure will be suppressed by this biased starting vector. To obtain all the low-frequency modes, we cannot choose a symmetric or anti-symmetric vector as the starting vector. This undesirable situation can usually be avoided by using a random vector as the starting vector.

To measure the efficiency of the Lanczos algorithm, we compare the CPU time required to find the solutions by the Lanczos algorithm with the CPU time required to find the solutions by RG (or RGG), shown in Section 2.5. For the examples considered, the Lanczos algorithm is comparable to RG and is less expensive than RGG. However, the virtue of the Lanczos algorithm is its being able to compute a small set of eigenpairs. To show this we run 20 and 40 step on Test Problems 1 and 2 respectively with various damping coefficients. Tables 5.3 and 5.4 show the results for partial solution of various experiments on Test Problems 1 and 2, respectively. We see that the first few eigenpairs can be extracted at a fairly low cost compared to the average cost of a complete solution. This is because the re-orthogonalization cost is greater at later steps in the Lanczos algorithm.

There are repeated eigenpairs in the $c = 0$ case of Test Problem 2; that is, 1^{st} and 2^{nd} modes have the same eigenvalues and so on (see Section 2.5). Since the Lanczos algorithm examines the Krylov subspace spanned by the vectors $(\mathbf{q}_1 , \mathbf{D}\mathbf{q}_1 , \mathbf{D}^2\mathbf{q}_1 , ... , \mathbf{D}^{m-1}\mathbf{q}_1)$, where $\mathbf{D} = \mathbf{B}^{-1}\mathbf{A}$, it produces multiple eigenvalues sequentially instead of simultaneously [P1]. This mechanism differs from the subspace iteration algorithm where multiple eigenvalues are obtained almost simultaneously. For example, in the partial solution of the $c = 0$ case of Test Problem 2, 24 eigenvectors, or 12 complex conjugate pairs (12 modes), are found. But the last three modes converged are the 11th, 13th and 15th modes instead of the 10th, 11th and 12th. Therefore, it is possible that some of the multiple eigenpairs associated with low-frequency modes may be missing in the partial solution obtained by the Lanczos algorithm.

The three dimensional space truss system in Test Problem 3 contains 120 degrees of freedom. The associated (**A**, **B**) is of the order 240. The Lanczos algorithm with the FRO and PRO is used to generate 60 Lanczos vectors. Of the 60 Ritz pairs obtained from these 60 Lanczos vectors, the least dominant 28 agree with the eigenvalues being approximated with at least 8 digit of accuracy. Similarly, 80 vectors are generated by Lanczos algorithm with the FRO and PRO in the relatively large system of Test Problem 4, where the associated (**A**, **B**) is of the order 1776. The least dominant 40 of the resulting 80 Ritz pairs agree with the eigenvalues being approximated with at least 8 digit of accuracy. In other words, on the average only about two Lanczos vectors are required to capture a new eigenvector for these two large problems. This implies that the Krylov subspace generated by $\mathbf{B}^{-1}\mathbf{A}$ is excellent for approximating the least dominant eigenspace of the systems in the above problems. Table 5.5 and Table 5.6 summarize the results of various experiments on Test problems 3 and 4 respectively.

The effectiveness and efficiency of the PRO scheme can be examined from the results in Tables 5.5 and 5.6. By maintaining semi-orthogonality between the Lanczos vectors with the PRO scheme, the resulting Ritz values are as accurate as those obtained with the FRO scheme. In addition, it is noted that about two thirds of the re-orthogonalization steps and a portion of the CPU time spent on generating the Lanczos vectors can be saved by using the PRO scheme instead of the FRO scheme. That is, some re-orthogonalization effort can be saved without sacrificing accuracy of the final solution when solving $\lambda \, \mathbf{A} \, \mathbf{z} = \mathbf{B} \, \mathbf{z}$ with the PRO scheme, as in the case of

$\omega^2 \mathbf{M} \psi = \mathbf{K} \psi$ [P1]. To measure the efficiency of an algorithm, one can compute the average cost, defined as the ratio of the total CPU time spent to the number of satisfactory eigenpairs obtained. The Lanczos algorithm is much more efficient than the subspace iteration algorithm if one compares the average cost of the Lanczos algorithm with the average cost of the subspace iteration algorithm, listed in Section 4.3.

Box 5.1 *Simple Lanczos Algorithm*

Step 1 :	Operation Count
pick a random vector $\mathbf{r}$	
$\mathbf{p} = \mathbf{A}\,\mathbf{r}$	$2\mu(\mathrm{M}) + \mu(\mathrm{C})$
solve $\mathbf{B}\,\mathbf{q} = \mathbf{p}$	$\nu(\mathrm{K})$
$\mathbf{p} = \mathbf{A}\,\mathbf{q}$	$2\mu(\mathrm{M}) + \mu(\mathrm{C})$
$\gamma_1 = sqrt\,[\,abs\,(\mathbf{q}^T\,\mathbf{p})\,]$	$2n$
$\delta_1 = sgn\,(\mathbf{q}^T\,\mathbf{p})$	
$\mathbf{p} \leftarrow \mathbf{p}\,/\,\gamma_1$	$2n$
$\mathbf{q} \leftarrow \mathbf{q}\,/\,\gamma_1$	$2n$
solve $\mathbf{B}\,\mathbf{r} = \mathbf{p}$	$\nu(\mathrm{K})$
$\alpha_1 = (\mathbf{r}^T\,\mathbf{p}) \cdot \delta_1$	$2n$
$\mathbf{r} \leftarrow \mathbf{r} - \alpha_1 \cdot \mathbf{q}$	$2n$
$\mathbf{oldp} = \mathbf{A}\,\mathbf{r}$	$2\mu(\mathrm{M}) + \mu(\mathrm{C})$
$\gamma_2 = sqrt[abs\,(\mathbf{r}^T\,\mathbf{oldp})]$	$2n$
$\delta_2 = sgn\,(\mathbf{r}^T\,\mathbf{oldp})$	
store $\mathbf{q}$ as $\mathbf{q}_1$	

Loop : For j = 2,3...	Operation Count
$\mathbf{oldq} \leftarrow \mathbf{q}$	
$\mathbf{oldp} \longleftarrow \mathbf{p}$	
$\mathbf{q} = \mathbf{r}\,/\,\gamma_j$	$2n$
$\mathbf{p} \leftarrow \mathbf{p}\,/\,\gamma_j$	$2n$
solve $\mathbf{B}\,\mathbf{r} = \mathbf{p}$	$\nu(\mathrm{K})$
$\alpha_j = (\mathbf{r}^T\,\mathbf{p}) \cdot \delta_j$	$2n$
$\beta_{j-1} = (\mathbf{r}^T\,\mathbf{oldp}) \cdot \delta_{j-1}$	$2n$
$\mathbf{r} \leftarrow \mathbf{r} - \alpha_j \cdot \mathbf{q}$	$2n$
$\mathbf{r} \leftarrow \mathbf{r} - \beta_{j-1} \cdot \mathbf{oldq}$	$2n$
$\mathbf{oldp} = \mathbf{A}\,\mathbf{r}$	$2\mu(\mathrm{M}) + \mu(\mathrm{C})$
$\gamma_{j+1} = sqrt\,[\,abs\,(\mathbf{r}^T\,\mathbf{oldp})\,]$	$2n$
$\delta_{j+1} = sgn\,(\mathbf{r}^T\,\mathbf{oldp})$	
store $\mathbf{q}$ as $\mathbf{q}_j$	

Table 5.1 *Full Solution of Test problem 1*

item	c = 0	c = 5	c = 5000
number of Lanczos vectors generated	80	80	80
CPU time spent on generating Lanczos vectors	21.2	21.0	21.0
CPU time spent on solving eigenproblem	157.6	112.7	100.9
total CPU time spent on solving the whole problem	192.2	147.2	135.4
the last residual norm $\mathbf{r}^T \mathbf{A} \mathbf{r}$	-0.6e-25	0.5e-30	0.2e-25

Table 5.2 *Full Solution of Test problem 2*

item	c = 0	c = 5	c = 5000
number of Lanczos vectors generated	160	160	160
CPU time spent on generating Lanczos vectors	128.9	129.0	128.4
CPU time spent on solving eigenproblem	492.3	672.2	720.0
total CPU time spent on solving the whole problem	709.2	888.9	936.0
the last residual norm $\mathbf{r}^T \mathbf{A} \mathbf{r}$	0.4e-30	0.8e-32	-0.2e-19

Table 5.3 *Partial Solution of Test problem 1*

item	c = 0	c = 5	c = 5000
number of Lanczos vectors generated	20	20	20
CPU time spent on generating Lanczos vectors	3.0	3.0	3.0
CPU time spent on solving eigenproblem	5.1	2.6	2.8
total CPU time spent on solving the whole problem	10.7	8.2	8.3
number of satisfactory eigenpairs obtained	10	10	10

Table 5.4 *Partial Solution of Test problem 2*

item	c = 0	c = 5	c = 5000
number of Lanczos vectors generated	40	40	40
CPU time spent on generating Lanczos vectors	14.6	14.5	14.6
CPU time spent on solving eigenproblem	19.7	15.9	19.8
total CPU time spent on solving the whole problem	42.1	38.2	42.2
number of satisfactory eigenpairs obtained	24	22	22

Table 5.5 *Partial Solution of Test Problem 3*

item	FRO	PRO
number of Lanczos vectors generated	60	60
number of re-orthogonalization	1770	602
CPU time spent on generating Lanczos vectors	40.3	32.6
CPU time spent on solving eigenproblem	50.8	51.7
total CPU time spent on solving the whole problem	113.9	106.7
number of satisfactory eigenpairs obtained	28	28

Table 5.6 *Partial Solution of Test problem 4*

item	FRO	PRO
number of Lanczos vectors generated	80	80
number of re-orthogonalization	3159	1246
CPU time spent on generating Lanczos vectors	536.6	473.5
CPU time spent on solving eigenproblem	100.9	101.2
total CPU time spent on solving the whole problem	893.2	830.9
number of satisfactory eigenpairs obtained	40	40

Chapter 6
Solution of Transient Problems

6.1 Introduction

The equation of motion for a transient dynamic problem is

$$\mathbf{M}\,\ddot{\mathbf{q}}(t) + \mathbf{C}\,\dot{\mathbf{q}}(t) + \mathbf{K}\,\mathbf{q}(t) = \mathbf{f}(t) \tag{6.1.1}$$

This system of second-order ordinary differential equations, in principle, can be solved with standard procedures for solving differential equations. However, when the system is large many procedures become very expensive unless we take advantage of the symmetry and sparseness of the coefficient matrices. In practical analysis, we are mainly interested in efficient methods. The time-domain methods currently used to solve structural dynamic problems can be divided into two general categories : direct integration methods and mode superposition methods.

In direct integration methods, the equations in (6.1.1) are integrated using a numerical step-by-step procedure. To this end, an approximation of $\mathbf{q}(t)$, $\dot{\mathbf{q}}(t)$ and $\ddot{\mathbf{q}}(t)$ between discrete time points are assumed, where the form assumed dictates the accuracy, stability, and cost of the method. The use of the approximation involves that Eq.(6.1.1) is satisfied only at the discrete points in time instead of at any time t. Since the nature of damping does not require special consideration in the direct integration methods, the solution of a generally damped system does not pose additional difficulty than already exists in the solution of a proportionally damped system. Therefore, we need not further elaborate on this category of methods.

In mode superposition methods, the equation of motion Eq.(6.1.1) is transformed into a set of uncoupled equations so that each one may be treated individually using a closed form or a numerical solution. The response of the system can be obtained by superposition of the solutions of these uncoupled equations. Unlike direct integration methods where the entire set of equations have to be solved at every time step, in mode superposition methods the solution of only a subset of uncoupled equations can approximate the response of the system very well. Since the uncoupled equations associated with a damped system are first-order and complex-valued, which is different from the second-order, real-valued uncoupled equations associated with a proportionally damped system, we present a detailed description for solution in the following section.

In some applications, we want to know the responses or the time histories of certain quantities at only a few chosen degrees of freedom in a very large system. Using a direct integration method, however, we must compute the responses of all the degrees of freedom at each time step since the responses of all the degrees of freedom at previous time steps are required for computing the responses of the desired degrees of freedom at the current time step. If a mode superposition method is used, we can compute the responses at only those required degrees of freedom.

In the analysis of a large undamped dynamic system, the Rayleigh-Ritz method is often used to reduce the large system of equations into a smaller one for economic reason. To reduce a large damped dynamic system, the procedures in the generalized Rayleigh-Ritz method or the projection method described in Chapter 3 can be used. For example, the Lanczos vectors $\mathbf{Q} = [\mathbf{q}_1 , \ldots , \mathbf{q}_m]$ generated by the procedures described in Chapter 5 can be used as the transformation matrix between the geometric coordinates $\mathbf{x}(t)$ and the generalized coordinates $\mathbf{u}(t)$. Substituting the transformation $\mathbf{x}(t) = \mathbf{Q}\,\mathbf{u}(t)$ and $\dot{\mathbf{x}}(t) = \mathbf{Q}\,\dot{\mathbf{u}}(t)$ into the reduced equation of motion $\mathbf{A}\,\dot{\mathbf{x}}(t) - \mathbf{B}\,\mathbf{x}(t) = \mathbf{y}(t)$ and pre-multiplying both sides by $\mathbf{Q}^{\mathrm{T}}\,\mathbf{A}\,\mathbf{B}^{-1}$, we obtain

$$\mathbf{Q}^{\mathrm{T}}\,\mathbf{A}\,\mathbf{B}^{-1}\,\mathbf{A}\,\mathbf{Q}\,\dot{\mathbf{u}}(t) - \mathbf{Q}^{\mathrm{T}}\,\mathbf{A}\,\mathbf{Q}\,\mathbf{u}(t) = \mathbf{Q}^{\mathrm{T}}\,\mathbf{A}\,\mathbf{B}^{-1}\,\mathbf{y}(t) \qquad (6.1.2)$$

Using the orthogonality properties $\mathbf{Q}^{\mathrm{T}}\,\mathbf{A}\,\mathbf{Q} = \mathbf{\Delta}$ and $\mathbf{Q}^{\mathrm{T}}\,\mathbf{A}\,\mathbf{B}^{-1}\,\mathbf{A}\,\mathbf{Q} = \mathbf{\Delta}\,\mathbf{T}$ derived in Section 5.3, we can simplify Eq.(6.1.2) to

$$\mathbf{\Delta}\,\mathbf{T}\,\dot{\mathbf{u}}(t) - \mathbf{\Delta}\,\mathbf{u}(t) = \mathbf{Q}^{\mathrm{T}}\,\mathbf{A}\,\mathbf{B}^{-1}\,\mathbf{y}(t) \qquad (6.1.3)$$

or

$$\mathbf{T}\,\dot{\mathbf{u}}(t) - \mathbf{u}(t) = \mathbf{\Delta}\,\mathbf{Q}^{\mathrm{T}}\,\mathbf{A}\,\mathbf{B}^{-1}\,\mathbf{y}(t) \qquad (6.1.4)$$

where $\mathbf{T}$ is an m by m tri-diagonal matrix and $\mathbf{\Delta} = \mathbf{\Delta}^{-1}$ is an m by m diagonal matrix. Note that Eq.(6.1.4) is smaller in size than $\mathbf{A}\,\dot{\mathbf{x}}(t) - \mathbf{B}\,\mathbf{x}(t) = \mathbf{y}(t)$ and is only slightly coupled; therefore, it is easier to solve. Since the approximate solution of $\mathbf{x}(t)$ is given by $\mathbf{Q}\,\mathbf{u}(t)$, the quality of this approximation depends entirely on how adequately the assumed set of displacements $\mathbf{Q}$ have captured the essential information of the original system. Although using Lanczos vectors generated from $(\mathbf{M}, \mathbf{K})$ to reduce the original large system of equations to a smaller one has been proved efficient for the analysis of undamped dynamic systems by [W2] and [N2], using Lanczos vectors generated from $(\mathbf{A}, \mathbf{B})$ to reduce the equations of a damped system, as shown above, remains to be explored.

6.2 Mode superposition method

To take advantage of the orthonormality properties developed in Section 2.4, we work with the reduced form of the equation of motion. Since the $2n$ eigenvectors constitute a complete basis, the state vector $\mathbf{x}(t)$ can be expressed as a linear combination of these eigenvectors [F1]; that is,

$$\mathbf{x}(t) = \sum_{j=1}^{2n} \mathbf{z}_j\, p_j(t) = \mathbf{Z}\,\mathbf{p}(t) \qquad (6.2.1)$$

where $\mathbf{p}(t)$ is a vector whose elements $p_i(t)$ are generally complex-valued and

$$\mathbf{Z} = \left[\, \mathbf{z}_1\, \mathbf{z}_2\, \ldots .\ \mathbf{z}_{2n} \right] \qquad (6.2.2)$$

is the *modal matrix* which transforms the generalized coordinates $\mathbf{p}(t)$ to geometric coordinates $\mathbf{x}(t)$. Substituting Eq.(6.2.1) and $\dot{\mathbf{x}}(t) = \mathbf{Z}\,\dot{\mathbf{p}}(t)$ into the reduced equation of motion $\mathbf{A}\,\dot{\mathbf{x}}(t) - \mathbf{B}\,\mathbf{x}(t) = \mathbf{y}(t)$ and pre-multiplying both sides by $\mathbf{Z}^{\mathrm{T}}$, we obtain

$$\mathbf{Z}^T \mathbf{A} \mathbf{Z} \dot{\mathbf{p}}(t) - \mathbf{Z}^T \mathbf{B} \mathbf{Z} \mathbf{p}(t) = \mathbf{Z}^T \mathbf{y}(t) \tag{6.2.3}$$

Making use of the orthonormality properties $\mathbf{Z}^T \mathbf{A} \mathbf{Z} = \mathbf{\Delta}$ and $\mathbf{Z}^T \mathbf{B} \mathbf{Z} = \mathbf{\Delta} \, \mathbf{\Lambda}$ we can rewrite Eq.(6.2.3) as

$$\dot{\mathbf{p}}(t) - \mathbf{\Lambda} \, \mathbf{p}(t) = \mathbf{\Delta} \, \mathbf{Z}^T \mathbf{y}(t) \tag{6.2.4}$$

which simply represents the following set of uncoupled equations

$$\dot{p}_j(t) - \lambda_j \, p_j(t) = \delta_j \, \mathbf{z}_j^T \mathbf{y}(t) = \delta_j \, \mathbf{w}_j^T \mathbf{f}(t) \qquad j = 1,2,3,....,2n \tag{6.2.5}$$

with δ_j being 1 for complex modes and 1 or -1 for real modes. These uncoupled equations can be solved individually. The response of the system under excitation is obtained by summation of the solutions of these uncoupled equations using Eq.(6.2.1).

Section 2.2 demonstrated that a pair of eigensolutions can be used to construct the damped modal equation. Now, we show that a pair of first-order uncoupled equations, either complex conjugate pair or real pair, corresponds to its second-order modal equation. To establish this result, we consider the following two homogeneous equations

$$\dot{p}_1(t) - \lambda_1 \, p_1(t) = 0 \qquad \dot{p}_2(t) - \lambda_2 \, p_2(t) = 0 \tag{6.2.6}$$

which are associated with either a complex conjugate pair or a real pair of eigensolutions. We can transfrom the two first-order equations into a second-order one as

$$\ddot{r}(t) - (\, \lambda_1 + \lambda_2 \,) \, \dot{r}(t) + (\, \lambda_1 \lambda_2 \,) \, r(t) = 0 \tag{6.2.7}$$

This can be easily verified by substituting $r(t) = p_1(t) + p_2(t)$ into the equation. Recall that $\lambda_1 + \lambda_2 = -2\xi\omega$ and $\lambda_1\lambda_2 = \omega^2$ for both underdamped modes and overdamped modes, so that Eq.(6.2.7) can be written as

$$\ddot{r}_1(t) + 2\xi\omega \, \dot{r}_1(t) + \omega^2 \, r_1(t) = 0 \tag{6.2.8}$$

which is simply a damped modal equation, as shown in Section 2.2. That is, the two equations in Eq.(6.2.6) correspond to a vibration mode.

Mode superposition method can be applied in two alternative ways to evaluate the response of a system under excitation : (1) the mode displacement method and (2) mode acceleration method.

In the mode displacement method, $2m$ $(m \leq n)$ values of $p_j(t)$, obtained by solving the first $2m$ equations of Eq.(6.2.5), are substituted directly into a truncated form of Eq.(6.2.1), i.e., into

$$\mathbf{x}(t) = \sum_{j=1}^{2m} \mathbf{z}_j \, p_j(t) \tag{6.2.9}$$

to obtain the approximate solution $\mathbf{x}(t)$. In the mode-acceleration method, Eq.(6.2.5) is solved for $p_j(t)$ giving

$$p_j(t) = \frac{1}{\lambda_j} [\, \dot{p}_j(t) - \delta_j \, \mathbf{z}_j^{\mathrm{T}} \, \mathbf{y}(t) \,] \tag{6.2.10}$$

This is then substituted into Eq.(6.2.9) to give the approximation

$$\mathbf{x}(t) = \sum_{j=1}^{2m} \mathbf{z}_j \, \frac{1}{\lambda_j} [\, \dot{p}_j(t) - \delta_j \, \mathbf{z}_j^{\mathrm{T}} \, \mathbf{y}(t) \,] \tag{6.2.11}$$

However, the second term of Eq.(6.2.11) need not be limited to the $2m$ modes. This is because of the following :

$$\begin{aligned} & \sum_{j=1}^{2n} \mathbf{z}_j \, \frac{1}{\lambda_j} \delta_j \, \mathbf{z}_j^{\mathrm{T}} \, \mathbf{y}(t) \\ &= \mathbf{Z} \, \Lambda^{-1} \, \Delta^{-1} \, \mathbf{Z}^{\mathrm{T}} \, \mathbf{y}(t) \\ &= \mathbf{B}^{-1} \, \mathbf{y}(t) \qquad\qquad (6.2.12) \\ &= \begin{bmatrix} -\mathbf{K}^{-1} & \mathbf{0} \\ \mathbf{0} & \mathbf{M}^{-1} \end{bmatrix} \begin{Bmatrix} \mathbf{f}(t) \\ \mathbf{0} \end{Bmatrix} \\ &= \begin{Bmatrix} -\mathbf{K}^{-1}\mathbf{f}(t) \\ \mathbf{0} \end{Bmatrix} \end{aligned}$$

The last term is simply a *pseudo-static response* that is equivalent to the solution of a static analysis at time t. Hence, in the mode-acceleration method the approximate solution is

$$\mathbf{x}(t) = \sum_{j=1}^{2m} \mathbf{z}_j \, \frac{1}{\lambda_j} \dot{p}_j(t) - \mathbf{B}^{-1}\mathbf{y}(t) \tag{6.2.13}$$

The summation in Eq.(6.2.13) represents a *dynamic correction*, which is added to the pseudo-static response to give an approximate solution. Note that if the spatial distribution of $\mathbf{f}(t)$, and hence $\mathbf{y}(t)$, does not vary with time, the pseudo-static displacement vector needs to be solved only once.

From the foregoing discussion, it is apparent that the solution obtained by the mode acceleration method is actually the solution obtained by the mode displacement method plus the pseudo-static response due to the remaining higher modes. Hence, with the same number of modes, the mode acceleration method will yield better results than the mode displacement method for certain classes of problems in which the static effect plays a dominant role. If all n modes are included in the summation, then both methods will give the exact solution.

6.3 Closed form solution

The complete solution for an uncoupled equation of motion, derived in the last section, may be written as the sum of the homogeneous solution and the particular solution. The homogeneous solution is due to the initial conditions while the particular solution is due to the externally applied loadings. We evaluate both solution in closed form in this section.

Free vibration. The homogeneous solution of an uncoupled equation given in Eq.(6.2.5) is represented by

$$p_j(t) = p_j(0)e^{\lambda_j t} \tag{6.3.1}$$

where the participation factor $p_j(0)$ is determined from the initial conditions of the system by

$$p_j(0) = \delta_j \, \mathbf{z}_j^{\mathrm{T}} \mathbf{A} \, \mathbf{x}(0) \tag{6.3.2}$$

which can be expanded as

$$p_j(0) = \delta_j \, [\, \lambda_j \, \mathbf{w}_j^{\mathrm{T}} \mathbf{M} \, \mathbf{q}(0) + \mathbf{w}_j^{\mathrm{T}} \mathbf{C} \, \mathbf{q}(0) + \mathbf{w}_j^{\mathrm{T}} \mathbf{M} \, \dot{\mathbf{q}}(0) \,] \tag{6.3.3}$$

That is, $p_j(0)$ depends on both the initial displacements and velocities of the system. We see from Eq.(6.3.3) that the participation factor can be either complex-valued or real-valued depending on whether the corresponding mode is underdamped or overdamped. Combining the j^{th} complex conjugate pair of solution, we obtain the response due to this underdamped mode as

$$p_j(0) \, e^{\alpha_j t} \, \Phi_j + \bar{p}_j(0) \, e^{\bar{\alpha}_j t} \, \bar{\Phi}_j \tag{6.3.4}$$

This is the sum of complex conjugate pair of vectors and therefore is real-valued. To identify the physical implication of this modal solution, we can rearrange this formulation to obtain the entirely real-valued expression. For this purpose, we can express $p_j(0)$ in terms of its modulus and phase angle as

$$p_j(0) = \frac{1}{2} a_j \, e^{i^* \theta_j} \tag{6.3.5}$$

Recall $\alpha_j = -\xi_j \omega_j + \tilde{\omega}_j i^*$ and $\Phi_j = \Phi_{Rj} + \Phi_{Ij} i^*$ and using the identity $e^{(\tilde{\omega}_j t + \theta_j) i^*} = \cos(\tilde{\omega}_j t + \theta_j) + \sin(\tilde{\omega}_j t + \theta_j) i^*$, we can write Eq.(6.3.4) as

$$a_j \, e^{-\xi_j \omega_j t} [\, \Phi_{Rj} \cos(\tilde{\omega}_j t + \theta_j) - \Phi_{Ij} \sin(\tilde{\omega}_j t + \theta_j) \,] \tag{6.3.6}$$

The above equation indicates that the j^{th} underdamped modal solution consists of the sum of two exponentially decaying harmonic motions with a circular frequency, $\tilde{\omega}_j$ and a damping ratio, ξ_j. The component motions lag behind one another by one-quarter the period $\tilde{T}_j = 2\pi / \tilde{\omega}_j$, and they are in different spatial configurations. We note that each point of the system undergoes a simple harmonic motion; however, the configuration of the system does not remain constant but changes continuously, repeating itself at intervals $\tilde{T}_j$. The quantity $\tilde{T}_j$ is thus known as the j^{th} damped natural period of the system.

Combining the j^{th} real pair of solution, we obtain the response due to this overdamped mode as

$$p_j(0)\, e^{\beta_j t}\, \Psi_j + \hat{\mathbf{p}}_j(0)\, e^{\hat{\beta}_j t}\, \hat{\Psi}_j \tag{6.3.7}$$

This indicates that the j^{th} overdamped modal solution consists of the superposition of two exponentially decaying functions, which are in different spatial configurations. Hence, the resulting motion is non-oscillatory. The configuration of the system is not constant, either.

The response of the system to arbitrary initial conditions is thus given by the superposition of the various modal solutions

$$\mathbf{x}(t) = \sum_{j=1}^{nc} a_j\, e^{-\xi_j \omega_j t}[\, \Phi_{\mathrm{R}j}\cos(\tilde{\omega}_j t + \theta_j) - \Phi_{\mathrm{I}j}\sin(\tilde{\omega}_j t + \theta_j)\,]$$

$$+ \sum_{j=1}^{nr} [\, p_j(0)e^{\beta_j}\, \Psi_j + \hat{p}_j(0)e^{\hat{\beta}_j t}\, \hat{\Psi}_j\,] \tag{6.3.8}$$

Forced vibration. The particular solution to the Eq.(6.2.5) for an arbitrary loading $\mathbf{f}(t)$ may be written in terms of a convolution integral

$$p_j(t) = \delta_j\, \mathbf{w}_j^{\mathrm{T}} \int_0^t e^{\lambda_j(t-\tau)}\, \mathbf{f}(\tau)\, d\tau \tag{6.3.9}$$

For complex modes, it is desirable to express the solution in terms of the real-valued quantities so that they may be physically interpreted. To this end, we recall that the *impulse response function* for a SDOF damped system with unit mass is

$$h_j(t) = \frac{1}{\tilde{\omega}_j} e^{-\xi_j \omega_j t}\, \sin\tilde{\omega}_j t \tag{6.3.10}$$

and its derivative with respect to time is

$$\dot{h}_j(t) = e^{-\xi_j \omega_j t}\, \cos\tilde{\omega}_j t - \xi_j \omega_j h_j(t) \tag{6.3.11}$$

In terms of these well-defined functions, we have the following expression

$$e^{\lambda_j t} = [\, \dot{h}_j(t) + \xi_j \omega_j h_j(t) \,] + \tilde{\omega}_j h_j(t)\, \mathrm{i}^* \qquad (6.3.12)$$

Accordingly, the real and imaginary part of $p_j(t)$ is represented by

$$p_{\mathrm{R}j}(t) = \boldsymbol{\phi}_{\mathrm{R}j}^{\mathrm{T}} \int_0^t [\, \dot{h}_j(t-\tau) + \xi_j \omega_j h_j(t-\tau) \,]\, \mathbf{f}(\tau)\, d\tau$$

$$- \boldsymbol{\phi}_{\mathrm{I}j}^{\mathrm{T}} \int_0^t \tilde{\omega}_j\, h_j(t-\tau)\, \mathbf{f}(\tau)\, d\tau \qquad (6.3.13a)$$

$$p_{\mathrm{I}j}(t) = \boldsymbol{\phi}_{\mathrm{I}j}^{\mathrm{T}} \int_0^t [\, \dot{h}_j(t-\tau) + \xi_j \omega_j h_j(t-\tau) \,]\, \mathbf{f}(\tau)\, d\tau$$

$$+ \boldsymbol{\phi}_{\mathrm{R}j}^{\mathrm{T}} \int_0^t \tilde{\omega}_j\, h_j(t-\tau)\, \mathbf{f}(\tau)\, d\tau \qquad (6.3.13b)$$

and the response due to the j^{th} mode is represented by

$$2\, [\, \boldsymbol{\Phi}_{\mathrm{R}j}\, p_{\mathrm{R}j}(t) - \boldsymbol{\Phi}_{\mathrm{I}j}\, p_{\mathrm{I}j}(t) \,] \qquad (6.3.14)$$

Eq.(6.3.14) indicates that the j^{th} underdamped modal solution consists of two oscillatory motions with spatial configurations $\boldsymbol{\Phi}_{\mathrm{R}j}$, $\boldsymbol{\Phi}_{\mathrm{I}j}$ and temporal variations $p_{\mathrm{R}j}(t)$, $p_{\mathrm{I}j}(t)$ respectively.

The response due to the j^{th} overdamped mode is simply

$$[\delta_j\, \boldsymbol{\psi}_j^{\mathrm{T}} \int_0^t e^{\beta_j (t-\tau)}\, \mathbf{f}(\tau)\, d\tau \,]\, \boldsymbol{\Psi}_j + [\hat{\delta}_j\, \hat{\boldsymbol{\psi}}_j^{\mathrm{T}} \int_0^t e^{\hat{\beta}_j (t-\tau)}\, \mathbf{f}(\tau)\, d\tau \,]\, \hat{\boldsymbol{\Psi}}_j \qquad (6.3.15)$$

Again, this indicates that the j^{th} overdamped modal solution consists of two exponentially decaying motions with spatial configurations $\boldsymbol{\Psi}_j$, $\hat{\boldsymbol{\Psi}}_j$ and decaying factors β_j, $\hat{\beta}_j$ respectively.

The response of the system due to applied loadings can thus be represented by the superposition of the tributary modal solutions; that is,

$$\mathbf{x}(t) = 2 \sum_{j=1}^{nc} [\, \boldsymbol{\Phi}_{\mathrm{R}j}\, p_{\mathrm{R}j}(t) - \boldsymbol{\Phi}_{\mathrm{I}j}\, p_{\mathrm{I}j}(t) \,] +$$

$$\sum_{j=1}^{nr} [\, (\delta_j\, \boldsymbol{\psi}_j^{\mathrm{T}} \int_0^t e^{\beta_j (t-\tau)}\, \mathbf{f}(\tau)\, d\tau \,)\, \boldsymbol{\Psi}_j + \qquad (6.3.16)$$

$$(\hat{\delta}_j\, \hat{\boldsymbol{\psi}}_j^{\mathrm{T}} \int_0^t e^{\hat{\beta}_j (t-\tau)}\, \mathbf{f}(\tau)\, d\tau \,)\, \hat{\boldsymbol{\Psi}}_j \,]$$

The general response of the system to both initial conditions and externally applied loadings can be obtained simply by combining the solutions represented by Eq.(6.3.8) and (6.3.16).

We see from the above discussion that the eigenvectors of a damped system still represent the vibration mode shapes of the system just as those of a undamped system. Although the undamped mode, obtained by analyzing an undamped system, is represented by only one single shape, the damped mode is composed of linear combination of two shapes, each of which undergoes different temporal variation. If we let a damped system vibrate freely, all points in the system undergo motion at the same frequency but at a different phase angle. In other words, not all points of the system necessarily pass through their equilibrium position simultaneously as they do in the undamped mode. As a result, there is no stationary *node* in the damped mode. If the undamped mode can be thought of as a *standing wave* pattern, the damped mode can be thought of as a *traveling wave* through the system. The representation of this travelling damped mode requires continuous description over the period of this mode and is thus much more laborious.

6.4 Numerical solution by exact method

In the last section, convolution integral expressions were obtained for the solution of uncoupled equations to arbitrary excitations. For simple forms of excitation these expressions can be evaluated in closed form. For more complicated forms of excitation a numerical scheme is required. Two general approaches can be used for this purpose : (1) interpolation of the excitation, or (2) approximation of derivatives in the differential equation. In many practical dynamic problems, e.g., the so-called *discrete time system*, the excitation function is not known in the form of an analytical expression but rather is supplied at a set of discrete points. A direct and accurate procedure for obtaining the response to this kind of excitation is to interpolate the excitation function and to solve the resulting equation exactly. In this approach, only the unknown excitation function is interpolated and no other numerical approximations in the integration process is made. For this reason it is called the *exact method*. In the following discussion, a piecewise linear interpolation of the excitation function is used, and the exact solution of the resulting modal equation is derived for the evaluation of the response quantities.

An uncoupled equation, which is a first-order differential equation, can be expressed as

$$\dot{p}(t) - \lambda\, p(t) = \delta\, \mathbf{w}^T \mathbf{f}(t) = f(t) \tag{6.4.1}$$

Assuming that $f(t)$ is represented by a piecewise linear function, Eq.(6.4.1) may be written as

$$\dot{p}(t) - \lambda\, p(t) = f_i + \frac{\Delta f}{\Delta t}\, t \tag{6.4.2}$$

where

$$\Delta t = t_{i+1} - t_i \tag{6.4.3}$$

$$\Delta f = f_{i+1} - f_i \tag{6.4.4}$$

Eq.(6.4.2) is valid between two consecutive discrete points i and $i+1$ and the solution, for $0 \le t \le \Delta t$, is

$$p(t) = a + b\, t + c\, e^{\lambda t} \tag{6.4.5}$$

where a, b and c are constants of integration. Substituting this solution into Eq.(6.4.2) and using the initial condition $p(t_i) = p(0)$, we obtain the following expressions for the integration constants

$$a = -\frac{1}{\lambda} f_i - \frac{1}{\lambda^2}\frac{\Delta f}{\Delta t} \tag{6.4.6}$$

$$b = -\frac{1}{\lambda}\frac{\Delta f}{\Delta t} \tag{6.4.7}$$

$$c = p(0) - a \tag{6.4.8}$$

For overdamped modes, these expressions are in terms of real quantities and can be directly substituted into Eq.(6.4.5) to find the response of the system by the mode superposition method. For underdamped modes, however, these expressions are in terms of complex quantities. To obtain the real and imaginary parts of $p(t)$ at any time t, we express the associated complex quantities in terms of their real and imaginary parts as

$$p(t) = p_{\mathrm{R}}(t) + p_{\mathrm{I}}(t)\,\mathrm{i}^* \tag{6.4.9}$$

$$\lambda = \alpha_{\mathrm{R}} + \alpha_{\mathrm{I}}\,\mathrm{i}^* \tag{6.4.10}$$

$$f = f_{\mathrm{R}} + f_{\mathrm{I}}\,\mathrm{i}^* \tag{6.4.11}$$

$$\frac{\Delta f}{\Delta t} = \frac{\Delta f_{\mathrm{R}}}{\Delta t} + \frac{\Delta f_{\mathrm{I}}}{\Delta t}\,\mathrm{i}^* \tag{6.4.12}$$

Substituting Eqs.(6.4.10), (6.4,11) and (6.4.12) into Eqs.(6.4.6) and (6.4.7) and simplifying them, we obtain the following expressions

$$\begin{Bmatrix} a_{\mathrm{R}} \\ a_{\mathrm{I}} \end{Bmatrix} = \begin{bmatrix} -\dfrac{\alpha_{\mathrm{R}}^2-\alpha_{\mathrm{I}}^2}{(\alpha_{\mathrm{R}}^2+\alpha_{\mathrm{I}}^2)^2} & -\dfrac{2\alpha_{\mathrm{R}}\alpha_{\mathrm{I}}}{(\alpha_{\mathrm{R}}^2+\alpha_{\mathrm{I}}^2)^2} \\ \dfrac{2\alpha_{\mathrm{R}}\alpha_{\mathrm{I}}}{(\alpha_{\mathrm{R}}^2+\alpha_{\mathrm{I}}^2)^2} & -\dfrac{\alpha_{\mathrm{R}}^2-\alpha_{\mathrm{I}}^2}{(\alpha_{\mathrm{R}}^2+\alpha_{\mathrm{I}}^2)^2} \end{bmatrix} \begin{Bmatrix} \dfrac{\Delta f_{\mathrm{R}}}{\Delta t} \\ \dfrac{\Delta f_{\mathrm{I}}}{\Delta t} \end{Bmatrix} + \begin{bmatrix} -\dfrac{\alpha_{\mathrm{R}}}{\alpha_{\mathrm{R}}^2+\alpha_{\mathrm{I}}^2} & -\dfrac{\alpha_{\mathrm{I}}}{\alpha_{\mathrm{R}}^2+\alpha_{\mathrm{I}}^2} \\ \dfrac{\alpha_{\mathrm{I}}}{\alpha_{\mathrm{R}}^2+\alpha_{\mathrm{I}}^2} & -\dfrac{\alpha_{\mathrm{R}}}{\alpha_{\mathrm{R}}^2+\alpha_{\mathrm{I}}^2} \end{bmatrix} \begin{Bmatrix} f_{\mathrm{R}} \\ f_{\mathrm{I}} \end{Bmatrix} \tag{6.4.13}$$

$$\begin{Bmatrix} b_{\mathrm{R}} \\ b_{\mathrm{I}} \end{Bmatrix} = \begin{bmatrix} -\dfrac{\alpha_{\mathrm{R}}}{\alpha_{\mathrm{R}}^2+\alpha_{\mathrm{I}}^2} & -\dfrac{\alpha_{\mathrm{I}}}{\alpha_{\mathrm{R}}^2+\alpha_{\mathrm{I}}^2} \\ \dfrac{\alpha_{\mathrm{I}}}{\alpha_{\mathrm{R}}^2+\alpha_{\mathrm{I}}^2} & -\dfrac{\alpha_{\mathrm{R}}}{\alpha_{\mathrm{R}}^2+\alpha_{\mathrm{I}}^2} \end{bmatrix} \begin{Bmatrix} \dfrac{\Delta f_{\mathrm{R}}}{\Delta t} \\ \dfrac{\Delta f_{\mathrm{I}}}{\Delta t} \end{Bmatrix} \tag{6.4.14}$$

Now, the solution $p(t)$ for $0 \le t \le \Delta t$ can be conveniently expressed as

$$\begin{Bmatrix} p_{\mathrm{R}}(t) \\ p_{\mathrm{I}}(t) \end{Bmatrix} = \begin{Bmatrix} a_{\mathrm{R}} + b_{\mathrm{R}}\, t \\ a_{\mathrm{I}} + b_{\mathrm{I}}\, t \end{Bmatrix} + \qquad (6.4.15)$$

$$\begin{bmatrix} e^{\alpha_R t}\cos(\alpha_I t) & -e^{\alpha_R t}\sin(\alpha_I t) \\ e^{\alpha_R t}\sin(\alpha_I t) & e^{\alpha_R t}\cos(\alpha_I t) \end{bmatrix} \begin{Bmatrix} p_{\mathrm{R}}(0) - a_{\mathrm{R}} \\ p_{\mathrm{I}}(0) - a_{\mathrm{I}} \end{Bmatrix}$$

Equation (6.4.15) can be used as a recurrence formula for evaluating the response p_{i+1} at time t_{i+1} given the response p_i at time t_i. This procedure is implemented in FEAP for computing the dynamic response of damped systems. As an example, we solve two cases of the beam structure in Test Problem 1, one with damper $c = 0$ and the other with $c = 5$. Figure 6.1 shows the detailed description of the structure and the applied loading. We plot displacement-time history where the loading is applied. Figure 6.2 shows the results of $c = 0$ case for using (1) only the first mode and (2) the first ten modes. The response obtained by using ten modes differs only slightly from the response obtained by using one mode. Figure 6.3 shows the results of $c = 5$ case for using (1) only the first mode, (2) the first two modes, and (3) the first ten modes. It is shown in Section 2.5 that for this system the first mode is an overdamped mode while the others are underdamped modes. We see that the response obtained by using ten modes differs only slightly from the response obtained by using two modes. Therefore, the mode displacement method is very effective for this particular problem. The presence of damper not only reduces the displacement but also makes the occurrence of maximum displacement earlier.

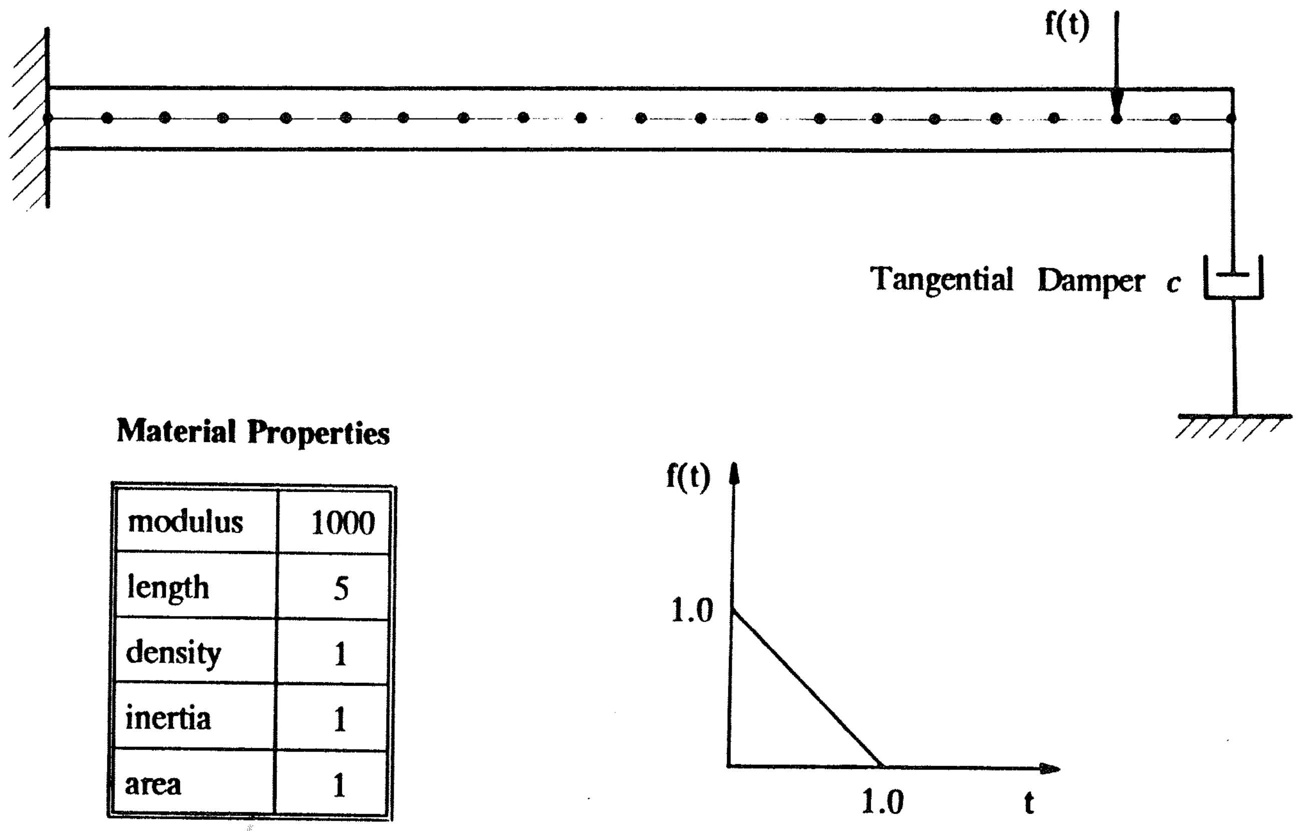

Material Properties

modulus	1000
length	5
density	1
inertia	1
area	1

Figure 6.1 damped dynamic system under loading

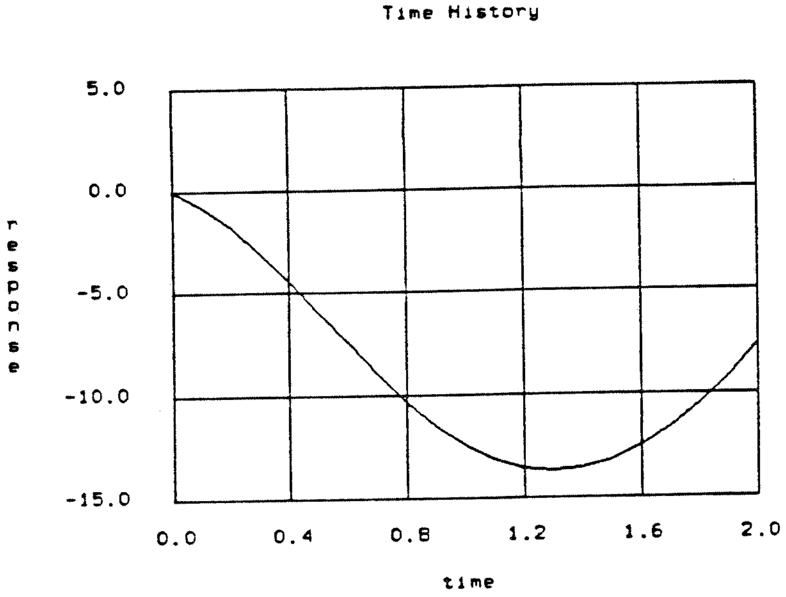

the first mode

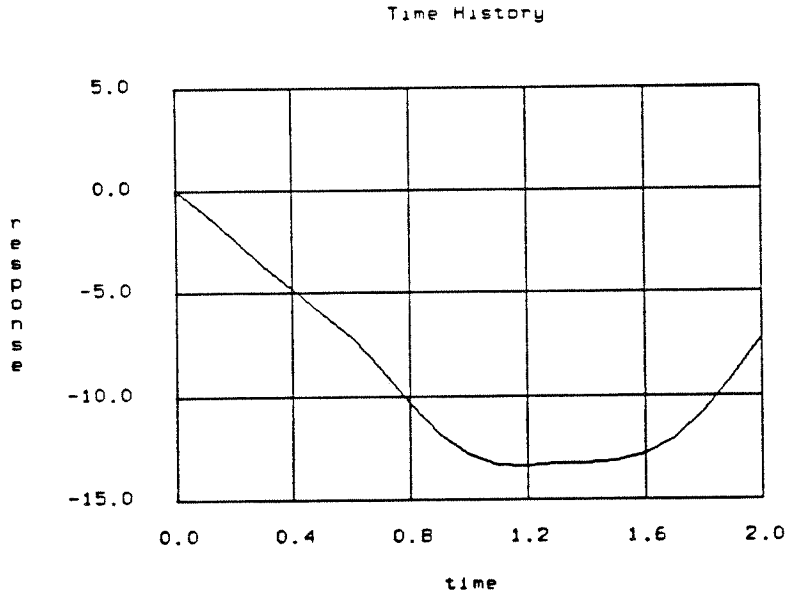

summation of the first ten modes

Figure 6.2 mode-displacement solution (c = 0)

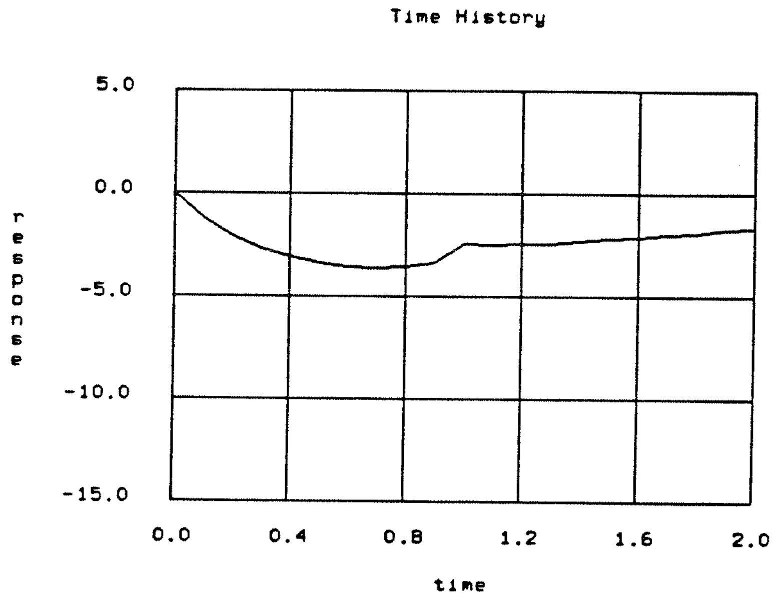

the first mode

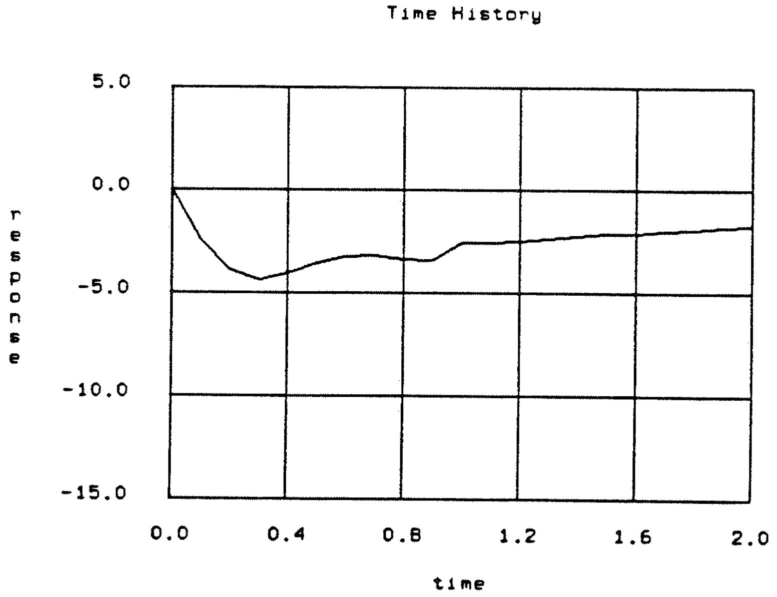

summation of the first two modes

Figure 6.3 mode-displacement solution (c = 5)

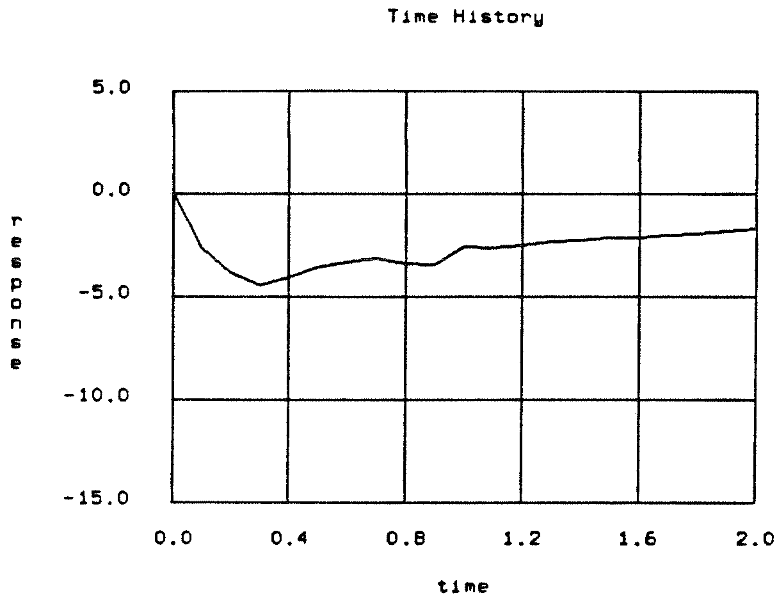

summation of the first ten modes

Figure 6.3 mode-displacement solution (c = 5)

Chapter 7
Conclusions

7.1 Summary

Both the subspace iteration algorithm and the Lanczos algorithm have been extended to extract the least dominant set of complex eigensolutions of a damped system. It should be noted that the amount of matrix-vector multiplications in one iteration of the subspace iteration algorithm is about the same as the one in the Lanczos algorithm. The Lanczos algorithm does not require iteration, therefore, it is faster than the subspace iteration algorithm. This is because the cost of matrix-vector multiplications dominates in large scale problems. However, the subspace iteration algorithm is stable while the Lanczos algorithm is very vulnerable to the round-off effect. The subspace iteration algorithm has advantages over the Lanczos algorithm and vice versa. In the case of solutions of parametric problems or many problems with only slight changes, the Lanczos algorithm used as the first step and the subspace iteration algorithm used for the other steps is recommended.

The eigensolutions are used to construct a set of decoupled equations which correspond to the damped modal equations of the dynamic system. Each of the decoupled equations is solved independently. The modal solutions are then superposed to give the response of the dynamic system. Frequently, only the first few modes are needed to approximate the solution satisfactorily.

7.2 Future Research

The Lanczos algorithm presented is efficient for the solution of viscously damped dynamic systems. It is suggested that an efficient scheme to solve the resulting tri-diagonal system be developed. This will further enhance the efficiency of the

Lanczos algorithm.

We have shown by examples that the Krylov subspace generated from $\mathbf{B}^{-1}\mathbf{A}$ is excellent in approximating the least dominant eigenspace of the damped systems considered. A rigorous discussion of the property of the Krylov subspace is desired because it will give an *a priori* estimation on how close the approximating space is to the desired eigenspace.

In the solution of an undamped dynamic problem, the Sturm sequence property is used to check whether the eigensolutions obtained are the required least dominant ones; however, there is no similar procedure for damped systems. To ascertain that there are no eigensolutions missed in the calculation, an efficient procedure to give the number of eigensolutions in a specified interval is desired.

The present study considers only damped nongyroscopic systems, whose damping matrix is symmetric. In a conservative gyroscopic system the damping matrix, sometimes referred to as *Coriolis* matrix, is skew-symmetric. The eigenvalues of such a system are pure imaginary and the eigenvectors are complex. More generally, the damping matrix may be non-symmetric if it includes both gyroscopic forces and viscous forces. The Lanczos method can be applied to solve the conservative gyroscopic system, as shown in [B2]. For the general system, the two-sided Lanczos algorithm, which generates both right and left vectors, must be used to accommodate the asymmetry of the **C** matrix. The subspace iteration algorithm, however, can still be applied in the present form to solve the general system since it does not require that the associated matrices be symmetric.

Although it is conventional to use the mode-displacement method or the mode-acceleration method to solve the transient dynamic problem; one can also use the Lanczos vectors generated from (**A**, **B**) to reduce the original system into a smaller tri-diagonal one, as suggested in Section 6.1. Further study should be directed towards quantitying the relative effectiveness and efficiency of this alternative method.

In using the mode superposition method, if the frequency of a certain mode is in the neighborhood of the frequency content of the applied loading, then the contribution of this mode must be included in the summation even though the participation factor of this mode is small. This is because of *resonance* where the response due to this mode is greatly amplified. Knowledge of eigenvalues is essential to avoid resonance in designing the systems under dynamic loadings. It is therefore recommended that one compare the frequency of a mode with the frequency contents of the loading, in addition to calculating the participation factor, to decide whether this mode should be included in the mode superposition. Moreover, in performing design of systems uncertainty in loading must be accommodated. In order to have reliable sensitivity analysis all modes within a specified range must be known, not just those excited by the input load specified.

References

[B1] Bathe, K. J., *Finite Element Procedures in Engineering Analysis,* Prentice-Hall, Englewood Cliffs, NJ, 1980.

[B2] Bauchau, O. A., "A solution of the Eigenproblem for Gyroscopic Systems with the Lanczos Algorithm", *Int. J. Numer. Methods Engrg.,* Vol. 23, 1986, pp. 1705-1713.

[B3] Bishop, R. E. D., and Johnson, D. C., *The Mechanics of Vibration,* Cambridge University Press, London, 1960.

[C1] Caughey, T. K., "Classical Normal Modes in Damped Linear Dynamic Systems," *J. Appl. Mech.* , Vol. 27, June 1960, pp. 269-271.

[C2] Clough, R. W., and Penzien, J., *Dynamics of Structures,* McGraw-Hill, New York, NY, 1975, pp. 935-950.

[C3] Craig, Jr. R. R., *Structural Dynamics - An Introduction to Computer Methods* Prentice-Hall, Englewood Cliffs, NJ, 1981.

[E1] EISPACK - The Eigensystem Subroutine Package, Argonne National Laboratories, 9700 S. Cass Ave., Argonne, IL.

[F1] Foss, K. A., "Co-Ordinates Which Uncouple the Equation of Motion of Damped linear Dynamic Systems," *J. Appl. Mech.,* Vol. 25, 1958, pp. 361-364.

[F2] Fox, L., *Introduction to Numerical Linear Algebra,* Clarendon Press, Oxford, 1964.

[F3] Frazer, R. A., Duncan, W. J., and Collar, A. R., *Elementary Matrices and Some Applications to Dynamics and Differential Equations,* Cambridge University Press, Cambridge, 1946.

[G1] Garbow, B. S., Boyle, J. M., Dongarra, J. J., and Moler, C. B., *Matrix Eigensystem Routines : EISPACK Guide Extension,* Springer-Verlag, New York, 1972.

[G2] George, A. and Liu, J. W-H., *Computer Solution of Large Sparse Positive Definite Systems,* Prentice-Hall, Englewood Cliffs, New Jersy, 1981.

[H1] Hughes, T. J. R., *The Finite Element Methods,* Prentice-Hall, Englewood Cliffs, New Jersy, 1987, pp. 570-631.

[H2] Hurty, W. C. and Rubinstein, M. F., *Dynamics of Structures,* Prentice-Hall, Englewood Cliffs, New Jersy, 1964, pp. 313-337.

[J1] Jennings, A., *Matrix Computation for Engineers and Scientists,* John Wiley & Sons, London, 1977.

[L1] Lancaster, P., "A Generalised Rayleigh-Quotient Iteration for Lambda-Matrices," *Arch. Rat. Mech. Anal.,* Vol. 8, 1961, pp. 309-322.

[L2] Lancaster, P., *Lambda-matrices and Vibrating Systems,* Pergamon Press, Oxford, 1966.

[M1] Meirovitch, L., *Computational Methods in Structural Dynamics,* Sijthoff & Noordhoff, 1980.

[N1] Nour-Omid, B., Parlett, B. N., and Taylor, R. L., "Lanczos versus Sub-space Iteration for the Solution of Eigenvalue problems," *Int. J. Numer. Methods Engrg.,* Vol. 19, 1983, pp. 859-871.

[N2] Nour-Omid, B., and Clough, R. W., "Dynamic Analysis of Structures Using Lanczos Coordinates," *Earthquake Engineering and Structural Dynamics,* Vol. 12, 1984, pp. 565-577.

[N3] Nour-Omid, B., Parlett, B. N., Ericsson T., and Jensen, P. S., "How to Implement the Spectral Transformation," *Mathematics of Computation,* Vol. 48, No. 178, April 1987, pp. 663-673.

[P1] Parlett, B. N., *The symmetric Eigenvalue Problem,* Prentice-Hall, Englewood Cliffs, NJ, 1980.

[P2] Parlett, B. N. and Scott, D. S., "The Lanczos Algorithm with Selective Orthogonalization," *Math. Comp.,* v.33, 1979, pp.21-238.

[S1] Scott, D. S., "Analysis of the Symmetric Lanczos Process" *Technical Report ERL-M78/40,* Electronics Research Laboratory, University of California, Berkeley, CA, 1978.

[S2] Simon, H. D., "The Lanczos Algorithm with Partial Reorthogonalization" *Math. Comp.,* v.42, 1984, pp.115-142.

[S3] Simon, H. D., "The Lanczos Algorithm for Solving Symmetric Linear Systems" *Technical Report PAM-74,* Center for Pure and Applied Mathematics, University of California, Berkeley, CA, 1982.

[S4] Smitch, B. T., Boyle, J. M., Ikebe, Y., Klema, V. C., and Moler, C. B., *Matrix Eigensystem Routines : EISPACK Guide,* 2nd ed., Springer-Verlag, New York, 1970.

[V1] Veletsos, A. and Ventura, C. E., "Modal Analysis of Non-Classically Damped Linear Systems," *Earthquake Engineering and Structural Dynamics,* Vol. 14, 1986, pp. 217-243.

[W1] Wilkinson, J. H., *The Algebraic Eigenvalue Problems,* Clarendon, Oxford, 1965.

[W2] Wilson, E. L., Yuan, M., and Dickens, J. M., "Dynamic Analysis by Direct Superposition of Ritz Vectors," *Earthquake Engineering and Structural Dynamics,* Vol. 10, 1982, pp. 813-821.

[Z1] Zienkiewicz, O. C., *The Finite Element Method,* third edition, McGraw-Hill, London, 1978.